Development of alkali-activated foamed materials combining both mining waste mud and expanded granulated cork

Imed Beghoura

Tese para obtenção do Grau de Doutor em
Engenharia Civil
(3º ciclo de estudos)

Orientador: Prof. Doutor João Paulo de Castro-Gomes

Juri:
Prof. Doutor Victor Manuel Pissarra Cavaleiro
Prof. Doutor Jorge Alberto Durán Suárez
Prof. Doutor José Luis Barroso de Aguiar
Prof. Doutor Szymon Dawszynski

Outubro de 2022

Dedication

I would like to dedicate this dissertation to my parents Abd-Elmoughith and Elamrya, who have sacrificed their lives to raise me and have supported me throughout my life and have encouraged me to pursue my passions in an academic setting. Undoubtedly, I would have never achieved this level of education without their support and attention. Although I have been far away from them during my Doctoral studies. I have always felt their presence in every single cell of my body, and they have always inspired and given me the hope to go through the challenges posed by academic life. I am glad that I can please them by accomplishing this phase of my scholarly life. I would also like to devote this dissertation to Baba Mansour and M'a Zouina, who have been present in my life and are like my second parents as well as to all my brothers and sisters, especially my brother Rahimou, without forgetting all those I loved, and they are no longer with us.

Acknowledgements

The completion of this doctoral dissertation was possible with the support of several people. I would like to express my sincere gratitude to all of them who, during the doctoral program, provided me with everything I needed.

First of all, I would like to express my deepest gratitude to my main supervisor, Full Professor Joao Paulo de Castro-Gomes for the continuous support of my doctoral study and related research, for his patience, motivation, enthusiasm, and immense knowledge. I would like to thank him for encouraging my research and for allowing me to grow as a research scientist. His advice on both research and my career has been priceless. I am also grateful for his motivation to present my work at international scientific conferences, thus giving me the opportunity to develop my prospects.

A special thanks also goes to the University of Beira Interior due to the wonderful people, Professors, technicians, secretaries, librarians, and others, who work in offices and departments and help students continuously, direct, or indirectly, to bring their research to an end. I am particularly grateful to my colleagues of research for their enthusiastic encouragement.

I would like to extend my thanks to all the REMINE Project partners for their scientific inputs and support. Furthermore, I would like to thank Alsitek Limited (Peterborough, UK) and Sofalca, Lda (Abrantes, Portugal) for their contribution to providing knowledge and materials.

I am also very grateful to the Santander Totta/UBI for financial support in the form of a Doctoral grant for a part of this investigation for 10 months in 2018.

Last but not the least, I would like to thank all my family big and small: my parents as well as my siblings for supporting me spiritually and financially throughout the writing of this dissertation and my life in general.

Abstract

In Portugal, the significant amount of mine waste mud from tungsten mining operations has led to growing concerns about their ecological and environmental impacts such as the occupation of large areas of land, generation of powder and the contamination of surface and underground water. Furthermore, natural by-products in general, and natural cork particles in particular, have been used to manufacture new materials which not only provide good thermal insulation but also have a limited impact on the environment and a lower cost. Alkali-activated foamed materials have been introduced in the field of alkali-activated materials which have been produced from different raw and waste materials. It has been proposed as a new idea that involves the production of lightweight materials, thus combining the performance and the benefits of energy-saving (Carbon footprint) with the reduction of the cradle-to-gate emission obtained. Besides, in order to reduce the density of the alkali-activated materials holes or lightweight aggregates can be added for such purposes. Therefore, in this research, novel alkali-activated lightweight foamed materials (AALFM) from a combination of tungsten mine waste mud (TWM), waste glass (WG), and metakaolin (Mk) using alkali activators solution of Sodium Silicate (SS) and Sodium Hydroxide (SH) was developed and combined with natural expanded granulated cork (EGC) using aluminium powder (Al) as a foaming agent.

The objective of this study is to develop a new alkali-activated foamed tungsten-based binder/mortar and to characterize the cork waste composite made from this binder/mortar and natural granulated aggregates (EG-Cork). Cork, which is the exterior bark of Quercus suber L., a natural, organic, and lightweight plant tissue with a high dimensional stability substance. Physical properties of tungsten-based alkali-activated binder/mortar such as bulk density, thermal conductivity and pore sizes distribution were provided. The formulations of the alkali-activated binders are based on a combination of tungsten waste mud (TWM), waste glass (WG), and metakaolin (Mk). The mechanical and thermal properties of alkali-activated foamed materials produced were then tested. The research work includes three main phases. The first part shows the feasibility to produce new improved lightweight foamed alkali-activated materials using Panasqueira tungsten waste mud (TWM) as major raw material incorporating expanded granulated cork (EGC). During this preliminary study, a series of mixes containing mining waste mud, milled waste glass, metakaolin and Ordinary Portland Cement, in different proportions, were prepared. The influence on porosity, density, and compressive strength of incorporating granulated expanded cork at different percentages was first studied with potential applications in artistic, architectural, and

historical heritage restoration. The second part investigates the influence of different precursors' particle sizes on the physical and mechanical properties, such as density, porosity, expansion volume, and pore size by image analysis. The design and development of tungsten-based alkali-activated foams (AAFs) were studied systematically. Moreover, the manufactured AAFs with enhanced compressive strength from non-calcined tungsten waste mud (raw material) by changing the precursor particle sizes showed results of the same level or even higher as other research results obtained with fly ash and MK. The third part of the research investigates the effect of the incorporation of expanded granulated cork (EGC) to produce alkali-activated lightweight foamed materials (AALFM) with thermal properties.

The findings indicate that experimental research on different combinations of raw materials particularly tungsten mining waste mud (TMWM) contribute to the development of alkali-activated materials (AAMs) and alkali-activated foamed materials (AAFMs). These new improved materials can be used as building materials with enhanced properties such as compressive strength, density, thermal conductivity, and fire resistance. This doctoral research contributes to a sustainable development by promoting the complete recycling and use of mining wastes as construction materials.

Keywords Alkali-activated materials, Tungsten Waste Mud, Expanded granulated Cork, Foamed materials, Aluminium powder, Compressive strength, Density, Porosity, Expansion Volume, Thermal Conductivity.

Resumo

Em Portugal, a quantidade significativa de lamas residuais provenientes das operações de mineração de tungsténio, tem gerado preocupações crescentes relativamente aos impactos ecológicos e ambientais, tais como, ocupação de grandes áreas de terreno, libertação de poeiras, e a contaminação de águas superficiais e subterrâneas. Nesta pesquisa, um novo material espumoso leve obtido por ativação alcalina (AALFM) de lamas residuais da mina de tungsténio (TWM) foi desenvolvido, utilizando pó de alumínio (Al) como agente de formação de espuma e, ainda, combinado com cortiça granulada expandida natural (EGC).

O trabalho de pesquisa comtemplou três fases principais. A primeira parte demonstra a viabilidade de produção de novos materiais expandidos ativados alcalinamente utilizando lamas residuais das minas de tungsténio da Panasqueira (TWM) como principal matéria-prima e, incorporando cortiça granulada expandida (EGC), com aplicações potenciais na restauração de património artístico, arquitetónico e histórico. Neste estudo preliminar, foram preparados conjuntos de misturas, contendo lamas residuais, resíduo de vidro moído, metacaulino e cimento Portland, em diferentes proporções. Em primeiro lugar, foi estudada a influência na porosidade, densidade e resistência à compressão da incorporação de cortiça expandida granulada em diferentes percentagens. A segunda parte investiga o projeto e o desenvolvimento de ligantes /argamassas espumosas ativadas alcalinamente com lamas das minas de tungsténio, utilizando três tamanhos de partícula de diferentes. As propriedades físicas e mecânicas, densidade, porosidade, volume de expansão e tamanho dos poros, foram estudados de forma sistemática. Além disso, foi também estudado o aprimoramento da resistência à compressão de espumas ativadas alcalinamente (AAFs), alterando os tamanhos das partículas precursoras. A terceira parte da investigação investiga o efeito da incorporação da cortiça granulada expandida (EGC) na produção de espumas leves ativadas alcalinamente (AALFM) nas suas propriedades térmicas. Os materiais espumosos ativados alcalinamente inserem-se no campo dos materiais obtidos por ativação alcalina, os quais têm sido produzidos a partir de diferentes matérias-primas e resíduos. Foi proposto como uma ideia nova que envolve a produção de materiais leves, combinando assim o desempenho e os benefícios da poupança de energia (pegada de carbono) com a redução da emissão "cradle-to-gate" obtida. Além disso, a fim de reduzir a densidade dos materiais ativados alcalinamente, podem ser adicionados orifícios ou agregados leves para esse fim.

Os resultados dos estudos experimentais permitem desenvolver diferentes tipos de materiais, utilizando resíduos de minas como matéria-prima. Este novo material produzido

pode ser usado como materiais de construção com propriedades aprimoradas, como resistência à compressão, densidade, condutividade térmica e resistência ao fogo. Esta investigação de doutoramento contribui para o desenvolvimento sustentável, promovendo a reciclagem completa e a utilização de resíduos de mineração como materiais de construção.

Palavras-chave Materiais ativados alcalinamente, lamas residuais de tungstênio, cortiça expandida, materiais em espuma, pó de alumínio, resistência à compressão, densidade, porosidade, volume de expansão, condutividade térmica.

Content

List of Figures

List of tables

List of abbreviations and acronyms

Materials

AAMs	Alkali-Activated Materials
AABs	Alkali-Activated Binders
LWMs	Lightweight Materials
AAFMs	Alkali-Activated Foamed Materials
AALFMs	Alkali-Activated Lightweight foamed materials
C-A-S-H	Calcium Aluminium Silicate Hydrate
N-A-S-H	Sodium Aluminium Silicate Hydrate
C-S-H	Calcium-Silicate-Hydrate
CH	Calcium Hydroxide
CF	Carbon Fibre
GGBFS	Granulated Ground Blast-Furnace Slag
TMWM	Tungsten Mining Waste Mud
WG	Waste Glass
MK	Metakaolin
OPC	Ordinary Portland Cement
EGC	Expanded Granulated Cork
RS	River Sand
RHA	Rice husk ash
P/A	Precursor / Activator ratio
Si/Al	Silicium/Aluminium Ratio
SH	Sodium Hydroxide (NaOH)
SS	Sodium silicate (Na_2SiO_3)
Al	Aluminium Powder
HP	Hydrogen Peroxide
SCM	Supplementary Cementitious Materials

Techniques

SEM	Scanning electron microscopy
EDS	Energy Dispersive X-Ray Spectroscopy
FTIR	Fourier-Transforms Infra-red
MIP	Mercury Intrusion Porosimetry
XRD	X-Ray Diffraction
Rc	Compressive Strength

Chapter 1 - General introduction

This chapter presents a general introduction, research background, and justification. The aims of the study are reviewed and underlined followed by hypothesis and motivations. The outline of the thesis and the research topics are discussed and highlighted.

1.1. Introduction

For several decades, we have been facing global environmental issues such as climate change, pollution, and environmental degradation due to human activities in different fields such as industry, construction, energy, and transport. From now on, in order to protect the environment, it is necessary to integrate all projects into a sustainable development approach. The construction sector is recognized as an activity that consumes the highest quantity of energy in the world, and the one that emits the second-highest rate of CO_2, after industry, in comparison with other activities. This shows that the construction sector is one of the areas that harm the environment the most. In the field of construction, the production of materials represents a very large share of CO_2 emissions and energy consumption, particularly due to the production of Portland cement. Consequently, studies are necessary to integrate the production of building materials into a sustainable development approach, and new construction materials must be developed to replace conventional ones. The production of these new materials must respect environmental criteria and the comfort and health of users. Likewise, their properties should be improved as much as possible [1].

1.2. Background and justification

At present Portland cement is an essential material in the construction of buildings and structures that are being widely utilized since 1900. Nevertheless, the aim is to reduce the use of Portland cement in buildings due to the significant carbon emissions as well as the environmental impacts caused by cement manufacture and the high cost of the production of Ordinary Portland Cement (OPC), For that reason, it is recommended to restrict the cement content of concrete in order to make it a more sustainable material [2] and this is possible through the substantial replacement of cement with supplementary materials. In the near future, Geopolymers or alkali-activated cementitious products will be used as new construction materials and will include high-performance substances which present low environmental impacts and that are produced at a relatively cheaper price [3]. The main role is to determine the characteristics and components of the final product derived from alkali-activated materials (AAMs). Many researchers studied the properties of geopolymers or alkali-activated materials by using different alumino-silicate resources (Fly Ash, Metakaolin, Slag, etc.). As known, Geopolymer is the name given to cementitious materials where the binder is entirely replaced by an inorganic polymer formed between a strong alkaline solution and an alumino-silicate source [4]. These products can be replaced with a binder in concrete as the main building material [5]. Future concerns with inadequate pozzolanic materials for alkali-activation owing to demands from the

cement and concrete industry of alkali-activated slags and fly ash (industrial wastes). Identified and secured additional non-conventional alkali-activation precursor materials. Alkali-activated materials (AAMs) have been used for more than 60 years and various researchers have also shown that AAMs can be considered eco-friendly materials because their production process consumes much less energy than that of Portland cement and emits very little CO_2. Studies showed the potential of alkali-activated binders (AABs), using a variety of raw materials from industrial and mining waste to manufacture AAMs. The basic mechanisms of the alkali-activation reaction have been understood [6]. The benefits of the use of alkali-activated materials are twofold. First, lowering the cement percentage of concrete reduces its carbon footprint. Secondly, due to the huge amount of supplementary cementitious materials (SCM) that are basically waste raw materials that must be kept in landfills and enclosures if not used. As a result, making effective use of these raw materials by integrating them into construction materials in large quantities might help ease the waste storage problem [7].

The target of resource efficiency is to separate economic growth from resource use. It encourages the economy to produce more with less, to offer more value with less input, to use resources sustainably, and to reduce their environmental effect. Eco-innovation is any type of invention that aims to make significant and measurable progress toward the objective of sustainable development by decreasing environmental impacts, increasing environmental resilience, or attaining more efficient and responsible use of natural resources [8]. Great interest in the prospect of using naturally available silico-aluminate and alumino-silicate resources and industrial wastes, such as coal fly ash, blast furnace slag, clay sediments, and others from quarrying and mining wastes, to reduce the environmental impact of the manufacture of new alkali-activated materials (AAMs). Furthermore, the synthesis of newly formed products occurs at low temperatures, often below 60 ° C. All of these considerations suggest a reduction in natural raw material usage and greenhouse gas emissions, particularly CO_2 when compared to typical cement-based products [9]. Many countries have conducted surveys on mining and quarrying waste products during the last two decades for the production of additional cementitious materials. The primary motivations for conducting such surveys are the need to conserve precious natural resources, decrease pollution, and conserve energy [10]. Over time, the build-up of waste from the mining and quarrying industries has resulted in the creation of huge deposits. These deposits cause a danger of environmental contamination and have substantial landscape consequences, lowering the quality of life for surrounding residents. Given that these wastes include certain dangerous chemicals, storing them directly on land may have detrimental environmental consequences (e.g., heavy metals) [11]. In the past few years, there has been a growing interest in materials derived from renewable resources, due to increasing concerns about the environment, waste accumulation and disposal, and the eventual depletion of fossil resources. Cork is a versatile material that has been utilized in a variety of applications. The most well-known uses of cork are in alcoholic beverage stoppers (natural and agglomerated cork), traditional floor covering with composite cork tiles (made by binding cork particles with different binders), in addition to thermal, acoustic, and vibration insulation with expanded cork-board in buildings and some other industrial fields [12]. Furthermore, it was found that it is possible to use abundant waste material

from the cork industry, cork powder, as a substitute for fines in mixtures of self-compacting concrete resulting in a good strength level and suitable durability for common applications [13].

1.3. Aims and structure of the thesis

The main objective of this doctoral research is to investigate and develop new tungsten-based alkali-activated lightweight foamed materials (AALFMs) binders/mortars, by incorporating expanded granulated cork (EGC) through a chemical foaming method. In this research, we used wastes from various sources such as tungsten waste mud (TWM) and industrial waste (waste glass), and others. These have the potential to be of significant importance from an environmental perspective and can promote a circular and stronger green economy. Furthermore, this study also aims at developing new enhanced tungsten-based alkali-activated binders/mortar foamed materials which incorporate natural expanded granulated cork (EGC) with the target of being able to improve building thermal performance.

The primary objective of this research study was to enhance the compressive strength, density and to investigate the expansion process of the produced alkali-activated lightweight foamed materials (AALFMs). It was also aimed to develop an improved tungsten-based alkali-activated foam (AAFs) by using precursors with different maximum particles sizes of (150 μm, 300 μm, and 500 μm) to obtain a low-cost and more sustainable, fire-resistant, and thermal insulating material with high porosity, and at the same time able to retain high ratios of compressive strength to porosity. Besides that, the novelty of this research is the study of the effect that different maximum precursor particle sizes have on the compressive strength, volume expansion, and pore size distribution of AAFs and the AALFMs. Given this, this doctoral research has as general objectives:

1. To develop and design mixes of materials and methods for the development of alkali-activated foamed materials incorporating expanded granulated cork (EGC) based on the demand from rheology and processing techniques.
2. To research the relationship between composition, microstructure, and physical-mechanical properties of tungsten-based alkali-activated foamed materials.
3. To investigate the possibility of enhancing mechanical properties (compressive strength, versus porosity and pore size distribution) of the alkali-activated foamed materials by varying the precursors' maximum particle sizes.
4. To study the expansion process (pore size and distribution) of alkali-activated foamed materials incorporating EG-Cork using aluminium powder.
5. To develop alkali-activated lightweight foamed materials incorporating natural expanded granulated cork particles (EGC) with good thermal properties.

1.4. Phases of research work and schedule

Table 1.1 – presents the different phases of the research work and the schedule set.

Table 1.1 - Phases of the research work and schedule.

Research/Literature review	Initially, the objectives of this doctoral work focus on the systematization of the concept of alkali-activated foamed materials (AAFMs). Considering that this research aims to develop a novel and improved tungsten-based alkali-activated binder/mortar lightweight foamed materials (AALFMs) through a chemical foaming method as well as incorporating expanded granulated cork (EGC), a review on the use of both parameters was carried out. The literature review identifies the various strategies for alkali activation technology, the most used raw materials in addition to the main construction characteristics. Moreover, the literature review draws the main topics discussed in the context of the production of alkali-activated foamed materials (AAFMs), including their benefits and contributions to building components *(Chapter 2).*
Mix design and properties	After exploring materials and methods, the design of alkali-activated foamed materials was established. Several formulations were tailored. Varied materials as well as foaming agents for the blowing process, namely aluminium powder and Hydrogen peroxide were used. Models and prototypes were generated with added value in industrial design, as well as material elements that can be used for thermal insulation applications *(Chapter 4).*
Microstructure and physical-mechanical properties	During this phase, the chemical reaction of the AAFMs and the microstructural characterization by SEM were carried out. A relationship between physical and mechanical properties, particularly, compressive strength, density, and porosity, was determined *(Chapter 4).*
Expansion process	During this phase, the expansion process (expansion volume, time of the reaction, measurement of gas produced) for different alkali-activated foamed materials (AAFMs) produced was examined *(Chapter 5).*
Thermal properties of the foamed material	During this phase, a study of the thermal conductivity of the produced foamed materials, in particular AAFs and AALFMs with the potential for use as foamed insulating materials was conducted. Results and discussion were highlighted *(Chapter 6).*

1.5. State of the art

1.5.1. Sustainable development in construction

European Commission (EC) recently adopted an ambitious new Circular Economy Package (CEP) to help European businesses and consumers to make the transition to a stronger and more circular green economy where resources are used more sustainably [14]. In order to properly recycle and reuse mine

tailings and waste concrete in a sustainable and ecologically friendly manner, the research employs a process known as alkali-activation. The activation of silica and alumina-containing materials with alkali or alkaline solution forms an amorphous to the semi-crystalline polymeric structure. In Portugal, according to research conducted by the Directorate-General for Energy and Geology, the residential sector corresponded to 16.4% of the final energy consumption in 2017. As demonstrated in Figure 1.1. industry and housing are two of the most significant sectors that have greater impacts associated with power generation, which in turn increases economic and environmental impacts, thus increasing greenhouse gas emissions [15].
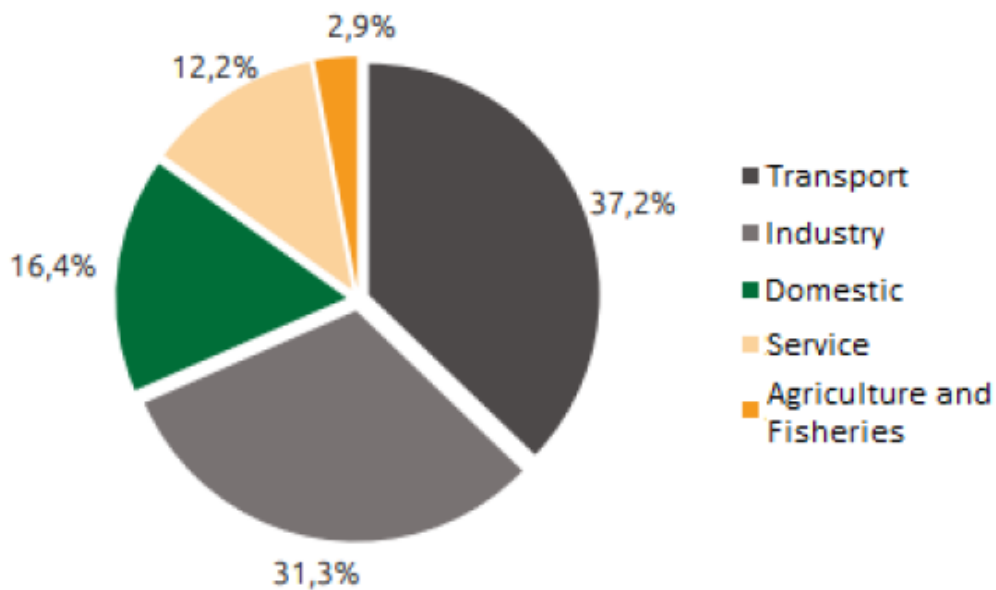
Figure 1.1 - Final energy demand in Portugal by sector, in 2017 [15].

Each year, a huge quantity of industrial waste is generated from different sectors including mining, power and energy, and construction. The significant amount of industrial waste deposits has led to growing concerns about their ecological and environmental impacts, such as the case of mining wastes [11]. The reuse of mineral wastes as precursor materials for alkali-activated binders (AABs) and applications have been conducted by many researchers and are now considered promising. Besides, the alkaline activation of aluminosilicate industrial by-products is widely known to yield binders whose properties make them comparable to or even stronger and more durable than ordinary Portland cement (OPC) [16][17]. Additionally, recent new ideas have led to the development of geopolymer/alkali-activated foam concrete. This idea combines the performance benefits and energy savings obtained with lightweight foam concrete, with the cradle-to-gate emissions reductions obtained through the use of a geopolymer binder derived from an industrial by-product, like fly ash [18].

Foamed concrete can be produced either by the pore-forming method or the mixed-foaming one [19]. The manufacturing of a stable mix of foamed concrete depends on many factors, such as the selection

of the foaming agent, the method used to prepare the foam to obtain a uniform air-void distribution, the selection of materials, strategies for mixture design, and the production of foamed concrete. Various foaming agents have been used to produce foamed concrete, including detergents, resin soap, glue resins, saponin, and hydrolysed proteins, such as keratin and similar materials [20]. Among the methods used to produce lightweight geopolymer/alkali-activated concrete by the foaming agent is the thermal expansion of (Na, K)-poly (sialate-multisiloxo) with ration Si: Al>>6 [21]. In addition, the density can be reduced by replacing part of the solids with air voids or lightweight aggregates. Several approaches can be followed to achieve this objective. In the method known as no-fines concrete, the fine aggregate is omitted; whereas in the so-called lightweight concretes, the normal aggregates are replaced by lightweight to reduce the density [22]. According to Davidovits, there is no standard formulation to fabricate a Geopolymer foam. The success of foamed geopolymer requires a delicate optimization of two parameters; (1) kinetics of peroxides decomposition with the production of oxygen, (2) increase in viscosity of the precondensated geopolymer [21]. For the foaming of inorganic polymers, hydrogen peroxide, aluminium powder, or sodium perborate can be used as chemical foaming agents. The reaction between the Al metal powder and alkaline activator proceeds quickly, during which the reaction releases hydrogen [23].

Lightweight concrete has been categorized into three groups (1) no-fines concrete; [24], (2) lightweight aggregate concrete; and (3) aerated/foamed concrete. Lightweight concrete can be prepared either by injecting air or by eliminating the finer aggregate sizes and substituting them with hollow, cellular, or porous aggregate. Moreover, lightweight aggregate concrete consists of lightweight aggregate (expanded shale, clay, or slate materials that have been fired in a rotary kiln to develop a porous structure) which can be used as a replacement for normal aggregates such as crushed stone or sand [25]. Several industries have investigated the use of granulated cork (EGC) as a lightweight aggregate (LWA) and numerous research projects have been conducted to evaluate the physical and mechanical characteristics of waste cork and to investigate its potential advantages as aggregates in concrete production [13]. Cork powders are an industrial by-product and because cork is a natural material, it has environmental advantages [26]. Finding alternative uses for industrial waste cork can have a great economic benefit. Cork granules have a low density and can be used as lightweight aggregate (LWA) in the production of concrete and mortars (specifically polymer-modified mortars) with improved thermal and acoustic insulation properties, as well as high durability, low permeability, and chemical and frost resistance. Cork has become widely utilized in a variety of construction applications as a lightweight, thermally insulating, and eco-friendly substance with several benefits [13]. Various research has been conducted to investigate the impact of cork granules on cement production compatibility [27]. Karade et al. 2006, investigated the incorporation of cork granules (both natural and expanded) and they were shown to be compatible with cement in hydration experiments and could be added up to 30% by the weight of cement [27]. Panesar and Shindman (2012), investigated the plastic, mechanical, transport, microstructural, and thermal properties of mortar and concrete when the cork was employed as a substitute for sand or stone [26].

1.4.2. Previous research work at UBI

From the early 2000s onwards, researchers at the University of Beira Interior (UBI) have been providing thorough information in the field of alkali-activation technology using mining waste aluminosilicate sources with a focus on tungsten-based alkali-activated materials. Torgal and Castro-Gomes published several articles [28][29][30] in which they addressed, at the time, the feasibility of using mine waste mud to produce environmentally friendly new binders and the nature of the preliminary hydration products formed. Alkali activation of tungsten mining waste mud (TWM) is considered to be very suitable for the production of alkali-activated materials (AAMs). The adhesion and green strength are the same as those produced from metakaolin and fly ash. Alkali activation of tungsten waste mud (TWM) has already been successfully used to produce artificial aggregates for water treatment systems [31]. Also, it has been used to produce modular pre-fabricated panels in combination with expanded cork (EGC) and incorporate pre-planted vegetation [32].

The future of mixture design and applications is to identify combinations of mine tailings with other waste components that have been treated with some success using alkali-activated slags both ground granulated blast furnace slag (GGBFS) and electric arc furnace slag (EAF-Slag), red clay brick waste (RCBW), fly ash or metakaolin-based binders in addition to other industrial products and by-products [33]. This way, it is possible to adapt individual solutions for the reuse of waste from mining and quarrying with the potential for many new applications.

Chapter 2 - Literature review

2.1. Literature review

This chapter presents a comprehensive overview of the importance of the research literature on the technology and properties of alkali-activated cementitious materials (AAMs), particularly alkali-activated lightweight foamed materials (AALFMs) in the existing literature. Their manufacturing processes and the hydration reactions along with the review of the major events and the outlining steps in the development of these new alkali-activated binders (AABs) are also described. The usage of lightweight aggregates mainly natural waste cork particles as well as the foaming methods for density reduction is also presented based on previous studies. In addition, the focus on utilizing alkali-activated binders (AABs) from mining and industrial wastes generation is presented with the potential to produce AALFMs mainly from tungsten mining waste mud (TMWM) and incorporating expanded granulated cork (EGC).

2.1.1. History of alkali-activated cement and main concepts

Cement-based materials are widely used in building construction. In fact, concrete is widely used and is considered the second most used material after water on Earth. Cement production emits the largest amount of CO_2 and generates around 2.2 billion tonnes of CO_2 approximately 8 % of the global total greenhouse emissions considering a range of 0.66 to 0.82 kg of CO_2 for every kilogram of Portland cement produced worldwide [34][35]. The emphasis is to reduce the global environmental and energetic impact of cement production. Research and construction communities all over the world reveal so far, a great interest in developing and performing new environmentally friendly sustainable materials alternative to Ordinary Portland cement (OPC) designed for concrete applications [36][37][38].

The first published work related to alkali-activated materials was by the German cement chemist and engineer Kühl in 1908 [39] in which he characterized the performance of a crystalline slag and an alkali sulphate or carbonate, with or without adding alkali metal oxides or hydroxides as 'developing material,' as "completely equivalent to the best Portland cement". Later in 1939, Feret utilized slag cement to establish models of alkali-activated binding systems. The activation of blast furnace slag (Si + Ca) with a mildly alkaline solution, having calcium silicate hydrate, or calcium silicate hydrogel, C-S-H as the main reaction product which is the same as the main component of hardened cement paste: the adhesive phase in hardened Portland cement [40]. Purdon, in 1940, was the first to demonstrate the alkaline activation of construction materials from non-Portland cement sloid by the synthesis of an alkali-slag blend with sodium hydroxide (High-calcium metallurgical slags) [41][42]. Victor Glukhovsky was the first person to investigate the possibility of preparing low-calcium and/or calcium-free cementitious materials clays and alkaline metal solutions thru analysing the binders used in ancient Roman and Egyptian structures, naming "soil cement" for the material produced by the

resulting investigation in 1957 [43]. This early investigation was followed by several formulations using a wide spectrum of materials, including blast furnace slag, clay, aluminosilicate rocks, and fly ash [44]. Several studies on the alkalinization of Na and K have been promoted for 'alkali-activated slag' coined by Glukhovsky and others and they built a storehouse in 1974 made of those cementitious systems [21].

In 1981, Davidovits published results obtained from the development of a series of blends based on the alkali activation of calcined clay or metakaolin (Mk), limestone, and dolomite (whose products he first called geopolymers back in 1978) [4]. These inorganic polymers are a tridimensionality structure formed by low-temperature polycondensation of aluminosilicates with excellent physical and chemical properties and a wide range of applications, including precast structures, along with non-structural elements, concrete pavements, and products [45]. Several raw materials can be used for the geopolymer synthesis from natural aluminosilicate minerals or industrial aluminosilicate wastes such as Class F fly ash, slag, and waste glass with highly alkaline solutions (the alkalis activators solutions are usually a mixture of alkali hydroxide and alkali silicate) [46]. These materials were initially developed after a series of fires in Europe and France in the 1970s mostly as a fire-resistant alternative to organic thermosetting polymers [47]. Geopolymer chemistry generally involves mechanisms such as the dissolution of silicates and aluminates in a strongly basic medium, followed by the polymerization of surface-active groups of particles with the dissolved species to form a solid geopolymer structure [42]. This consists of a network of more or less amorphous SiO_4 and AlO_4, where silicon and aluminium are in IV-fold coordination with oxygen. The presence of alkaline ions such as Na^+, K^+, and Li^+ in the network is necessary to compensate for the negative charge of Al^{3+} in IV-fold coordination. The geopolymerization involves the dissolution and poly-condensation process that occurs at room temperature or slightly higher temperature producing a Si-O-Al polymeric framework with SiO_4 and AlO_4 linked tetrahedrally by sharing oxygen atom [48].

Over the last decades, alkali-activated materials have received rapidly increasing interest due to their excellent physical, mechanical, and thermal properties. Geopolymers or alkali-activated materials possess excellent properties such as good fire and acid resistance, lower permeability, higher unconfined compressive strength, low shrinkage, low thermal conductivity, and good resistance to freeze-thaw cycles [3]. In 1986, the results of the work by Pavel Krivenko using the principles that govern the physical and mechanical properties of concrete prepared with alkaline activated slag were published [49]. Geocements were developed as a result of Prof. V. Glukhovsky's theory that the structure development mechanisms in alkaline aluminosilicate binders are related to geological transformations of aluminosilicate minerals in nature. Since only these phases are characterised by smooth dehydration and subsequent re-crystallisation into stable anhydrous alkaline alumino-silicates without destruction of the framework, optimised thermomechanical properties of metakaolin- and fly ash-based Geocements can be achieved in compositions with an average amount of thermostable zeolites [50][51]. Alkali activation processes of Portland cement, pulverized Portland cement clinker, blast-furnace slags, kaolinite materials, and other inorganic wastes have received a lot

of interest. The research on high-strength gypsum-free Portland cement (alkali-activated) lasted several years and ended up in a stage of industrial feasibility [52].

In 1999, Palomo [53] described the mechanism of activation of fly ash with highly alkaline solutions. Concurrently, Della M. Roy [37] published research results about alkali-activated types of cement, reviewed the history of their development, and discussed their compositions following the alkaline activation system as defined earlier by Glukhovsky in addition to their current circumstances. These materials were developed as an alternative to organic polymers. Alkali-activated cementitious materials can be classified into three main categories [54]: (1) moderately calcium-rich cement, (2) low-calcium cement, and (3) hybrid cement [55]. Alkali-activated materials can be produced from two parts i.e., a solid component (aluminate silicate source) and an alkaline solution activator (caustic alkalis or alkaline salts) [56][47]. These materials are commonly discussed based on similarities with natural zeolites and low-basic calcium hydro-aluminosilicates, and they may be processed and placed using equipment and knowledge similar to that used in the placement of Portland cement concretes. Moreover, for the development of these materials, several types of aluminate silicate sources can be utilized for their synthesis: metakaolin, blast furnace slag and fly ash are among the most common [21][18]. Table 2.1. chronologically reviews some important events outlining steps in the development of alkali-activated types of cement.

Alkali-activated materials (AAMs) have appeared as environmentally friendly alternative cementitious materials to the OPC since the optimally tailored alkali-activated/geopolymer materials for engineering applications could help to reduce CO_2 emissions by 80% in OPC manufacturing [5][108]. Alkali-activated materials and geopolymers characteristics, as well as their applications, are currently being investigated in a variety of industrial and scientific areas, including contemporary inorganic chemistry, colloid chemistry, physical chemistry, geology, mineralogy, and various engineering process technologies [21]. These products are alkali-activated aluminosilicate materials with a substantially lower CO_2 footprint than standard Portland cement (OPC), as well as extremely strong strength and chemical resistance properties and a range of other potentially beneficial characteristics. Even though widespread usage of geopolymer technology is restricted by several factors, the most significant of which is the lack of long-term durability evidence in this relatively new research area. It is widely accepted that a technology that cannot find use is irrelevant [109]. Consequently, several research studies are currently debating how to overcome the challenges related to the widespread use of geopolymers [43][42][101].

Table 2.1 - *Alkali-activated cement timeline (updated from (Palomo et al. 2014))* [54].

Author	Year	Significance	Ref.
Kühl	1930	Slag setting in the presence of dry potash	[57]
Feret	1939	Utilization of slag in cement	[58]
Purdon	1940	Alkali slag combination	[59]
Glukhovsky	1959	Theoretical basis and development of alkaline types of Cements.	[60]
Glukhovsky	1965	First called "alkaline cement"	[61]
P. R. Jochens	1969	Utilization of slags for the manufacture of cement.	[44]
Davidovits	1979	The first who gives the name Geopolymer.	[62]
Malinowski	1979	Ancient aqueducts characterized	[63]
Davidovits	1981	Geopolymer chemistry and applications.	[64]
Forss	1983	F-cement (Slag-alkali-superplasticizer)	[65]
Davidovits et al.	1983	Patent of ''Pyrament'' cement	[66]
Roy and Langton	1984	Ancient building materials characterized	[67]
Philip G. Malone	1985	Potential applications of alkali-activated alumino-silicate binders in the military.	[68]
Krivenko	1986	DSc thesis, R_2O-RO-SiO_2-H_2O	[69]
Małolepszy and Petri	1986	Activation of synthetic melilite slags.	[70]
Malek et al.	1986	Slag cement-low level radioactive wastes forms	[71]
Davidovits	1987	Ancient and modern concretes compared.	[72]
Roy et al.	1989	Ancient concretes analogues.	[67]
Deja and Małolepszy	1989	Resistance to chlorides shown.	[73]
Kaushal et al.	1989	Adiabatic cured nuclear wastes from alkaline mixtures.	[74]
Majundar et al.	1989	C12A7-slag activation	[75]
Talling and Brandstetr	1989	Alkali-activated slag	[76]
Roy et al.	1990	Rapid setting alkali-activated cements.	[77]
Wu et al.	1990	Activation of slag cement	[78]
Roy et al.	1992	Alkali-activated cements: an overview.	[79]
Palomo and Glasser	1992	CBC with metakaolin.	[80]
Roy and Malek	1993	Slag cement.	[81]
Glukhovsky	1994	Ancient, modern, and future concretes.	[82]
Krivenko	1994	Alkaline cement.	[83]
Wang and Scivener	1995	Slag and alkali-activated microstructure.	[84]
Caijun Shi	1996	Strength, pore structure and permeability of alkali-activated slag	[85]
Fernandez-Jimenez and Puertas	1997	Kinetic studies of alkali-activated slag cements	[40]
Katz	1998	Microstructure of alkali-activated fly ash	[86]

Davidovits	1999	Chemistry of geopolymeric systems, technology.	[87]
Palomo et al.	1999	Production of hardened cementitious materials from alkali-activated type F fly ashes	[53]
Roy	1999	Opportunities and challenges of alkali-activated Cements.	[88]
Gong and Yang	2000	Alkali-activated red mud-slag cement	[89]
Puertas	2000	Alkali-activated fly ash/slag cement.	[90]
Bakharev	2001-2002	Alkali-activated slag concrete	[91]
Palomo and Palacios	2003	Immobilization of hazardous wastes	[92]
M. Grutzeck et al.	2004	Zeolite formation in alkali-activated cementitious systems	[93]
Sun	2006	Sialite technology	[94]
Shi	2006	First book on Alkali Activated cement.	[95]
Duxson	2007	Geopolymer technology: the current state of the art.	[96]
Hajimohammadi et al.	2008	One-part geopolymer	[97]
Provis and Deventer	2009	Geopolymers: structure, processing, properties, and industrial applications.	[42]
Luis Oliveira et al.	2012	Ceramic materials waste from the red-clay ceramic industry in Portugal as a partial cement substitute in mortar and concrete.	[98]
Rachit Ghosh et al.	2013	Fly Ash based-geopolymer -excellent short-and long-term properties-	[99]
Provis and Deventer	2014	Alkali-Activated Materials: State-of-the-Art Report	[100]
B. Singh et al.	2015	Geopolymer concrete: A review of some recent developments	[101]
John L. Provis et al.	2015	Advances in understanding alkali-activated materials	[102]
Part Wei Ken et al.	2015	An overview on the influence of various factors on the properties of geopolymer concrete derived from industrial by-products.	[103]
P. Krivenko	2017	Why Alkaline Activation – 60 Years of the Theory and Practice of Alkali-Activated Materials.	[104]
John L. Provis	2018	Brief discussion of the class of cementing materials known as 'alkali-activated binders.	[105]
Aiguo Wang et al.	2020	The Durability of Alkali-Activated Materials in Comparison with Ordinary Portland Cements and Concretes: A Review	[106]
Furqan Farooq et al.	2021	Geopolymer concrete as sustainable material: A state of the art review	[107]

Alkali-activated binders (AABs) are generally made up of one or more mineral components that contain aluminium and silicon oxides, as well as one or more activators. The activators will include alkali metal ions and will create an environment with a high pH value, usually great than 13. (e.g., alkali silicates, hydroxides, sulphates, or carbonates). Furthermore, alkali-activated technology has allowed for the valorisation of a wide range of mining and industrial wastes that are inappropriate for

the production of ordinary Portland cement (OPC) [42]. The alkali-activation reaction is exothermic and occurs at atmospheric pressure and temperatures below 100 degrees Celsius. Despite the extensive studies on the activation of various aluminosilicate materials and the production of a diverse variety of alkali-activated materials, the specific process that occurs during alkali-activation (geopolymerization) remains unknown [110]. Despite the considerable number of research reports and data available on alkali-activated technology, very few practical applications of modern alkali-activated products have been reported. Some conventional inorganic materials, such as expanded perlite, expanded vermiculite, and rock wool cannot meet the energy-saving requirements of modern buildings, as their manufacture requires high energy and resource consumption [111][112]. The major role and motivations of inorganic polymers "geopolymers" as a component in the development of a sustainable concrete industry have been investigated.

2.1.2. Terminology associated with chemically activated cementitious materials

In the past few decades, various research in this field has been published using different classified names for the produced materials through chemical activation using cementitious technology. Alkali-activated binders (AABs) are cement-free building materials that have a variety of advantages over Ordinary Portland cement-based (OPC) formulations, including superior performance. In addition, alkali-activated and/or geopolymer compounds are rapidly developing as an alternative to OPC as the binder of concrete. In comparison to OPC, which produces a significant amount of greenhouse gases, alkali-activated once creates comparatively minimal CO_2 emissions. Waste products from various sectors are frequently used as key raw materials in the creation of alkali-activated and/or geopolymer construction materials [113].

The fundamental technology used to make alkali-activated binders, similar to the other alternative binders discussed, is not new. The Belgian scientist Purdon developed these binders in greater depth, He first introduced the reaction of an alkali source with alumina and silica-containing solid precursor to form a new-rapid hardening binder (a solid material) with performance comparable to hardened Portland cement in 1940. Purdon used alkaline solutions and lime to activate blast furnace slags, thus achieving good rates of strength development and final strengths. He also mentioned the improved tensile and flexural strength of slag-alkali cement, as well as the low solubility of the hardened binder phases and low heat evolution and said that this method of concrete production is best suited to premixed and precast applications where the activator dosage can be precisely controlled. However, the sensitivity of the activation conditions to the quantity of water supplied, as well as the difficulty associated with handling concentrated caustic solutions, were identified as possible issues [2]. More than 30 different blast furnace slags were examined and shown to have rates of strength development and ultimate strengths equivalent to Portland cements when activated with NaOH solutions as well as combinations of $Ca(OH)_2$ and other sodium salts [43]. Alkali, such as sodium hydroxide and potassium hydroxide, was originally used to test iron ground granulated blast furnace slag (GGBFS) to determine whether the slag would be set when added to Portland cement (OPC) [66].

Over the following few decades, the greatest research advances in the field of alkali-activated materials came from a Ukrainian research group directed by Glukhovsky through the combination of various aluminosilicate wastes. These binders are classified into two types based on the composition of their starting materials'; alkaline binding systems and acidic binding systems and alkaline-earth alkali binding systems $Me_2O-Me_2O_3-SiO_2-H2O$ and $Me_2O-MeO-Me_2O_3-SiO_2-H_2O$. Various slags and clays were combined with alkaline industrial waste solutions to produce a family of cement-alternative binders for so-called 'soil cement' building applications and the corresponding "soil silicates" concretes [43], as well Pavel Krivenko later in 1994 [83]. They succeeded in developing alkali-activated mixtures based on a variety of precursors and activators chemistries, including low and high calcium binder systems. Davidovits, a French material scientist is known for inventing geopolymer chemistry, and patenting various aluminosilicate-based formulations for niche applications in the early 1980s. He was the first to use the term 'geopolymer' to describe these materials [48]. As a result of the work of several researchers, alkali-activated mixtures based on a variety of precursors and activators were produced, including low and high-calcium binder systems. Alkali-activated materials have been used in a variety of applications [50]. The alkali-activated types of cement are also known under other names; Table 2.2. shows the different nomenclature given to alkali-activated binders as well as the research group that identified them.

Table 2.2 - Different terms linked to alkaline cementitious materials [50].

Terms	Investigator
Alkali-slag cement or alkali-activated slag cement	Purdon (1940)
Soil Silicates	Glukhovsky (1957)
Geopolymers	Davidovits (1973)
Alkali-activated cement	Narang, Chopra (1983)
F-Cement (slag–alkali–superplasticizer)	Forss (1983)
Gypsum-Free Portland Cement	Odler, Skalny, Brunauer (1983)
SKJ-Binder	Changgo (1991)
Geocements	Krivenko & Associates (1991)
Alkaline Cements	Krivenko (1994)

2.1.3. Alkali-activation mechanism: a conceptual model

The exact mechanism of alkali-activation, although extensively explored and investigated, is not yet completely defined: the usage of various types of precursors generates significant modifications in the chemistry of the reaction, changing the quality and properties of the final compounds [56]. For this reason, there are several studies and papers in the literature in which many authors have attempted to identify and describe the various phases of alkali-activation and what occurs during them [114]. Purdon in 1940 was the first to propose a process of alkali-activation involving the mixing of sodium

hydroxide (NaOH) with a variety of minerals and glass rich in silicon and/or aluminium including blast furnace slag. He discovered that the involved mechanism takes place in two steps [59]:

• First: the release of silica, alumina, and lime.

• Second: formation of hydrated calcium silicates, aluminates as well as the generation of alkali solution.

In other words, it was proposed that the hardening stage involves dissolving Si and Al in an alkaline medium, such as a sodium hydroxide solution, followed by the precipitation of calcium silicate or aluminium hydrate, indicating that alkali hydroxides serve as catalysts in this process [115].

Glukhovsky developed a three-stage concept for alkali activation of aluminosilicate materials, comprising "destruction coagulation," "coagulation-condensation," and "condensation-crystallization" as primary steps. The initial disaggregation phase is based on the disintegration of the starting material's Si-O-Si and Al-O-Si covalent bonds. The disaggregation occurs only when the ionic force is changed by adding electron donor ions, as when the pH of the medium solution rises. The second step involves the build-up of disaggregated products that coagulate into a coagulated structure, leading to polycondensation, which is catalysed by the OH- ion. Aluminates have a function in this reaction as well; whereas they behave as catalysers in the destruction phase, they are structural components in the second and third steps. The last (third) step involves the formation of a condensed structure, which includes the formation of alkali-activated network structures [42]. The alkali-activation reaction begins when aluminosilicate material is dissolved in an alkaline medium, the silicon-oxygen and aluminoxane bonds are broken, besides the dissolved aluminate monomer and silicate salt diffuse from the surface of the solid particles to the intercellular spaces of the particles. The alkali silicates in the activator react with the aluminate monomer and silicate salt to form the gel phase. The water generated during the polymerization reaction is progressively released when the gel phase hardens. Following Purdon's initial studies and based on the current literature review [42], Figure 2.1. presents a scheme of general models for the alkali activation of alumino-siliceous materials [114].
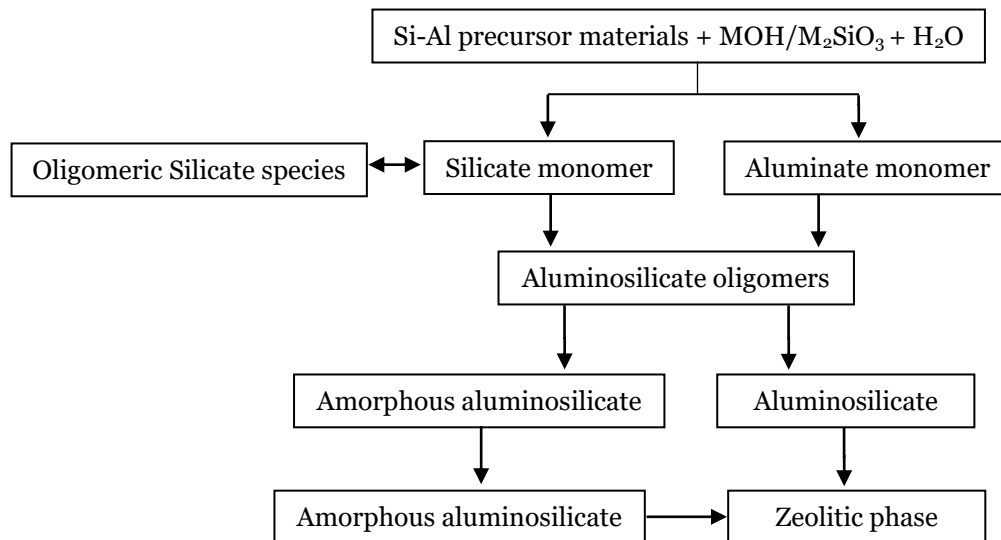
Figure 2.1 - *Scheme for the mechanism of the alkali-activation.*

Where M is a monovalent alkali-action, like sodium or potassium.

2.1.4. Alkali-activated materials versus Portland cement

Portland cement (OPC) is the main component of concrete. This binder combines aggregates and water to form a solid, compact, and mechanically sustainable framework. However, excessive OPC usage is a major concern, since the manufacture of OPC is energy-intensive, and it is easy to understand, considering the massive quantities of concrete produced. Cement currently contributes to a significant portion (8% – 10%) of worldwide carbon dioxide (CO_2) [116][117] as well as nitrous oxide (N_2O), and methane (CH_4) emissions. Both of these challenges have emerged as a source of worldwide concern. At the same time, the world moves towards the concept of alternative sustainable development. Alkali-activated materials (AAMs) are the widest categorization, which includes basically any binder system formed from the interaction of an alkali metal source (solid or liquid) with a solid alumino-silicate powder. This solid source can be a calcium silicate, as in the alkali-activation of more common clinkers, or it can be a more aluminosilicate-rich precursor, such as metallurgical slag, natural pozzolan, fly-ash, or bottom ash. Alkali sources can include alkali hydroxides, silicates, carbonates, sulphates, aluminates, or oxides - in short, any soluble material that can deliver alkali metal cations, raise the pH of the reaction mixture, and speed up the dissolving of the solid precursor [100]. The various sources of the alkaline activation of aluminosilicates can be explained by diverse factors. The most important are those relating to the search for alternatives to the OPC manufacturing process, which has a significant environmental impact and produces significant greenhouse gas emissions (primarily CO_2) from various generation sources during the manufacturing process.

Alkali activation technology has expanded substantially throughout the world, with over 100 active research centres (academic and commercial) currently functioning worldwide, with extensive research and development work taking place on every inhabited continent. Much of this work has focused on

developing materials with acceptable performance based on the specific raw materials available in each location; there is a large number of technical publications available in the literature that report the basic physical and/or microstructural properties of alkali-activated binders derived from specific combinations of raw materials and alkaline activators [100]. Alkali activation technology also provides the opportunity for the utilisation of waste streams that might be of significant benefit for the new cement-free blending material such as slags, and mine tailings wastes [118]. It has shown that these materials can be effectively converted into valuable materials by alkali activation, while they are of little or no benefit as mineral additions to OPC.

The interest in comparing alkali-activated materials (AAMs) with Portland cement binders (OPC) comes particularly from arguments concerning durability and strength retention, in addition to the strong thermal and fire resistance properties. Although C-S-H gel is a key element of both Portland cement paste (OPC) and alkali-activated binders (AAB), concluding that its presence is responsible for durability is quite incorrect. The degree of gel cross-linking appears to be connected to environmental stability, and the presence of lower amounts of calcium and high levels of tetrahedral aluminium (usually charge-balanced by alkalis, as in the case of zeolites) is extremely favourable in this area [119]. Thus, the examination of some ancient materials may be used to derive conclusions about the durability of modern types of cement, and these tendencies appear to remark favourably on the fundamental chemical durability of aluminosilicate-based (as opposed to calcium silicate-based) binders.

2.1.5. The global business of alkali-activated materials

Alkali-activated materials' commercial future, similar to that of many other alternative concrete binders, depends not only on technological preparedness but also on economic and societal suitability. Although standardisation is an essential aspect of commercialization, it is just a tiny portion of the whole process (contrary to common belief) [43]. Alkali-activated binders have a wide range of current and potential applications. Some alkali-activated binder uses are still in the early stages of research, while others have already been industrialized and commercialized. Alkali-activated cement is the most common application in terms of volume and it has been commercialized in many countries, being Australia the most notable due to Earth Friendly Concrete [120], but it has also been manufactured and studied by several other international research institutes. Alkali-activated concrete was developed by Zeobond Group in collaboration with several teams of business partners that are driving the commercialization of alkali-activated material technologies. These include, for instance, the Centre for Sustainable Resource Processing, which has been making progress in this field over the past decade in Melbourne, Australia, to overcome the barriers of alkali-activated concrete commercial's adoption under the name E-Crete cement binder using a combination of fly ash, slag, and alkaline activators. This project, which was finished in 2009, comprised the restoration of a huge embankment retaining wall at Melbourne's Swan St Bridge was cast in-situ to demonstrate that alkali-activated materials are not limited to pre-cast applications (Figure 2.2). VicRoads chose E-Crete for this project because of its high-profile position and stringent specifications. For this application, 40 MPa structural concrete [121] was required, with longer slump retention and the capacity to be pumped as criteria. The steel

reinforcement was monitored throughout time with equipment put on the wall. On the other hand, National standards such as the European cement standard, are more prescriptive, thus requiring concrete to use a Portland cement-based binder.

Figure 2.2 - E-Crete retaining wall at the Swan Street bridge in Melbourne, Australia [121].

To prove that alkali-activated materials are not restricted to pre-cast applications, the Westgate Freeway Alliance utilized E-Crete in 25 MPa walkways on Brady St in Port Melbourne (Figure 2.3). In 2010, VicRoads approved E-Crete grades 20, 25, and 32 MPa in the standard for ordinary concrete paving and non-structural usage in footpaths and kerb and guttering [122]. Several parties were involved in this project, including VicRoads, Melbourne City Council, Port Melbourne City Council, and the Alliance partners.

Figure 2.3 - In-situ production of E-Crete footpaths at Brady St in Port Melbourne, Australia [122].

In Europe, the Dutch company ASCEM has commercially been putting together pre-cast products; concrete pavement units of 2 x 2m were manufactured, and pipes using patented fly-ash reprocessing technology to produce the necessary precursors for their products under the brand name Stelcon® [123]. This was accomplished with the help of a machine that compacts earth-moist concrete to create concrete pipelines. The uniformity and green body strength of pipes are critical during the manufacturing process. The green pipe is promptly removed and brought to a climate room, where it is kept. The pipes were successfully constructed and were hauled outdoors the next day for storage as shown in Figure 2.4.
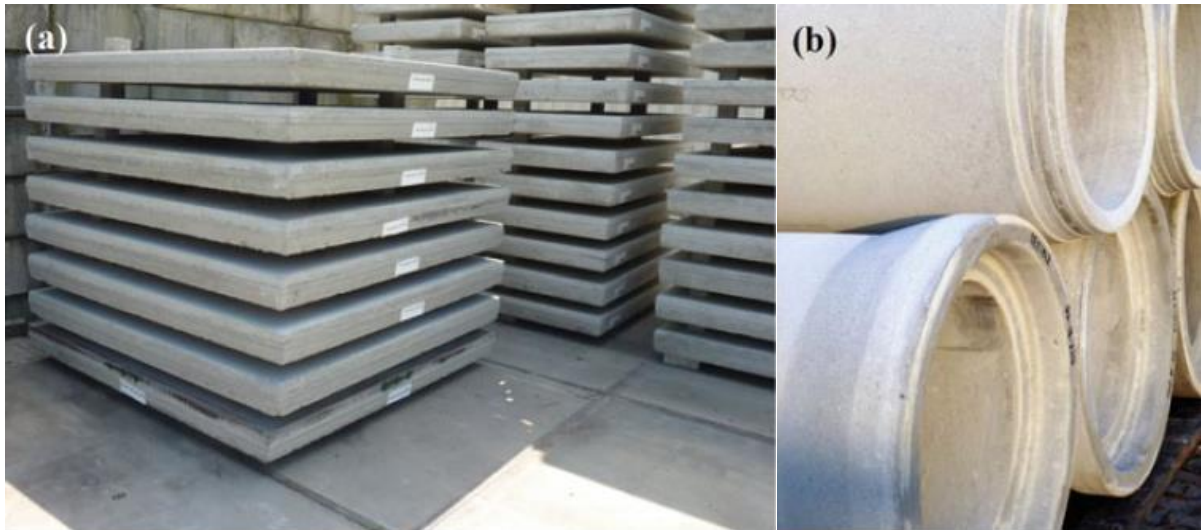
Figure 2.4 - *Products in outdoor storage: (a) slabs; (b) pipes [123].*

2.1.6. Advances in alkali-activation of non-conventional materials

The use of non-conventional materials in the building and construction industry is attracting more and more attention, and their introduction has brought both possibilities and problems to academics and engineers throughout the world. Currently, innovative research focuses on the type of precursors through the alkali-activation technology (the potential of using non-conventional materials). Academics and engineers have spent the last three decades or more conducting substantial studies to industrialize alternative technologies to build a more sustainable structure. Bakharev (2005), Bilodeau and Malhotra (1998), Bilodeau et al. (2001), Cheng and Chiu (2003), Davidovits et al. (2001), Cheng and Chiu (2003), Davidovits et al (1990), Davidovits (1994), Hardjito and Rangan (2005), Li et al. (2004), Malhotra (2002), Wallah and Rangan (2006), Rangan (2008), just to name a few, have begun looking for replacement ingredients to replace OPC completely or partially in concrete manufacturing.

In the EU, mining and quarrying wastes represent around 28% of all wastes generated from industrial activities and residences [124]. The majority of mining and quarrying wastes, as well as other industrial wastes, can be used in earthworks and buildings, particularly the coarser fractions into asphalt pavements and concrete [125]. They can also be used as a raw materials in industrial applications when the high value of the product does not restrict it from being reused due to transportation costs [126]. Other research has been focusing on producing polymer-based composite materials with technical-artistic value added [127].

2.1.7. Precursors

Starting material plays a significant role in the formation of alkali-activated and geopolymer materials. Numerous research has been carried out in order to develop various methods to improve the durability of alkali-activated cement and concrete. A wide range of materials is presently being used for the alkali-activation (geopolymerization). Various pozzolanic, supplementary cementitious materials (SCM), chemicals, and mineral additives are examples of these materials [128].

Theoretically, the basic requirements for alkali-activation are materials rich in Si (e.g., fly ash as well as rice husk ash) along with materials rich in Al (e.g., kaolin) to undergo alkali-activation (geopolymerization). Some other materials such as Ordinary Portland cement (OPC), kiln dust, etc. can also be utilized as a reactive filler material or a setting additive which helps in the development of good mechanical properties [129]. So far, the following are some of the most important materials used for the alkali-activation (geopolymerization) investigations. Furthermore, waste materials such as slag, fly ash, rice husk-ash, tungsten mining waste mud, as well as calcined clays (Metakaolin) are utilized as the primary precursors, which contain unreacted, amorphous silica and alumina [130].

2.1.7.1. Metakaolin

Metakaolin (MK) has often been used as a reference to understand and improve the knowledge of alkali-activated binders [131][132]. Calcined clay -or metakaolin- is produced by the dihydroxylation of the mineral clay kaolinite between 650° C and 800° C. Both kaolin and kaolinite are naturally occurring minerals. It is a pozzolanic substance made up of smaller particles than those of Portland cement. Davidovits utilised metakaolin in his research as the main precursor and named the produced material as geopolymer. Metakaolin is substantially more reactive than other pozzolans (such as fly ash, which is equivalent to silica fume), thus assisting in the acceleration of concrete hardening processes. Metakaolin enhances concrete's early strength, making it acceptable for precast applications [56]. It is like most other pozzolans, and it improves the long-term strength of the concrete by minimizing the impacts of alkali-silica reactions (which may severely destroy concrete) and enhancing chemical resistance. It also lightens the colour of concrete, allowing the incorporation of a coloured tint [133].

The production of metakaolin is more expensive than other supplementary cementitious materials (SCMs) because it must be activated by heating the raw material at relatively high temperatures. Unless, unless adequate water-reducing admixtures are utilized, the use of metakaolin can increase water consumption during concrete production by over 20%. Metakaolin-based geopolymers have less field experience than other supplementary cementitious materials (SCMs), and their use (as with silica fume) appears to be limited to high-strength lightweight concretes and the precast/poured mould sector due to its limitations [134].

2.1.7.2. Fly ash

Fly ash is a by-product of the combustion formed during electricity generation. It consists of the remnants of clays, sand, and organic matter present in the coal, which is collected by electrostatic precipitators in the chimney of a furnace. Pulverized Fly Ash (PFA) is categorized into two categories: Class C fly ash and Class F fly ash. The quantity of calcium, silica, alumina, and iron in the ash is the main difference between these classes [135].

•Class C – Fly ash normally derives from lignite or sub-bituminous coal. This class of fly ash, besides having pozzolanic properties, also has some cementitious properties. Furthermore, this fly ash has a high CaO content [136].

•Class F – Fly ash is a type of ash that is often formed when anthracite or bituminous coal is burned. This fly ash contains siliceous or siliceous and aluminous material, which itself possesses little or no cementitious value. However, this siliceous or siliceous and aluminous material may, in its finely divided form and the presence of moisture, chemically react with sodium hydroxide at normal temperatures to form cementitious compounds [137].

2.1.7.3. Ground granulated blast-furnace slag

Among many of the various types of slags that can be chemically activated, ground granulated blast furnace slags (GGBFS) are certainly the most common and are used not only in the field of chemical activation but also in the cement and concrete industries [138]. GGBFS sometimes referred to as alkali-activated slag (AAS) is mainly an industrial by-product resulting from iron and steel manufacture, generated in the blast furnace and rapidly cooled, and is characterised by appropriate amounts of CaO (30% - 50%), SiO_2 (28% – 38%), Al_2O_3 (8% – 24%), MgO (1% – 18%), and Fe_2O_3. GGBFS has many advantages in the concrete industry, including being relatively not expensive, maintaining excellent thermal properties, and high resistant tendency to chemical attacks [139]. Furthermore, major components of the slag products include calcium oxide, silicon dioxide, aluminium oxide, and magnesium oxide which are mostly present in commercial silicate glasses. Typical slag products are granulated, ground, and mixed with 3.5 - 5.5 percent water glass or sodium hydroxide. Alkali-activation produces a low-basic, highly amorphous calcium silicate hydrate (C-S-H) gel product possessing high aluminium content. Its chemical composition and high reactivity make it a suitable material for alkali activation [38][66]. The chemical component of GGBFS consists mainly of the $CaO–SiO_2–MgO–Al_2O_3$ system and is described as a mixture of phases with compositions resembling Gehlenite ($Ca_2Al[AlSiO_7]$) and Åkermanite ($Ca_2Mg[Si_2O_7]$), as well as a depolymerized calcium aluminosilicate glass [66].

According to an investigation carried out by several authors, saturated GGBFS pastes have much larger porosity volumes and chemical shrinkage than ordinary Portland cement (OPC) which is a substantial issue during setting. Drying shrinkage results from hydration heat and is increased with an increase in dosage and modulus of water glass activators [140][141]. Alternatively, the degree of hydration reaction is increased as the alkali concentration in the mixed paste increases. Additionally, reduction in pore volumes occurs as the alkaline concentration in the paste mix increases improving the microstructural properties of the C-S-H product. Meanwhile, shrinkage in GGBFS pastes is more significant than OPC pastes by comparison, but GGBFS sustains much higher ultimate strength and remains a sustainable raw material for commercial usage [142].

2.1.7.4. Rice husk ash

Rice husks (also known as rice hulls) are the firm protective coatings that protect rice grains throughout the growing season. Rice husk ash (RHA) is a kind of sustainable biomass energy that is created by burning rice husk primarily for the creation of power. It can be used as a construction material, fertilizer, insulating material, or fuel. RHA is another pozzolanic substance made from rice husk combustion. When entirely burned, the ash can have a Blaine number of up to 3,600, whereas cement has a Blaine number of between 2,800 and 3,000, indicating that it is finer than cement [143][144].

The major component of ash is silica (which comprises 90 - 95 wt. %). This fine silica will produce concrete that is extremely compacted. In addition, ash is an excellent heat insulator. Because of its fineness, ash is an excellent choice for sealing fine fractures in civil constructions, where it may penetrate deeper than a traditional cement-sand combination. It exists mostly in amorphous and partially crystalline phases (although the ratio of amorphous to crystalline phases of silica is affected by the time and temperature of burning), with carbon persisting as the principal contaminant and other trace elements such as K and Ca [145].

2.1.7.5. Waste glass powder

Glass is a non-crystalline amorphous solid material that is generally transparent and has been widely used in technological, practical applications, and decorative usage. The type of glass made is based on the chemical compound silica, silicon dioxide, the main component of sand. Glass contributes significantly to household and industrial waste due to its weight and density. Nowadays, non-recyclable waste glass is becoming a concern for solid waste management in several local regions of the European Union (EU). The majority of non-recyclable glass is the mixed colour broken glass manufactured by the bottling industry and disposed of in landfills. Furthermore, because glass is a non-biodegradable substance, dumping glass in landfills has a negative influence on the environment. At the same time, due to the enormous demand for pozzolanic/precursor materials used in cement and concrete production by the construction industry the available pozzolanic/precursor resources will be insufficient worldwide, thus being necessary to the search for alternatives to meet the growing needs of concrete and cement production. However, according to Eurostat, 18 million tonnes of glass waste was generated in 2012, with just 35% of that being recycled [124].

Additionally, this massive volume of waste glass available for reuse has attracted much interest throughout the world due to the increased disposal costs and environmental concerns, besides, pushing the construction industry to use waste glass in concrete as a partial replacement of fine or coarse aggregates. However, due to the strong reaction between the alkali in cement and the reactive silica in the glass, studies of the use of waste glass in concrete as part of the coarse aggregates were not satisfactory due to a drop in strength caused by simultaneously occurring expansions [146]. Furthermore, Caijun Shi et al., 2007, conducted an additional investigation of glass, revealing that, despite the traditional alkali-silica reaction theories used to explain the expansion of cement concrete

containing mixed waste glasses as aggregates, the expansion phenomena are different from those of conventional alkali-silica reaction caused by certain aggregate types [147]. Additionally, Figg, in 1981, noticed some differences between alkaline-silica reaction expansion caused by natural aggregates and that caused by glass aggregate [148].

Glass particle size has recently been discovered to be a critical factor for alkali-silica reaction to occur [149]. Particularly, aggregate fineness favours alkali-silica reaction expansion which is a surface area dependent phenomenon. It seems that there is a minimum particle size, depending on the structure of the glass, where the maximum expansion occurs. Thus, it was found that if the glass was ground to a particle size of 300 μm or smaller, the alkali-silica reaction induced expansion could be reduced [147]. In fact, data reported in the literature show that if the waste glass is finely grounded, under 75 μm, this effect does not occur and the structural integrity of mortar containing fine glass is guaranteed. It is also well known that typical pozzolanic materials might feature high silica content, an amorphous structure and have a large surface area. Last but not least, Luis Oliveira et al. 2012, conducted research using waste glass and red-clay ceramic as cement mortar components and found promising results, thus showing a high potential for the utilisation of waste glass in concrete and mortar as a partial replacement for expensive material such as PFA and cement [98].

2.1.7.6. Mining wastes

The mining and quarrying sector is the second-largest generator of rubbish in the EU 27, accounting for 26.3 percent of total waste generated. It has the potential to contain considerable amounts of hazardous compounds. Mining waste is created as a result of the extraction and processing of mineral resources. It comprises topsoil overburden (which is removed to obtain access to mineral deposits), waste rock, and tailings, among other things (after the extraction of the valuable mineral). Data from SMART Trash partners' respective EU Member States demonstrate that mining and quarrying operations contribute very little to national total waste creation, with contributions ranging from 0% to less than 2% in 5 out of 6 EU Member States [150]. Mine tailings are responsible for the majority of environmental problems associated with the extractive sector, with hazards growing as the number of low-grade ore mined increases and extreme weather events become more common. Tailings recycling in raw-material-intensive applications is an intriguing alternative to the costly tailings management and restoration efforts. The use of mining waste to produce alkali-activated binders includes the influence of calcination processes in the reactivity of the mine waste, as well as how the mix design parameters influence strength gain besides to what is the nature of the reaction products formed in the new binders. It also includes some physical and mechanical properties particularly the adhesion between the mine waste binders and ordinary Portland cement (OPC) concrete. In addition, it describes durability performance from abrasion [151].

Currently, large amounts of inorganic waste from mining and quarrying are being generated each year across the world, and these raw waste materials have a range of utilisation in building construction industries, in addition to other products, such as waste glass [29]. Therefore, relevant research is being conducted to produce alkali-activated materials from mining waste, and the focus is to reuse the

waste material by integrating it into the manufacture and development of new materials and, at the same time, preserve the environment [28][151]. Several types of research have been undertaken on the reuse of mining and quarrying waste indicating the significant potential of recycling waste materials. Since the majority of mining and quarrying waste comes from the grinding of rocks, it may be utilized in buildings and earthworks, especially the coarser fractions. According to research conducted, the potential for reusing mining and quarrying waste on a national scale is limited by transportation governments and economic factors, and the main applications included are in asphalt pavements and aggregates for concrete productions [152][153][154].

The University of Arizona in the United States has undertaken further ground-breaking research on the alkali-activation of mining waste. A feasibility study on using copper mine tailings for the production of environmentally friendly bricks using alkali-activation technology was successfully completed. The novel approach does not involve clay or shale, nor does it require high-temperature kiln fire comparable to the conventional bricks production process, resulting in considerable environmental and ecological benefits. The findings revealed that copper mine tailings might be utilized to make eco-friendly bricks using alkali-activation technology in order to fulfil ASTM criteria [155]. Furthermore, at the University of Arizona in the United States, an investigation on the use of fly ash-modified mine tailings as a building material through alkali-activation was performed. Due to the extremely high Si/Al ratio of the mine tailings, class F fly ash was used to adjust the Si/Al ratio. Adding fly ash to mine tailings improved the compressive strength results of the alkali-activated materials produced. The addition of fly ash to mine tailings improved the impact primarily by lowering the mix's Si/Al ratio to the range of the optimal Si/Al ratio [156]. Some forms of mining waste with the potential of alkali-activated precursors are reviewed in Table 2.3.

2.1.8. Activators

The alkali-activation requires chemical activators. The alkalis component as an activator is a compound of the elements from the first group in the periodic table, containing water, silica, and alkalis. The chemistry of the alkaline activating solutions that can be coupled with aluminosilicate precursors to produce new cementitious materials is required [42]. As a result, such materials are also called alkali-activated aluminosilicate binders or alkali-activated cementitious materials [50]. The main activators utilized are Sodium/Potassium hydroxides (SH/PH) and Sodium Silicate (SS), known as water glass.

Sodium hydroxide (SH) also known as lye and caustic soda, is an inorganic compound with the formula (NaOH) and sodium silicate (SS), also called water glass ($nSiO2Na2O$) are most frequently used either individually or as a blend. However, Potassium Hydroxide (KOH) and potassium water glass ($nSiO_2K_2O$) are also fairly common [161] as well as Calcium Hydroxide ($Ca(OH)_2$), also known as slaked lime [132]. SH is the most used due to its wide availability and low viscosity. Sodium hydroxide (SH) concentration is a fundamental parameter because its influences the mechanical properties of alkali-activated materials [162].

Table 2.3 - *Wastes with the potential for alkali-activated precursors from the scientific literature.*

Wastes (Mineral)	Ideal stoichiometry of the mineral	Classification	Reactivity in alkali-activation	Ref.
Iron Ore	SiO_2	Magnetite, titanomagnetite, massive hematite	-	[157]
Copper	Copper (Cu)	Metals and intermetallic Alloys, Copper-cupalite family	-	[158]
Tungsten	$KAl2(AlSi3O10)(F,OH)2$	Phyllosilicate/Mica group (2:1 layer lattice aluminosilicate)	Excellent, calcination at 950 °C, 120 min	[29]
Chromite Ore	$(Fe, Mg)Cr_2O_4$	Oxide minerals Spinel group Spinel structural group	-	[159]
Vanadium	SiO_2	Vanadium hydrate mica	-	[160]
Lepidolite	$K(Li, Al)_3(Si, Al)_4O10(F, OH)_2$	Phyllosilicate/Mica group	-	[142]
Kyanite	Al_2SiO_5	Neosilicate/Al_2SiO_5 group	-	[142]
Sillimanite	Al_2SiO_5	Neosilicate/Al_2SiO_5 group	-	[142]
Spodumene	$LiAlSi_2O_6$	Inosilicate/Sodium pyroxene series	-	[142]
Andalusite	Al_2SiO_5	Neosilicate/Al_2SiO_5 group	-	[142]
Celsian	$BaAl_2Si_2O_8$	Framework silicate	-	[142]
Grossular	$Ca_3Al_2(SiO_4)_3$	Neosilicate/Garnet group	-	[142]

2.1.8.1. Nature and concentration of the activators

Sodium hydroxide (SH) and water glass sodium silicate (SS) are commonly used for the activation of raw materials and the dissolution of silica and aluminium is directly dependent on the concentration of NaOH. A higher concentration of hydroxide ions improves the solubility of aluminosilicate [123]. Several authors have proved an enhancement of mechanical strength through an increase of the NaOH solution concentration. However, an excessive concentration of sodium hydroxide has the opposite effect on the mechanical features.

Panias et al. 2007 verified that the compressive strength of fly-ash alkali-activated binder is not a monotonous function of NaOH concentration, since a decrease in strength occurs going from 6.6 M to

10.25 M, while an increase has been found between 4.47 M and 6.6 M [110]. Furthermore, the properties of the alkali-activated materials (AAMs) may also be deeply influenced by the presence of sodium silicate (SS) in the activating solution, which provides the addition of soluble silica to the mixture. Several authors have supported the idea that the use of sodium silicate (SS), blended with sodium hydroxide (SH), has a positive effect on the mechanical features of the produced materials. However, the addition of water glass in the activating solution affects not only the mechanical properties but also the durability and the physical features of the final materials [163].

2.1.8.2. Precursor/Activator ratio

According to several studies, the type and concentration of the activator were found to be the most important parameters in the alkali-activation process. Besides, the fineness of the precursor was the most essential factor in terms of physical properties [164][165]. The precursor-to-activator (P/A) ratio between the solid powder (precursors) and the liquid component (chemical activator and water) plays a fundamental role in the alkali activation, thus affecting the mechanical performance and physical properties significantly. The higher water content in the mixture is directly related to an increase of total porosity, as well as to strength decrease. However, the adequate presence of liquid is required for a good outcome of the dissolution phase, since it plays the role of the medium through which dissolved aluminosilicate ions can move [103].

According to Panias et al. (2007), water content has been demonstrated to be an important parameter in the synthesis of fly ash-based geopolymers for mechanical strength improvement. Water is crucial throughout the dissolution, polycondensation, and hardening stages of geopolymerization since reducing the amount of water used in the production of geopolymers increased their compressive strength. Besides, the amount of sodium hydroxide was found to have a substantial impact on the compressive strength, whereas the concentration of sodium hydroxide in the aqueous phase of the geopolymeric system influences both the dissolving process and the bonding of the solid particles in the final structure. Moreover, the degree of sodium silicate solution used in the production of geopolymers was shown to have a significant influence on the compressive strength achieved. The concentration of soluble silicate and the dominant silicate species in the geopolymeric system is controlled by a sodium silicate solution, which improves the mechanical strength of the materials generated [110].

2.2. Industrial and mining waste production

Each year, a vast amount of industrial waste is generated from different sectors including mining, power and energy, and construction. Several countries have conducted inquiries about mining waste materials. The key factors for undertaking such inquiries are the need to conserve limited natural resources, reduce environmental pollution by mitigating emissions and conserve energy [166]. In European countries, mining and quarrying wastes represent 15% of total waste in Western Europe and 31% in Eastern Europe according to the most recent Eurostat data on the total waste generation in the EU-28 for 2012 (see Figure 2.5). The mining and quarrying industry in Western Europe is the most

concentrated and active in the world. It also makes a significant contribution to the European economy. The extractive sector employs over 500 000 people and produces around 3 billion tonnes with a value of around $50 billion. Over 20% of the European Union's Gross Domestic Product is projected to be dependent on the extractive industry in some way [14]. Mine tailings present a potential precursor source for alkali-activation since the most common abundant minerals on the Earth's crust are aluminosilicates (i.e., tungsten), which is also reflected in the compositions of the tailings. However, the alkali-reactivity of the mine tailings is generally low, and it presents the most influencing factor in tailings-based alkali activation. Thus, pre-treatments are required in order to enhance reactivity.

Nowadays, for a circular and stronger green economy, a new ambitious circular economy package was adopted by the European Commission (EC) to help businesses and European Consumers make the transition in which resources are used more sustainably [167]. The significant amount of industrial waste deposits has led to growing concerns about their ecological and environmental impacts, such as the case of mining wastes [11]. Furthermore, the public and the consumer prefer "green" products and processes. For that research and development activities are focused on the development of new products based on industrial wastes, such as the case of mining wastes. Thus, in order to maintain natural biodiversity, the scientific community must make significant efforts to find alternative applications for mining and quarrying waste.
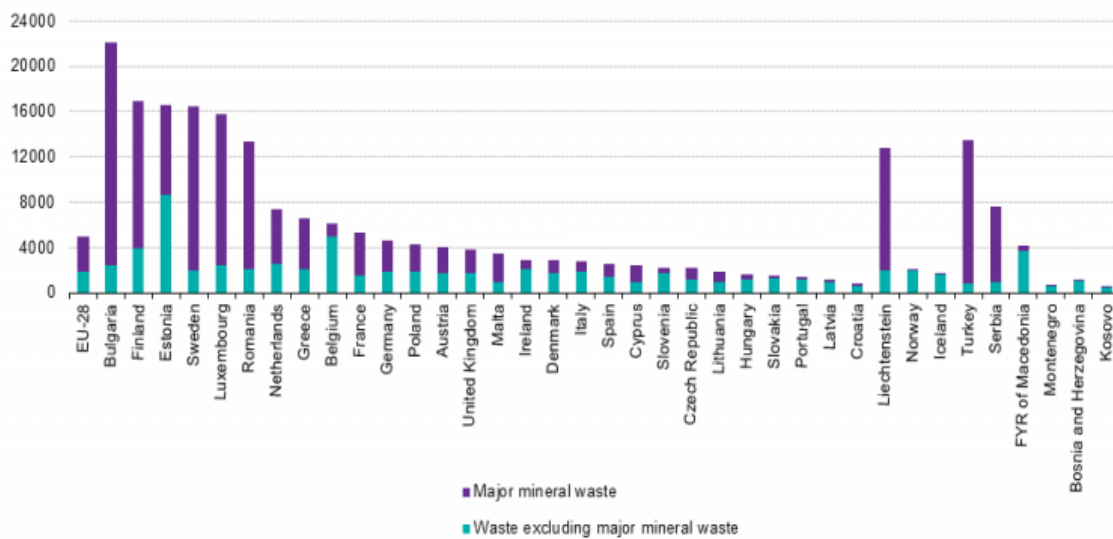
Figure 2.5 - Waste generation (including mineral waste), EU-28, 2012.

2.2.1. Alkali-activation using tungsten mining waste

A pertinent example is the Panasqueira tungsten mining waste mud (TMWM) produced at the mining exploration, in Covilhã, district of Castelo Branco, Portugal. This waste has good reactivity with alkaline activators such as calcium hydroxide, due to its high alkali concentration. The mechanical strength of the cement produced from this waste, initially cured at room temperature, was later improved by mixing the waste mud (TMWM) with different sources of silica (river sand (RS) and

amorphous grounded waste glass (WG)) and cured at moderate temperatures [168][169][170]. The reuse of mining waste is highly esteemed nowadays since the advantages of these residues lie in the fact that they have a very high alumina-silicate content, and for this reason, they can be used to produce alkali-activated materials.

2.2.2. The Panasqueira tungsten mining waste mud

The Panasqueira mine is situated in the centre of Portugal, in the district of Castelo Branco, on the southern slope of the Serra da Estrela mountain range, the highest in the Portuguese mainland, approximately 300 km northeast of Lisbon and is 200 km southeast of Porto. In 1886, the first prospecting license was issued at Panasqueira, and two years later, the first reference to wolframite was made. The underground mine at Panasqueira was created in 1896 to mine tungsten. And it has been operating almost continuously since then, except for a brief period at the end of World War II and a second shutdown in the mid-1990s. Cabeco do Piao (now Rio) was the first place where wolframite ore was discovered, and the first sites mined near current workings were Vale das Freiras, Vale da Ermida, and Barroca Grande. The separate concessions were consolidated into a single mining region known as the "Couto Mineiro da Panasqueira," which encompassed the same land as the current concession [171]. Between 1947 and 2014, approximately 31 million tonnes of rock were mined, which generated approximately 111,123 tonnes of tungsten concentrate, 5,383 tonnes of tin concentrate, and 31,702 tonnes of copper concentrate [172]. Figure 2.6. presents a panoramic view of the Panasqueira tungsten mining complex, as well as of the waste mud deposits.

The research focused on the reuse of waste materials (mining and quarrying) by integrating them into new materials manufacture such as typical applications including its use in asphalt pavements [152], in addition to other materials, such as metakaolin [129], coal fly ash and waste glass [173]. The reuse of mineral wastes as precursor materials for alkali-activated binders is most promising by the EU and other countries, from an environmental, technical, and economic point of view [174][17]. Tungsten mining waste mud (TMWM) is being used to produce alkali-activated binders as a new cementitious material obtained from dehydroxylated mine waste powder mixed with minor quantities of calcium hydroxide that can be easily activated with sodium hydroxide and water glass (Sodium silicate) solutions to produce an alkali-activated binder [115]. Little research has been conducted on this cementitious material, although so far it was noticed that TMWM has low water absorption, a very high early-age strength, and very good adhesion characteristics in comparison to OPC [175]. Research carried out by Torgal et al. 2008, on abrasion and acid resistance, showed that alkali-activated Tungsten-based binders presented a low level of weight loss in comparison to OPC-based binders, which presented severe weight loss. Furthermore, TMWM binders showed good acid resistance, higher than OPC binders [28]. According to Torgal et al. 2008, thermal treatment is responsible for increased reactivity in tungsten mining waste mud (TMWM). The X-ray diffraction (XRD) results revealed that the mining waste utilized was mostly muscovite and quartz [174].

Figure 2.6 - Panasqueira Tungsten mine, Covilhã, Portugal; (A): Panoramic view of the mine complex, and (B): waste mud deposits.

First, this research attempted to develop a new alkali-activated binder (AAB) by reusing waste mud from a tungsten mining exploration that presents very good reactivity with alkaline activators and calcium hydroxide, for high alkali concentrations and curing at room temperature. Later, improved alkali-activation conditions were found by combining mining waste mud with different sources of silica (namely, amorphous ground waste glass (WG), and river sand (RS), in addition to others) and cured at moderated temperatures, as presented in Table 2.4.

The alkaline activation of other alumino-siliceous industrial by-products is widely known to yield binders which make their properties comparable or even stronger and more durable than

Conventional Portland Cement [16][17]. Moreover, cost comparisons show that this alkali-activated cement repair solution is by far the most cost-efficient [168]. The possibility to replace Ordinary Portland cement (OPC) with those new alkali-activated binders (AABs) using tungsten mining waste mud (TMWM) was investigated by many researchers by enhanced environmental and durability performance [151][179].

Table 2.4 - Compressive strength (Rc) of alkali-activated binders using Panasqueira mining waste mud (TMWM).

Author	Year	Mix composition / (Curing conditions)	Rc (MPa)	Ref
F. Pacheco-Torgal	2006	90 % Mining waste mud[c)] + 10 % Calcium hydroxide Sodium hydroxide (16M) + Sodium silicate (28 days curing at room temperature)	30	[176]
F. Pacheco-Torgal	2008	90 % Mining waste mud[c)] + 10 % Calcium hydroxide Sodium hydroxide (24M) + Sodium silicate (28 days curing at room temperature)	28	[28]
F. Pacheco-Torgal	2009	90 % Mining waste Mud[c)] + 10 % Calcium hydroxide Sodium hydroxide (24M) + Sodium silicate (28 days curing at room temperature)	28	[168]
J. Centeio	2011	65 % Mining waste Mud[c)] + 35 % Sand Sodium hydroxide (10M) + Sodium silicate (3 days at 60°C curing temperature)	11	[177]
G. Kastiukas	2016	80 % Mining Waste Mud[n)] + 20 % Milled Glass Sodium hydroxide (10M) + Sodium silicate (24h at 60°C then curing at room temperature and testing at 28 days)	22	[31]
I. Beghoura et al.	2017	80 % Mining Waste Mud[n)] + 10 % Milled Glass + 5 % Metakaolin + 5 % Cement Sodium hydroxide (10M) + Sodium silicate (24h at 60°C then curing at room temperature and testing at 28 days)	19.5	[114]
N. Sedira et al.	2018	50 % TMWM + 50 % Red CBW Sodium hydroxide (10M) + Sodium silicate L60 (24h at 60°C then curing at room temperature and testing at 28 days)	59	[178]
I. Beghoura et al.	2019	70 % Mining Waste Mud[n)] + 20 % Milled Glass + 10 % Metakaolin Sodium Hydroxide (10M) + Sodium Silicate (24h at 60°C then curing at room temperature and testing at 28 days)	16.10	[165]

c)–calcined   n)–non-calcined

2.3. Alkali-activated foamed materials

Research in the field of alkali-activated materials (AAMs) has led to the development of several new or improved types of alkali-activated foamed Materials (AAFMs) [180][181]. Recently, a novel idea which involves the production of alkali-activated foamed materials (AAFMs) has been suggested [182]. These new foamed materials (FMs) combine the performance and benefits of energy savings (a lower

carbon footprint) obtained with alkali-activated foamed materials (AAFs) with the cradle-to-gate emissions reductions obtained [51][23] by using alkali-activated binders (AABs) derived from an industrial by-product, like fly ash [183] as well as foaming agents. Currently, foamed concrete is an innovative product for the construction industry [184]. It differs from conventional concrete, since it has a very low density, usually ranging between 300 and 1800 kg/m^3, and compares favourably with the density of normal concrete at approximately 2400 kg/m^3 [25]. It has several additional attractive advantages such as good thermal and acoustic insulation [185], better fire resistance, and ease of fabrication [186]. Besides, in order to reduce the density of the foamed alkali-activated materials [22], holes or lightweight aggregates [187][188] can be added for such a purpose.

The typical approach for the fabrication of alkali-activated foamed materials is borrowed from the procedure used in the cement industry, which consists of the addition of an aqueous alkali-activated slurry and other components (such as Al powder) that are capable of generating in-situ gaseous H_2 due to the oxidation reaction which occurs with metallic Si or Al in a highly alkaline environment [189][190][191]. Alkali-activated foams (AAFs) can be made using different methods. Among the methods used to produce alkali-activated foamed lightweight materials is the thermal expansion of (Na, K)-poly (silicate-multisiloxo) with ration Si: Al >> 6 [62]. Aluminium powder (Al) has been used to produce a large variety of alkali-activated types of cement that have been developed during the last two decades [188][36] in accordance with different criteria such as technology, environment, economy, and geographical rationality. Several examples of alkali-activated foams (AAFs) which have been obtained from different raw and waste materials have been reported in the literature [183][192][193]. In the next two pages Table 2.5. reviews some important events outlining steps in the development of alkali-activated foamed materials, also known as geopolymeric foamed materials, over the last two decades (updated from I. Beghoura et al. 2019, [114]).

31

Table 2.5 - Alkali-activated foamed materials timeline.

Authors	Year	Study/Impact	Foaming Agent	Production Process	Ref
E.P. Kearsley	2001	Effects of replacing large volumes of cement on the properties of foamed concrete.	Foamtech (hydrolysed proteins)	Pore-forming	[20]
Indrek Kulaots	2003	Possibility of standardizing the adsorption for use with coal fly ash pozzolans.	Air-entraining	Air bubbles	[194]
V. Vaow et al.	2010	The ability of geopolymerization technology for production of thermal insulating foamy inorganic polymers.	H_2O_2	Gas foaming	[195]
R. Arellano Aguilar et al.	2010	Effect of composition, curing temperature and density on the strength, thermal conductivity, microstructures, and composition of reaction products of aerated concretes based composite geopolymeric binders of Mk–FA using BFS as a lightweight aggregate.	Al	Gas foaming	[22]
E. Prud'homme et al.	2011	The preparation of geopolymer foams based on potassium silicate, industrial waste, and several types of clays.	Silica fume	Gas foaming	[190]
S. Delair et al.	2012	The characterization of the behaviour of inorganic foams in aqueous media.	Silica fume	Gas foaming	[196]
M. Mustafa et al.	2012	The possibility of producing foam concrete by using a geopolymer system.	NaOH and superplasticizer	Pre-foaming	[136]
H. Esmaily	2012	Use of alkali-activated slag (AAS) in place of usual cementitious materials in the production of autoclave aerated concrete.	Al	Gas foaming	[197]
Kun-Hsien Yang	2013	The feasibility of using reservoir sludge as a raw material in the production of foamed inorganic polymers with different densities.	No details	Pre-formed air bubbles	[198]
G. Masi et al	2014	Foaming to reduce the density of geopolymeric Materials.	Al - H_2O_2	Gas foaming and mix foaming	[199]
Z. Abdollahnejad	2015	Properties of foam geopolymers.	H_2O_2 - $NaBO_3$	Gas foaming	[200]
Jay G. Sanjayan	2015	Investigation of lightweight geopolymer aerated by aluminium powder.	Al	Gas foaming	[23]
P. Hlavácek et al.	2015	Synthesis of inorganic fly ash-based foam.	Al	Gas foaming	[201]
E. Kamseu	2015	The effective thermal conductivity of porous geopolymer composites.	Al	Gas foaming	[202]
Rui M. Novais	2016	The influence of the blowing agent content.	H_2O_2	Gas foaming	[203]
V. Ducman	2016	Characterization of geopolymer fly ash-based foams obtained with the addition of Al powder or H2O2 as foaming agents.	Al - H_2O_2	Gas foaming	[204]

Ailar Hajimohammadi	2017	Lightweight geopolymers foamed with aluminium powder.	Al	Gas foaming	[205]
Ailar Hajimohammadi	2017	The impact of aluminium reaction on the phase evolution of fly-ash based geopolymers.	Al	Gas foaming	[206]
Imed Beghoura et al.	2017	A preliminary study aimed at the feasibility to produce a new improved lightweight foamed alkali-activated materials incorporating expanded cork	Al - H_2O_2	Gas foaming	[114]
Imed Beghoura et al.	2017	Expansion volume of alkali-activated foamed cork composites from tungsten mining mud waste with aluminium	Al	Gas foaming	[207]
Gediminas Kastiukas	2018	Investigating the potential of producing a high-performance foamed alkali-activated material.	Al	Gas foaming	[208]
A. Hajimohammadi et al.	2018	Enhancing the strength of pre-made foams for foam concrete applications.	Sodium dodecyl sulphate	mechanical and chemical foaming methods	[209]
Imed Beghoura et al.	2019	The effect of using different Precursors' particle sizes on the AAFs compressive strength, volume expansion and pore size distribution.	Al	Gas foaming	[165]
Juan He et al.	2019	Effect of foaming agent on physical and mechanical properties of alkali-activated slag foamed concrete.	AOS SDS-K_{12} AES	pre-foaming	[210]
Shashwat Soni et al.	2020	Effect of Protein Based Foaming Agent on Geopolymer Foamed Concrete.	Protein based	Pre-formed air bubbles	[211]
Trong-Phuoc Huynh et al.	2020	Performance Evaluation of Pre-foamed Ultra-lightweight Composites Incorporating Various Proportions of Slag.	No details	Pre-formed air bubbles	[212]
Rafał Krzywon and Szymon Dawczynski	2021	Research on foamed geopolymers reinforced with glass fibre meshes.	H_2O_2	Gas foaming	[213]
Imed Beghoura et al.	2021	Development of an alkali-activated lightweight foamed material (AA-LFM) with enhanced density.	Al	Gas foaming	[214]
Nurliyana Ariffin et al.	2021	Effect of Aluminium Powder on Kaolin-Based Geopolymer Characteristic and Removal of Cu^{2+}.	Al	Gas foaming	[215]

33

Concrete and mortars based on Portland cement (OPC) are non-flammable inorganic materials. However, at temperatures over 100° C, the hydration water in calcium hydro silicates progressively evaporates and the material quickly loses its strength. At low temperatures between 100° C and 400° C, this process is rather slow, but it accelerates quickly at higher temperatures. Incorporating lightweight materials such as expanded perlite or vermiculite, as well as other inorganic lightweight aggregates, improves temperature resistance. These compositions are utilized as steel structure fireproofing materials, although they only preserve the structural steel for a limited time. Using calcium aluminate cement in mortars and concrete improves significantly high-temperature resistance [216].

Jay G. Sanjayan et al. (2015) aims to produce aerated fly ash-based geopolymer pastes by using different amounts of aluminium powder. The density, compressive strength, macro, and micro-structure of the produced samples were studied. Different sodium silicate to sodium hydroxide (NaOH) and alkali activator to fly ash ratios are investigated and the effect of percentage of aluminium powder on foam-ability is surveyed [23]. The reaction between the Al metal powder and the alkaline activator proceeds quickly [201]. It is evident from all pictures (Figure 2.7) that many unreacted fly ash particles remained in the aerated sample [23].
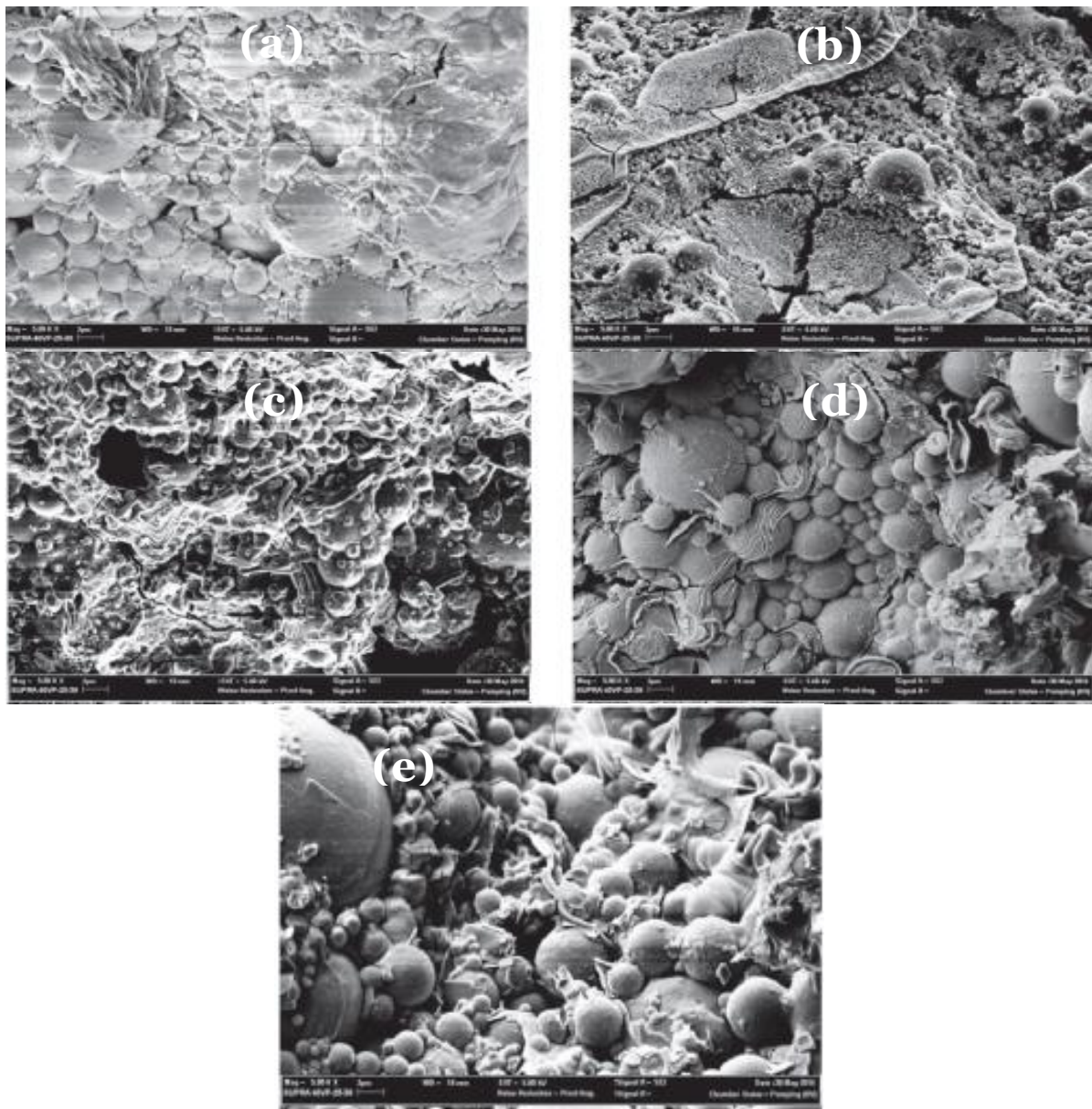
Figure 2.7 - *SEM micrograph of aerated geopolymer samples: (a); SS /SH = 2.5, AA/FA = 0.35,*
wt.% of Al = 5.0 (b); SS/SH = 2.5. AA/FA = 0.35, wt.% of Al = 3.0 (c); SS/SH = 1, AA/FA = 0.3, wt.%
of Al = 5.0 (d); SS/SH=1, AA/FA = 0.3, wt.% of Al = 1.5 and (e); SS/SH = 2.5, AA/FA = 0.25, wt.% of
Al =5.0 [23].

Mustafa Al Bakri et al. [25] used fly-ash, sodium silicate, sodium hydroxide (NaOH), and a foaming
agent to produce the foam geopolymer concrete. The average density of LW1 is 1650 kg/m^3 and for
LW2 is 1667 kg/m^3. Figure 2.8 (a, b) shows the foamed geopolymer concrete of LW1 and LW2 at
different magnifications. Conversely, at magnifications of 2000× and 5000×, microcracks were
observed in the LW1 samples (Figure 2.8. (c, e)), which contributed to their lower strength by
increasing their water absorption and porosity [25].
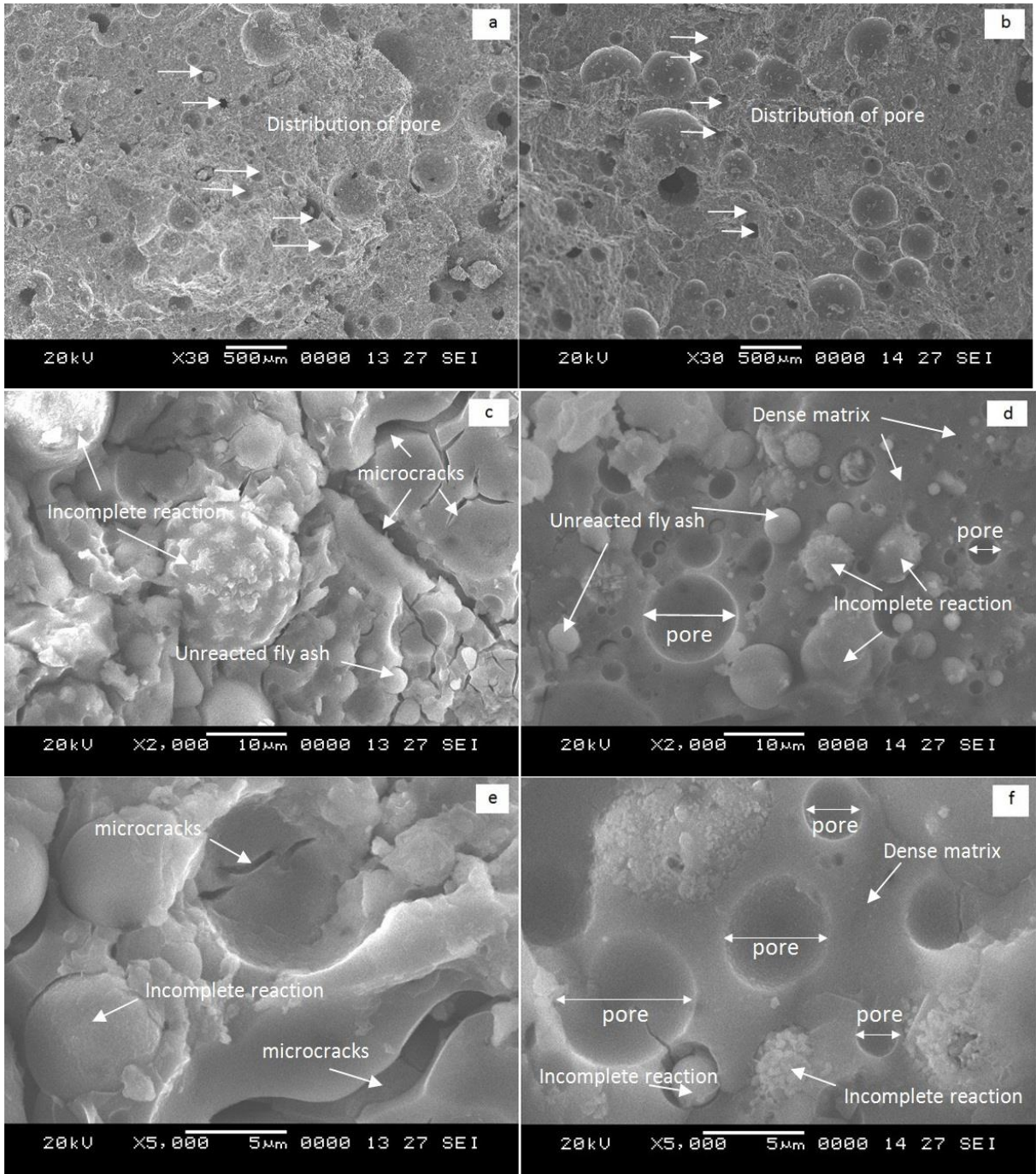
Figure 2.8 - (a) Distribution of pores for LW1; (b) Distribution of pores for LW2; (c) LW1 at a magnification of 2000×; (d) LW2 at a magnification of 2000×; (e) LW1 at a magnification of 5000×; (f) LW2 at a magnification of 5000× [25].

The LW2 samples, which had a denser matrix (Figure 2.8. (d, f)) than the LW1 samples, produced foamed geopolymer concrete that had greater strength. These stronger samples were heat-cured, which facilitated the complete reaction between the fly ash and the alkaline activator to form an aluminosilicate gel. Soon after the mixing process, the gel covered the fly ash particles and produced a dense matrix (complete reaction). Nevertheless, there were still some instances of incomplete reaction, as evidenced by the fact that the surface of the fly ash was covered with aluminosilicate gel

rather than a dense matrix has been formed. This situation was observed on both samples [25]. Unreacted fly ash was present in both samples. Fly ash with its original spherical shape was located on the nearby dense matrix. From the SEM analysis, it was determined that the existence of microcracks and the incomplete formation of the dense matrix had caused water absorption and porosity of the LW1 samples to increase, thereby impairing their strength [25].

Alkali-activated foams (AAFs) appear to be a very promising material since they are formed at temperatures below 100° C and possess properties like foamed glass or foamed ceramics, both of which are normally produced at high temperatures, normally above 900 ° C. Among many products that are based on alkali-activated precursors, the main precursor for alkali-activated is fly ash [201][204].

2.3.1. Classification of alkali-activated foamed materials

The two main methods are pore-forming and mixed foaming [184]. Many materials have been proposed and evaluated in the literature due to their use as foaming agents. The two common classes of foaming agents are physical and chemical. Physical foaming agents provide gas for the expansion of polymers by changing in physical state. Chemical foaming agents are inorganic or organic substances with a low molecular weight that are usually delivered in powder or pellet form [217]. Sodium bicarbonate, ammonium carbonate, ammonium bicarbonate, calcium azide, and aluminium powder are examples of inorganic chemical foaming agents [218]. The chemical foaming agents provide a gas (or gases) by undergoing a chemical reaction, which results in the dissolution (or decomposition) of the original molecule. In most cases, the decomposition of chemical foaming agents is thermally induced, although there are a few examples where decomposition is chemically initiated. Almost all chemical foaming agents are solids [217]. Several foaming agents, as well as detergents, resin soap, glue resins, saponin, and hydrolysed proteins, such as keratin and similar materials [20][25][219], have been produced for this purpose.

Based on the pore formation methods: The pore-forming agent (foaming agent mixed with a part of mixing solution or water) and the mixed foaming (foaming agent mixed with the precursor) are the two main methods which have already been used to produce a foamed material [184]. A large kind of foaming agents has been produced for this purpose, as well as detergents, resin soap, glue resins, saponin, and hydrolysed proteins, such as keratin and similar materials [20].

Air-entraining method (gas concrete): Gas-forming chemicals are mixed into lime or cement mortar during the liquid or plastic stage, resulting in a mass of increased volume and when the gas escapes, leaves a porous structure. Aluminium powder, hydrogen peroxide/bleaching powder and calcium carbide liberate hydrogen, oxygen, and acetylene, respectively. Among these, aluminium powder is the most commonly used aerating agent. The efficiency of the aluminium powder process is influenced by its fineness, purity, and alkalinity of cement, along with the means taken to prevent the escape of gas before the hardening of the mortar. In the case of Portland cements with low alkalinity, the addition of sodium hydroxide or lime supplements is required [184].

Combined pore-forming method: Production of cellular concrete by combining foaming and air-entraining methods has also been adopted using aluminium powder and glue resin [19][220]. Among the methods used to produce alkali-activated foamed materials is the thermal expansion of (Na, K)-poly (sialate-multisiloxo) with ration Si: Al>>6 [221]. In addition, to reduce the density of the foamed alkali-activated materials [51][188], holes or lightweight aggregates [22] can be added for such purposes. Over the last few years, several examples of alkali-activated foams have been obtained from different raw and waste materials [192][222].

Various chemical foaming agents can be used in the Si-Al precursor materials + MOH/M_2SiO_3 Oligomeric silicate species Silicate monomer Aluminate monomer Aluminosilicate oligomers Amorphous aluminosilicate polymer Amorphous aluminosilicate gel Aluminosilicate nuclei Zeolitic phase foaming process of inorganic polymers. Chemical foaming agents also known as thermal decomposable foaming agents are solids or liquids at room temperature that break down at a certain temperature, and that release a gas, such as nitrogen, hydrogen, carbon dioxide, or carbon monoxide when heated. They are usually made by combining a chemical foaming agent with a solid polymer and heating the combination while keeping it under pressure [223]. Aluminium powder has been used to produce foams of inorganic polymers [219][201][23] as well Hydrogen-peroxide [195][224] sodium-perborate [200] as a chemical foaming agent. Accordingly, to Davidovits there is no standard formulation to fabricate an alkali-activated foam using hydrogen-peroxide. The success of such foamed material requires a delicate optimization of two parameters [221]; (1) kinetics of peroxides decomposition with the production of oxygen; (2) increase in viscosity of the geopolymer precondensate.

Foaming agents have been utilized in a variety of industries, including building construction, due to their range of benefits including enhanced thermal stability, low density, thermal insulation, and unique material characteristics of the buildings, and they have long been a focus of research. Besides, foams have a wide range of applications. There are two main types of foaming agents:

- Inorganic: Hydrogen peroxide, aluminium powder, sodium perborate.
- Organic: expanded and extruded polystyrene.

For the foaming of inorganic polymers, hydrogen-peroxide [195], aluminium powder [23][201][137], or sodium-perborate [225] can be used as a chemical foaming agents. Furthermore, the reaction between the aluminium metal powder (Al) and alkaline activator proceeds quickly and during the reaction, hydrogen gas is released as the reaction shown in equation 2.1 [220].

$$2Al + 2NaOH + 2H_2O \implies 2NaAlO_2 + 3H_2 \qquad (2.1)$$
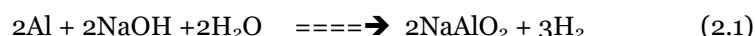
Besides, the hydrogen peroxide (H2O2) is thermodynamically unstable and therefore can be easily decomposed to water and oxygen gas (see reaction (2.2)) with the latter playing the role of the geopolymeric paste blowing agent [195]:

$$2H_2O_2 \rightarrow 2H_2O + O_2 \qquad\qquad (2.2)$$

2.3.2. Properties of alkali-activated foamed materials

Foamed materials (FMs) namely (aerated concrete) have the potential to be a viable alternative to conventional concrete. It has a high strength-to-weight ratio and is relatively lightweight. The use of FMs minimizes dead loads on the building and foundations, contribute to energy saving and reduce construction labour costs. It also has the potential to be utilized as a structural material and decreases the manufacturing and shipping costs of construction components when compared to conventional concrete. Alkali-activated foamed materials (AAFMs) have been extensively investigated in recent years, due to the great performance and low environmental impact which combines the benefits and operating energy saving achieved by foamed alkali-activated materials with the reductions of cradle-to-gate emissions. Alkali-activated foams (AAFs) obtained from the use of alkali-activated binder (AABs) derived from a variety of raw materials with a wide range of chemical and mineralogical compositions and surfaces, through different foaming methods and a variety of foaming agents, as well as alkali activator solutions. Physical and mechanical properties, as well as chemical and functional characteristics, were carried out, as briefly described in the following section.

2.3.2.1. Physical properties

Microstructure:

The mechanism of pore production (e.g., gas release or foaming) has an impact on the microstructure and consequently, on the characteristics of foamed materials (FMs). The FMs have a solid microporous matrix and macropores that define their structure. The macropores emerge as the mass expands due to air gaps and the micropores appear in the walls between the macropores [226]. Macropores have been defined as pores larger than 60 μm in diameter [227]. The orientation of cement hydration products is dramatically affected due to the existence of voids. The typical pore systems in aerated concrete are shown in Figure 2.9. The porous structure of aerated concrete is also characterized by its artificial air pores, inter-cluster pores, and inter-particle pores in terms of pore size distribution characteristics, and the distribution of pores in the matrix has an impact on its properties [228]. Another widely accepted method divides pores with a size range from 50 to 500 μm (pore sizes of 5 μm diameter are considered large in ordinary mortars) introduced by aerating or surface-active agents, microcapillaries of 50 nm or less formed in the walls between the air pores (referred to as micropores [226] and very few pores with a radius of 50 nm to 50 μm, so-called microcapillaries [229].

Although the air void network is relatively identical, the structure of autoclaved aerated concrete and unautoclaved aerated concrete differs due to differences in the hydration products, which explains the differences in their characteristics. A portion of the fine siliceous material combines chemically with calcareous material, such as lime and lime freed by cement hydration, during autoclaving, and producing a microcrystalline structure with a substantially lower specific surface. Due to the presence of increased pore water, unautoclaved aerated concrete has a greater volume of fine pores, according

to Tada and Nakano [229]. The macropore size distribution has been found to not affect compressive strength [226].
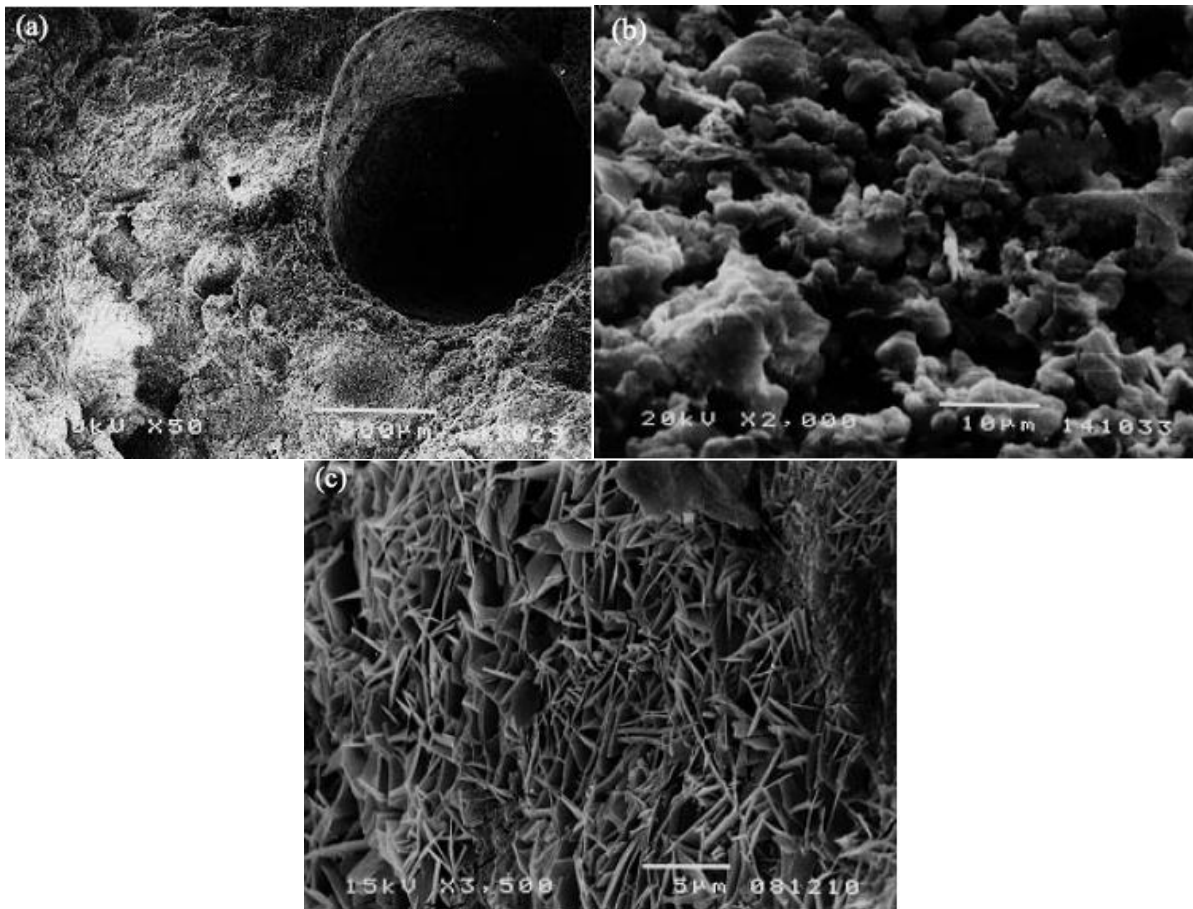
Figure 2.9 - Aerated concrete's porous systems: (a) man-made air pore; (b) pores between blocks; (c) pores between particles [230].

Density:

As several physical properties of foamed materials (FMs) depend on the density (300 - 1800 kg/m^3), density qualification is required. The moisture state (oven-dry or in equilibrium with the environment) must also be specified when specifying the density. The autoclave material is perhaps 15% to 25% heavier than oven-dry material. For very low density, this value can be as high as 45 percent. The carbonation process is responsible for a considerable rise in autoclaved aerated concrete density with increasing relative humidity and temperature which is proportionate to the original dry density [231].

As previously stated, foamed materials with a variety of densities for specific applications can be produced by altering the composition, which changes the pore structure, size, and distribution. For optimal structural and functional qualities, a stable and ideally spherical cell structure is required [228][232]. To get homogeneous density products, the pores must also be distributed consistently throughout the body mass. The development of bigger macropores in the matrix has been shown to considerably lower the density. The density of aerated concrete is proportional to its compacity and

porosity, whereas compacity (t) is the ratio of density to a specific weight and the percentage of porosity is (1-t) * 100.

2.3.2.2. Chemical properties

The X-ray powder diffraction investigations on autoclaved aerated concrete have demonstrated that the major reaction product is a calcium silicate hydrate Ca-rich (C-S-H) belonging to the tobermorite group [226][229]. The reaction product is a combination of crystalline, semi-crystalline, and near amorphous tobermorite [226]. It is also interesting to note that calcium silicate is the primary hydrate phase present. The specific surface of these reaction products is dramatically lower than that of wet curing. Microcapillaries in autoclaved aerated concrete are plate-shaped crystals of 11.3 Å tobermorite with a double-chain silicate structure, as shown by SEM, which generate differential pore distribution in gas formation and foaming processes [229] due to their growth rate and degree of orientation. They also do not exhibit any signs of ageing. As confirmed by analytical transmission electron microscopy, the tobermorite exhibits abnormal behaviour, in that their basal spacing of 11.3 Å does not drop to 9.3 Å even at 300° C. Throughout moist-curing, unautoclaved aerated concrete transform from needle-shaped hydrates to hexagonal hydrates, and subsequently, to block-shaped calcite crystals [229].

2.3.2.3. Mechanical properties

Properties such as strength, permeability, diffusivity, shrinkage, and creep of foamed concrete (FC) are directly related to its porosity and pore size distribution. The geopolymer foam possesses relatively high compressive strength (5.5MPa - 10.9MPa) [225][201]. However, increasing the liquid/solid ratio and the amount of foaming agent (Al powder or hydrogen-peroxide) in the geopolymer paste leads to a certain decrease of compressive strength [225].

Compressive strength:

Compressive strength generally increases linearly with density. Compressive strength values at various densities (Table 2.6) have been published in the literature. As high temperature and pressure result in a stable form of tobermorite, autoclaving considerably boosts compressive strength. For several forms of aerated concrete, the link between autoclaving pressure, time, and compressive strength has been observed. The intensity of NAAC increases from 30 to 80 percent between 28 days and 6 months, and very slightly beyond that. A portion of this rise can be ascribed to the carbonation process [231]. The compressive strength of a material changes inversely to its moisture content. There is an increase in strength after drying to balance it with the normal environment and an even higher gain when completely dried out. As a result, testing on materials that have reached an equilibrium with their environment is advised. To quantify the increase in compressive strength from wet to dry conditions, a correction factor has been developed.

Fly ash as a partial/complete filler substitute in the production of unautoclaved aerated concrete and autoclaved aerated concrete has demonstrated higher compressive strength to density ratio results. The impact of density on the compressive strength of autoclaved aerated concrete made from slate

debris has also been shown. To determine the compressive strength of aerated concrete, many relationships have been proposed. The modified form of Feret's equation which relates the strength (S), water-cement (w/c), and air-cement (a/c) ratios for foamed are given as: S= K $[1/(1 + (w/c) + (a/c))]^n$, where K and n are empirical constants. Durack and Weiqing developed a strength-to-gel-space ratio equation for foamed concrete developed with patented foaming chemicals.

Table 2.6 - *Properties of AAFMs*

Dry density (kg/m³)	Compressive strength (MPa)	Static modulus of elasticity (k N/mm²)	Thermal conductivity (W/m °C)
400	1.3 to 2.8	0.18 to 1.17	0.07 to 0.11
500	2.0 to 4.4	1.24 to 1.84	0.08 to 0.13
600	2.8 to 6.3	1.76 to 2.64	0.11 to 0.17
700	3.9 to 8.5	2.42 to 3.58	0.13 to 0.21

2.3.2.4. Functional properties

Water absorption and capillarity:

Due to the porous nature of aerated concrete, there is a significant interaction between water, water vapour and the porous system and multiple moisture transport mechanisms occur. Pores are vacant in dry conditions, and water vapour transport takes precedence, but certain pores are filled in higher humidity areas. For an element in contact with water, capillary suction is the most common. Due to these processes, it is demanding to predict the impact of pore size distribution and water content on moisture migration [228].

Water vapour transfer is described in terms of water vapour permeability and moisture diffusion coefficient, whereas water transfer is defined by capillary suction and water permeability [228]. The moisture transport phenomena in porous materials have been characterized by an easily quantifiable feature termed sorptivity, which is based on the unsaturated flow theory. It involves absorbing and transferring water via capillarity. The water transmission property has been demonstrated to be better explained by sorptivity than by permeability. The principle of capillary hygroscopicity is similar to that of sorption. These figures provide a good estimate of the pores' fineness.

Durability:

Autoclaved aerated concrete is mostly composed of tobermorite, which is far more stable than the materials created in typically cured aerated concrete, making it more long-lasting. Aerated concrete, on the other hand, has a significant porosity, thus enabling liquids and gases to pass through. This might result in matrix damage. At saturation levels between 20% to 40%, freeze-thaw responses have been observed to be considerable in autoclaved aerated concrete. The sample becomes brittle and splits entirely at greater saturation levels [233]. When sulphate assault is expected, protective

measures utilizing bitumen-based materials are required. Carbonation can cause an increase in density. Yet, this is usually not a substantial problem until the CO2 exposure is excessive.

Thermal conductivity:

Thermal conductivity production in building materials has attracted much interest in the past few decades due to its low cost and environmentally friendly processing technology. Thermal conductivity is influenced mainly by density, moisture content, and material composition [234]. Since thermal conductivity is essentially a function of density, it makes little difference whether the product is moist cured or autoclaved in terms of thermal conductivity. The number of pores and their distribution are also important factors in thermal insulation. The smaller the pores, the better the insulation.

Geopolymer foam has a low thermal conductivity, high mechanical characteristics, and very high-temperature stability. According to Davidovits all geopolymer foams (the precursor for geopolymers is mainly metakaolin) are incombustible and they are classified as Al materials. When exposed to fire, a release of toxic breaks down products is not possible [21]. Therefore, geopolymer foams are highly recommended for all applications where safety is critical. Geopolymer with Macro-encapsulated LWA has a lower thermal conductivity than that of ordinary cement mortar. Moreover, the size of the ME-LWA used in the geopolymer panel preparation compared with sand is also a contributing element in the reduction of the thermal conductivity of the geopolymer [31]. Increasing the foaming agent level in the geopolymeric paste have a significant impact on the thermal conductivity value because it creates holes in the paste which, in turn, increase the porosity volume as well as the reduction in apparent density as demonstrated by Vaou and Panias (2010). The thermal conductivity of foam geopolymer paste was reduced from 0.053 W/mK to 0.03 W/mK when the hydrogen peroxide (H_2O_2) concentration was increased from 0.7 percent to 2.02 percent [235]. According to the findings, the thermal conductivity of foamed geopolymers is connected to their cellular structure. Controlling the type, size, shape, and volume of the cells can also result in a significant reduction in the thermal conductivity of the produced material. These findings are in harmony with the state-of-the-art in thermal insulation foamed plastics, where thermal conductivity is first linked to the thermal conductivity of the filling gas, then to the apparent density of foams, and finally to the morphology of the cellular structure [236].

Fire resistance:

Aerated concrete's fire resistance is higher than or equal to that of conventional dense concrete in practice [232], hence its usage poses no risk of flame propagation. One key explanation for this behaviour is that the material is rather homogenous, as opposed to typical concrete, which has diverse rates of expansion, cracking, and disintegration due to the presence of coarse aggregate. The closed pore structure of aerated concrete pays off in terms of fire resistance, as heat transfer by radiation is inversely proportional to the number of air-solid contacts crossed. This, along with their low heat conductivity and diffusivity, suggests that aerated concrete has superior fire-resistance.

Pavel Krivenko and Georgiy Kovalchuk (2015) studied the heat-resistant of alkali-activated fly ash cellular concrete by regulating the microstructure creation in the $Na_2O-Al_2O_3-SiO_2-H_2O$ system as a result of hydration and dehydration processes during heating. The innovative cement system using alkali-activated fly ash can be tailored by hydration products with a unique combination of properties which are similar to zeolites is made up of 90% industrial by-products. Heat-resistant cellular concrete made from alkali-activated fly ash has a compressive strength of up to 16 MPa and thermal resistance of up to 34 cycles in the air (20° C – 800° C). High-temperature composite materials are one of the most potential areas of application (masonries, ovens, furnaces, etc.) for alkali-activated fly ash. Therefore, the materials should be heat-resistant enough to maintain high strength and minimal thermal shrinkage at the service temperature, and (2) have low thermal conductivity, i.e., are lightweight. Depending on the unit weight, cellular concretes are known to combine great mechanical strength with low thermal conductivity, although classic cellular concretes based on lime or OPC are not heat resistant [188].

Acoustical properties:

According to Valore [232], aerated concrete does not have any distinctive or considerable sound insulation properties. The rationale given is that the mass law, which is a function of the frequency and surface density of the component, determines the transmission loss of airborne sound. In addition to the mass law, Tada relates the TL to the stiffness and internal resistance of the wall and provides an acoustic performance design of aerated concrete based on bulk density and thickness [229]. According to Leitch, the closed porous structure affects the sound insulation, exactly as thermal and fire insulation does.

2.4. Alkali-activated materials with lightweight aggregates

Reducing density in building materials is increasingly being reported in the literature as it is effective in terms of improving thermal insulation properties. One of the existing methods is the use of lightweight aggregates. Various raw materials are suitable for the synthesis of alkali-activated materials (AAMs) such as fly ash [225], perlite [195], and metakaolin [22], among others. The use of lightweight aggregate (LWA) as an alternative to the normal weight aggregate in the building materials have shown density reduction for concrete structures. The density of the resulting concrete is determined by the used aggregate. The coarse aggregates could be replaced by lightweight aggregates (LWA) in conjunction with natural fines, or LWA can be used for both coarse and fine aggregates. Coated lightweight phase change material (PCM) produced from the coated PCM-LWA can be used as impregnated aggregates, and they are commercially available and compliant with EN 13055-1 expanded clay LWA supplied by Argex S.A [31]. Table 2.7. shows other types of lightweight aggregates, made from a variety of raw materials.

Aguilar et al. 2010, investigated alkali-activated lightweight concretes produced using binders made of metakaolin with 0 and 25% fly ash, activated with 15.2 % Na_2O using sodium silicate with a modulus of $SiO_2/Na_2O = 1.2$. Concretes with densities of 1200, 900, and 600 kg/m³ were produced by bubbling

with the addition of aluminium powder. In certain formulations, the lightweight aggregate of blast furnace slag was added to a binder: aggregate ratio of 1:1; curing was performed at 20° C and 75° C.

Table 2.7 - *Lightweight aggregates from different source components.*

Aggregate type	*Trade name*	*Dry density kg/m³*
Furnace clinker	-	720-1040
Processed fly ash/pfa	Lytag	770-960
Foamed blast furnace slag	-	670-920
Expanded clay, shale, and slate	Aglite, Leca, Solite	320-960
Pumice	-	480-880
Pelletized expanded slag	Pellite	800-1000
Wood and plastic particles	-	320-480
Expanded vermiculite	-	60-160

Scanning electron microscopy was used to acquire the morphological characteristics of the Mk, FA, Al powder, and BFS sand as shown in Figure 2.10. The Mk particles have a hexagonal sheet shape, whereas the FA particles are typically spherical and of uneven size. Images show that the morphology of the Al powder is irregular, and the GGBFS granules have a high porous texture [22].
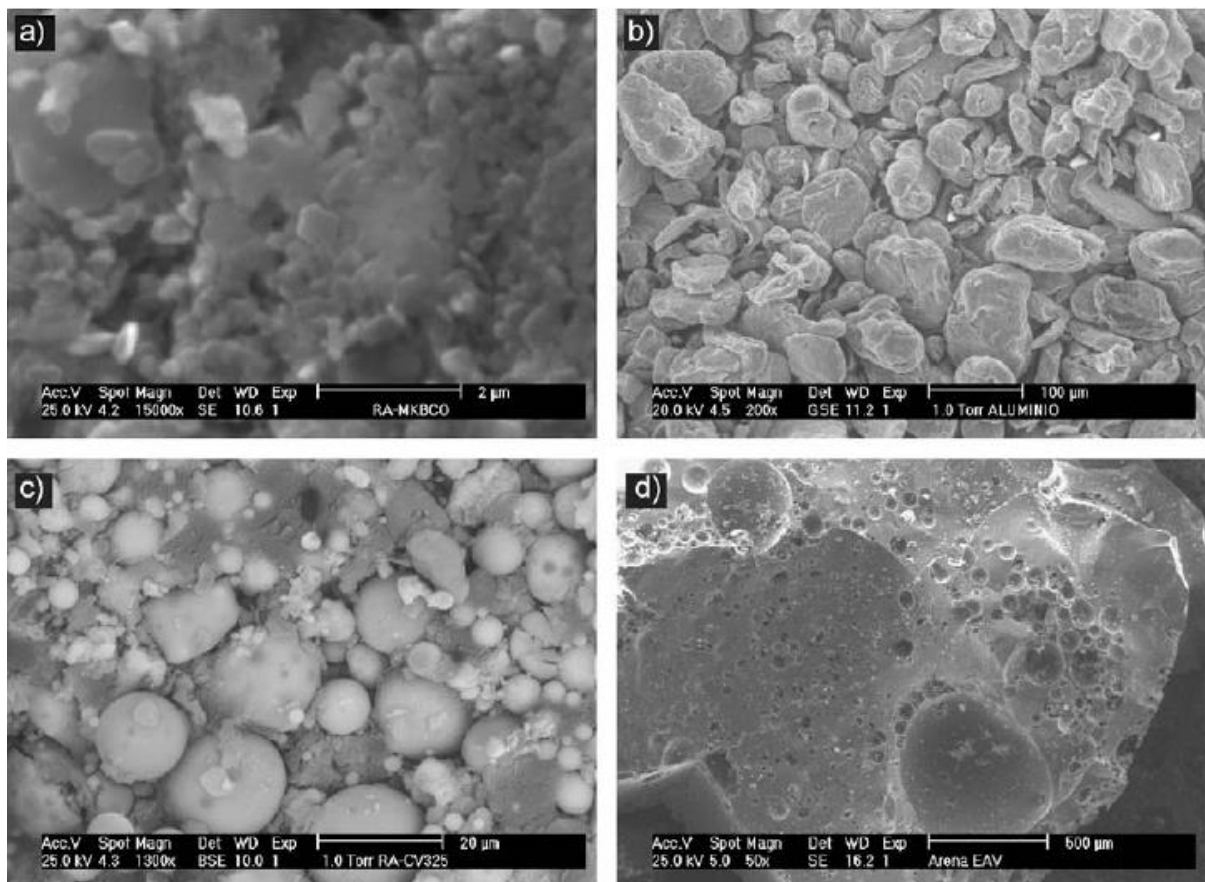
Figure 2.10 - *Microscopic images for the produced lightweight concrete (a) Mk, (b) Al powder, (c) FA, and (d) GGBFS sand* [22].

Besides, density reduction of alkali-activated materials (AAMs) can be performed by using lightweight aggregate as an alternative to the normal weight granules where they show better thermal insulating features. AAMs with lightweight aggregates for non-structural applications are usually produced with artificial aggregates such as expanded clay, expanded polystyrene (EPS), or natural expanded granulated cork particles (EGC) [237].

2.5. Alkali-activated materials applications

2.5.1. Advantages of using alkali-activated materials

From an analysis of relevant literature, it is obvious that employing alkali-activated cementitious materials (concretes/mortars) in the building sector provides various benefits. Several researchers stated that a variety of uses derives directly from many beneficial features that alkali-activated binders (AABs) compounds can develop during and after the alkali activation, essentially as an alternative to Ordinary Portland Cement (OPC) in the construction industry, also in other niche applications. Alkali-activated concrete and mortars were developed in the 20th century, allowing for commercial manufacturing and use in a variety of construction developments in Europe, China, and a few other nations. This is because of its improved durability, chemical and thermal resistance, adhesion to reinforcements/aggregates, quick growth of mechanical strength, and economic value as an industrial by-product material. Thus, this long, and extensive research about alkali-activated materials allowed gaining a lot of experience and knowledge in the production and application of these materials.

Alkali-activated binders, mortars, and concretes are used in the manufacture of concrete infrastructures, structural elements, heat-resistant pavement, hazardous metal immobilization, and sub-aqueous marine products. Outstanding alkali-activated constructions go back to 1960 when a two-storey building was built with alkali-activated concrete in Ukraine as shown in Figure 2.11. In addition, in 1985, French and English nuclear power stations equipped their plants with air filters in which joints and dust-free sealants are made of alkali-activated material, providing a temperature safety cover up to 500° C. Moreover, in 1999, a group of Ukrainian scientists demonstrated their interest in cementitious materials applications by investigating several concrete structures made of alkali-activated-based materials. Tubing, anti-soil-slippage collectors, sloping edges of railway embankments, silage trenches and multi-storey buildings were among the constructions used [54]. Furthermore, lately in 2014, Brisbane West Well camp Airport (BWWA), in Toowoomba Queensland, Australia, established a significant milestone in engineering being the world's largest alkali-activated concrete project, with approximately 40,000 m^3 (100,000 tons) of alkali-activated concrete used. These two remarkable constructions show how alkali-activated materials are being used in the building sector, thus having a positive environmental impact [42].

Figure 2.11 - *The first low and high rise residential constructions OPC-free manufactured using alkali-activated cement concrete in the 1970s, Ukraine* [54].

Several features of these materials, such as a rapid setting and hardening, low shrinkage, high resistance to a range of acids and salt solutions, the capability to incorporate toxic metal in their constitution have led to their employment in the immobilisation of toxic waste, such as lead and chromium [42]. The significance of these investigations can be observed in the outcomes that have been obtained. Alkali-activated based concretes and mortars continue to function well in all of the outstanding results. In some cases, it can even outperform OPC-based structures. These investigations have also demonstrated that the characteristics of concretes and mortars are significantly reliant on the raw materials used, as well as the conditions of service and the overall age of the structure, as demonstrated by performance testing and microstructure analysis. From a concrete design point of view, alkali-activated materials, when properly defined and synthesised, are capable of satisfying the criteria of Ultimate and Serviceability limit states.

2.5.2. Environmental and economic benefits

Alkali-activated cementitious materials (concretes and mortars) production is environmental-friendly, which contributes to reducing the environmental concerns related to OPC. This can be accomplished by replacing OPC with a commercially sustainable alternative, hence eliminating gaseous emissions (mainly CO2) during OPC manufacture. The production of one ton of OPC releases approximately one ton of pollution gas of CO2 into the atmosphere. This is added to the fuel and energy consumption required for the production of OPC, which releases harmful gases into the atmosphere. On the other hand, using pozzolanic by-products from power plants would prevent these materials from being disposed into landfills in their hazardous state, thus reducing the pollution emitted and the negative environmental impact of those materials. Currently, PFA and GGBS are disposed of in landfills, thus increasing the risk of leaching metals into groundwater. However, alkali-activated cementitious reproduction would reduce this risk. Furthermore, using alkali-activated cementitious materials in comparison to OPC would save approximately 0.25 million tons of coal, thus preventing 1.5 million tons of CO_2, and saving 80 million power units [238].

Furthermore, the economic impact of the manufacture of alkali-activated mortars and concretes are significant. The high temperatures necessary for OPC manufacturing (about 1450° C) make it a costly and energy-intensive process. As a result, alkali-activated materials manufacture lowers costs and saves a significant amount of energy in the production of OPC. Additionally, as previously stated, the pozzolanic materials utilized in the manufacturing of alkali-activated materials (AAMs) are easily available as by-products of industrial coal power plants, mining, and quarrying activities, which makes them affordable to obtain. According to Fernandez-Jimenez and Palomo (2005), only 30% to 40% of available fly ash material is used, leaving the majority to be disposed of in landfills. As a consequence, the more of these substances are utilized, the cleaner the landscape and air will be, thus resulting in a green environment. Resolving this rising challenge by recycling into building materials will benefit both the economy and the environment [239].

Other benefits of alkali-activated materials have been revealed in many types of studies, in addition to the characteristics mentioned above. The diverse materials employed as precursors, as well as varied preparation parameters like curing time, temperature, and chemical ratios, all have an impact on the final compounds and hence their properties. The following are some of the characteristics of the alkali-activated materials [96][129][240]:

- High compressive strength, even higher than that of OPC;
- Rapid and controllable setting and hardening;
- Low shrinkage, controlled cracking,
- Low thermal conductivity and fire resistance;
- No toxic fumes when heated;
- Low-cost material (10% – 30% less than OPC);
- Good abrasion resistance; High surface definition.

2.6. Alkali-activated foamed materials applications

Alkali-activated foamed materials (AAFMs) are defined as lightweight cellular materials which can be classified as lightweight foamed materials (LWFM) concrete/mortar (density under 2000 kg/m³) with random air-voids created from foaming agents in the mixture. Furthermore, foamed materials are recognized for their fire, heat resistance, and thermal insulation, these main properties must not be overlooked, as fire protection of structures is one of the most widespread applications for alkali-activated foamed materials. The benefits of using wastes derived from mining can be further enhanced when they are used as a host precursor for alkali-activation systems. Besides all of the above characteristics, several research works and patents have been submitted and approved in different countries, demonstrating the feasibility of various applications [64]. There have been several proposal applications for these materials by Davidovits and other authors as listed:

- Fire-resistant wood panels, insulated panels, and walls;
- Ceramic tiles; OPC-free concretes and mortars;

- Repair, renovation, and strengthening of structures and infrastructure;
- Toxic and radioactive waste encapsulation;
- High-tech fireproof uses in aviation and automobiles;
- Artefact made of decorative stone;
- Refractory materials, such as thermal shock refractory;
- Application in an aluminium foundry;
- Work on the restoration.

Although the alkali-activation method has several advantages and potential uses, it is evident that it also has considerable shortcomings. Limited understanding of the involved mechanisms of alkali activation, complicated by a wide variety of chemical and mineralogical compositions of the components, the use of alkaline solutions, which are harmful to health, and the use of silicates, particularly sodium silicate, which have a high environmental impact, are just some of the problems that prevent the diffusion and commercialization of alkali-activated binders [138].

2.7. Waste from cork production

2.7.1. Production of cork

Portugal is the world's largest cork producer and the major manufacturer of cork products. The most significant waste from cork processing is "cork powder", which includes crude cork impurities, cork material powder, cork particles with dimensions lower than permitted for granulates (typically less than 0.5 mm), and occasionally bigger fragments. Cork, the exterior bark of *Quercus suber L.,* is a plant tissue composed of the suberin (30% – 60%), lignin (19% – 22%), polysaccharides (12% – 20%), and extractives (9% – 20%) make up the majority of the cork's chemical composition. The structure of the cork is cellular or alveolar and with a very peculiar morphology consisting of tiny hollow hexagonal prismatic cells stacked in base-to-base rows [241]. Cork has specific features to possess unique properties such as very low density, hydrophobic character, resilience, low thermal conductivity, fire resistance, good insulation properties, and elastic behaviour, among others [242].

The cork bark is dried in the sun before being boiled to soften it then used in a variety of applications. The cork remainder is utilized in a variety of applications, including construction as agglomerated cork products [243]. Cork forests cover more than 720 thousand hectares in Portugal. Cork oak is also found in Mediterranean countries including Spain, Italy, France, Morocco, and Algeria [244]. To manufacture granulated expanded cork, it must first be heated to soften it before fully expanding the lenticels. Similarly, to manufacture a bottle's cork stopper, the nicest portions of the cork are punched out. The cork cells will first collapse and wrinkle after boiling (for about 1 hour), but the internal gas in the cells will expand to create a very tight, homogeneous cell structure [245]. During the production process, the cork waste generated is pulverized and utilized to manufacture agglomerated cork products. Cork powder is collected and burnt as part of the grinding process to help power the factory. Chemical components that are extracted during cork processing can be recovered and used as

beneficial by-products including tannin (used for curing leather), hard wax (used in products like paraffin, paint, and soap), resinous gum (helps vanish adhere to copper and aluminium), and phonic acid (used to make plastics and musk-scented toiletries) [246].

In recent years, there has been a great interest in materials generated from renewable resources, due to the increasing concerns associated with the environment, waste accumulation and disposal, and the eventual depletion of fossil resources [247]. Cork is natural, organic, and lightweight with a high dimensional stability substance. Cork can be used in a wide range of applications due to its various features, such as lightweight filler in thermal insulating solutions, aggregate for concrete, reduced weight concrete panels as well as acoustic insulation in floating floors. Figure 2.12. shows the cellular structure of cork as well as cork particles.

Figure 2.12 - Cellular structure of natural Cork (A) and (B): cork particles

2.7.2. Cork uses in cementitious materials

Since Portugal is the world's largest cork producer, it may prove economically interesting to find other applications for the usage of industrial waste from the processing of this material [244]. Cork, a natural, organic, and lightweight product with high dimensional stability was used in a wide range of applications in constructions besides the artificial lightweight aggregate (LWA). Their features allow the cork to be used, such as lightweight filler in thermal insulating solutions, aggregate for concrete, reduced weight concrete panels, and also for acoustic insulation in floating floors [13]. Nowadays, cork is used in a wide range of applications in the building as a solution of lightweight, thermally insulating, and shows good environmental advantages [13]. Panesar and Shindman (2012) studied the impact of cork used as an alternative of sand or an alternative of stone on the plastic, mechanical, transport, microstructural and thermal properties of mortar and concrete [26]. Karade et al. (2006) studied the influence of cork granules for the manufacture compatibility with cement and the hydration test results showed that cork granules (both natural and expanded) are compatible with cement and can be added up to 30% by weight of cement [27].

2.7.2.1. Cork for thermal and acoustic insulation of buildings

The use of expanded cork (mainly agglomerate cork boards), as thermal and acoustic insulation in buildings, potentially contribute to minimizing the environmental impact of traditional raw materials. Additionally, an enlarged cork could serve to regulate permeability and improve water retention, thus reducing the requirement for irrigation [248]. When compared to traditional alternatives, the environmental performance of this material has already been improved by several authors [249][250][251]. For instance, Maria Manso and Castro-Gomes developed a new modular green wall system during the last quarter of 2013, the modular system was examined for three different periods (cycles) in the central region of Portugal. The thermal behaviour of the covered wall (with a modular system) and how it affects the inside environment as well as the non-covered wall were carried out using an experimental setup in a Mediterranean climate [248]. Andreia Cortês et al. (2019) examined the expanded cork agglomerate as a sustainable alternative to the typical materials used in green vertical systems. The findings of this study indicate that expanded cork agglomerate is a feasible and environmentally friendly alternative to be used in green vertical systems, with the ability to optimize retention and drainage features by adjusting the produced density to meet local weather conditions [252]. Corkboards ensure maximum thermal insulation and significant acoustic insulation, because of their hollow cellular structure, tiny cells, and thin cell walls. The expanded cork agglomerates (cork boards) are made without the use of adhesive using cork grains in a closed autoclave at a high temperature (about 300° C) and pressure (around 40 kPa). It has a low density and a high gas content, which results in low thermal conductivity, thus making them a desirable material for thermal insulation [245].

GEOGREEN system is a modular system with an independent support structure that allows landscaped surfaces to be created in new structures or the rehabilitation/adaption of existing buildings (see Figure 2.13). It is a technology that permits separate parts to be connected to form continuous green surfaces. It was created to be more adaptable than the existing green roof and wall systems and it can be used to create both horizontal and vertical planted surfaces, considering their unique characteristics. It may be customized for surfaces of various shapes, sizes, slopes, and accessibility. The system was created to make installation and maintenance easier by allowing each module to be inserted and replaced independently during normal operation [32].

The modular system is made of eco-friendly materials and incorporates the usage of industrial waste. It distinguishes itself from other current systems by employing unusual materials and incorporating specific thermal, acoustic, and environmental benefits that other systems do not. Each system module is made up of an alkali-activated tungsten-base plate (a blend of tungsten mining waste mud and other waste materials incorporating EGC granules) and a black expanded cork agglomerate top plate, as shown in Figure 2.13 (a and b). The system is able to absorb water and slowly supply it to the plants by enhancing the water absorption capacity of the alkali-activated plate, thus reducing water loss and irrigation requirements. The expanded cork black agglomerate presents itself as a natural and sustainable material with low density, strong thermal and acoustic insulation, and adequate mechanical resistance to support inserted plants [248].
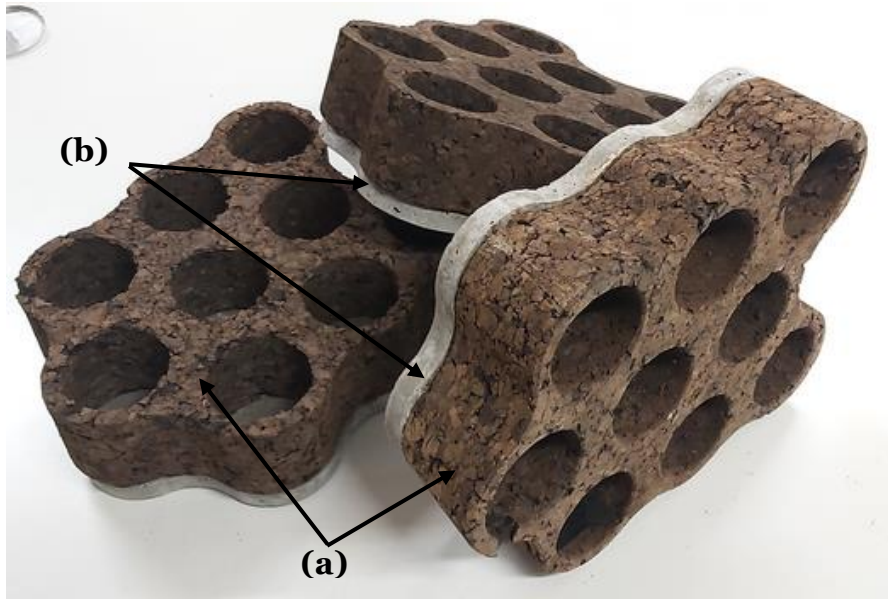
Figure 2.13 - *Geogreen modular system made up of two parts: (a); Tungsten- based alkali-activated base plate and (b) an expanded corkboard insulator.*

There are two types of cork: agglomerate composite cork and expanded cork, both of which can be used as insulating materials. The difference between them is in the transformation process: the first uses suberin, a natural resin that is heated at high temperatures to function as a binder, while the second requires extra components for the binder to be environmentally beneficial. Cork that has been expanded is sold as a board or granules. Due to the high thermal and acoustic insulation performance of cork, It can be used as acoustic, anti-vibration, or thermal insulation in walls, roofs, formwork, and even facades. In addition to being thermal and acoustic insulators, these products are decorative and increase house comfort.

2.7.2.2. Cork as lightweight aggregate

The use of natural EG-cork particles has been studied in various industries as lightweight aggregates. Branco et al. (2006), have developed a research project to assess the physical and mechanical properties of waste cork and explore its potential benefits when used as aggregates in concrete production [13]. Cork granules are a by-product [27] from the industry and the fact that cork is a natural product their usage has eco-efficient advantages. Cork granules are of low density and could be utilized as a lightweight aggregate for concrete and mortars manufacturing (namely polymer-modified mortars) with superior thermal and acoustic insulation properties and higher deformability [253], as well as high durability, very low permeability, and high resistance to chemical and frost attack [254].

Several investigations on the mechanical characteristics of cork under compression have been conducted [255]. Rosa and Fortes [256] studied the cork compression up to 80 % strain and found that the recovery rate reduces with time and rises with the degree of deformation applied earlier. The tensile behaviour of cork, as well as radial bending, have also been investigated [257][258]. The mechanical behaviour of cork is linked to its structural characteristics as well as the quantity and size

of flaws, according to the investigations. However, the impact of cork density on compression and recovery qualities has received less attention, especially for strains of 20% to 30%, which correspond to cork stopper deformation in the bottle and bottling, respectively. Ofélia Anjos et al. (2014) investigated the effect of cork in this piece. The impact of cork density on the mechanical behaviour of cork during compression, as well as subsequent dimension recovery. The mean density and porosity of samples evaluated in each compression direction are identical for each density class, thus allowing the effect of compression direction to be studied for the various cork density classes. Porosity rose as density climbed from lower to higher. The density class impact on porosity was highly significant, accounting for 73 percent of the total variation [259]. The main objectives of incorporating natural waste cork into building materials are to reduce the density, and provide excellent thermal insulation, and combustion protection due to its very high resistance to fire. Moreover, one of the strong advantages of cork waste usage besides the environmental benefits is the cost savings.

2.8. Summary

As outlined in this chapter, research on the alkali-activated materials (AAMs) as well as alkali-activated foamed materials (AAFMs) exhibit superior mechanical and physical properties including high early strength, low shrinkage, good thermal and fire resistance, and good chemical resistance. AAMs tend to be a more environmentally friendly alternative to OPC. Moreover, one of the most significant waste sources in the EU is mining waste and the majority is disposed of in heaps (after the extraction of the valuable mineral) and the reuse and integration of these waste resources in the building industry has the potential for eco-friendly materials in addition to being cost-effective. Furthermore, the alkali activation technology has great qualities to make it a sustainable and environmentally beneficial choice for improving life services and infrastructure as well as lowering maintenance costs. However, the lack of suitable application is the major concern for these new materials since numerous investigations have been carried out but received less attention. The following conclusions can be drawn:

- Alkali-activated materials (AAMs) have been discovered to differ greatly from Portland Cement-based (OPC) systems, not only in chemical formation but also in the manufacturing process; this has been the key barrier to understanding, exploiting, and commercialising this technology.
- The research and development history of chemically activated materials are still in its early stages; there has been a significant leap in determining fundamental concepts related to its hardening process and microstructure.
- Alkali-activated foams (AAFs) appear to be a very promising material since they are formed at temperatures below 100° C and possess properties like foamed glass or foamed ceramics, both of which are generally produced at highly elevated temperatures, over 900° C. Several products that are based on alkali-activated precursors derived from various raw and waste materials have been reported in the literature. Among many, the main precursor for AAMs and AAFs is fly ash.

- It is possible to produce aerated concrete Metakaolin-based geopolymer with different densities throughout hydrogen gas generated by the Al powder foaming agent in alkaline media [22].

- Fly ash, alkaline activators, and aluminium powder (Al) led to the design, synthesis, and optimization of fly ash foams (FAF) [201].

- Heat curing enhanced the degree of geopolymerization and, as a result, the compressive strength of the material increased [25].

- Alkali-activated foamed materials and/or geopolymers are fire-resistant materials and hence, fabricating lightweight geopolymers with enhanced thermal resistivity can be considered as an effective way of their usage.

- Research has also begun to evaluate a range of different waste precursor materials suitable for chemical activation, as well as the main factors that influence the properties of chemically-activated materials. However, due to the lack of standardisation and limited control over precursor resources, the knowledge gathered for one type of chemically activated materials cannot always apply to another.

- In order to achieve more eco-friendly buildings and constructions, the use of different by-products and natural resources such as cork, have become increasingly important to improve the energy and acoustic performance of buildings.

- There are still many essential procedures to be fulfilled before the alkali-activated materials industry can be recognised, particularly its long-term durability performance.

Chapter 3 - Materials and experimental Methods

In the first section of this chapter, the materials used are described in detail, and an evaluation of the characteristics of the aluminosilicate materials like tungsten waste mud (TWM) and others is carried out. In the second section the experimental methods, mixture design procedures, as well as curing conditions of different stages of this research work, are described. In addition, the tests performed are also presented.

3.1. Materials

The dry mixture composition (precursors) in this investigation consisted mainly of tungsten waste mud (TWM), grounded waste glass (WG), metakaolin (MK), as well as a liquid solution mixture composed of sodium silicate (SS) Na_2SiO_3 and sodium hydroxide (SH) NaOH. In addition, expanded granulated cork (EGC) was incorporated in this research together with the alkali-activated binder (AAB) to develop a new alkali-activated lightweight foamed materials (AALFMs) by using a chemical foaming process with aluminium powder (Al) besides hydrogen peroxide (HP) as a foaming agent. Moreover, river sand (RS) was used for the synthesis of alkali-activated foamed mortar (AA-FM). As described in the next section properties such as density, compressive strength, and porosity were determined in the produced alkali-activated binder/mortar containing different percentages of expanded cork (EGC) particles. Microstructure characterization was carried out by SEM.
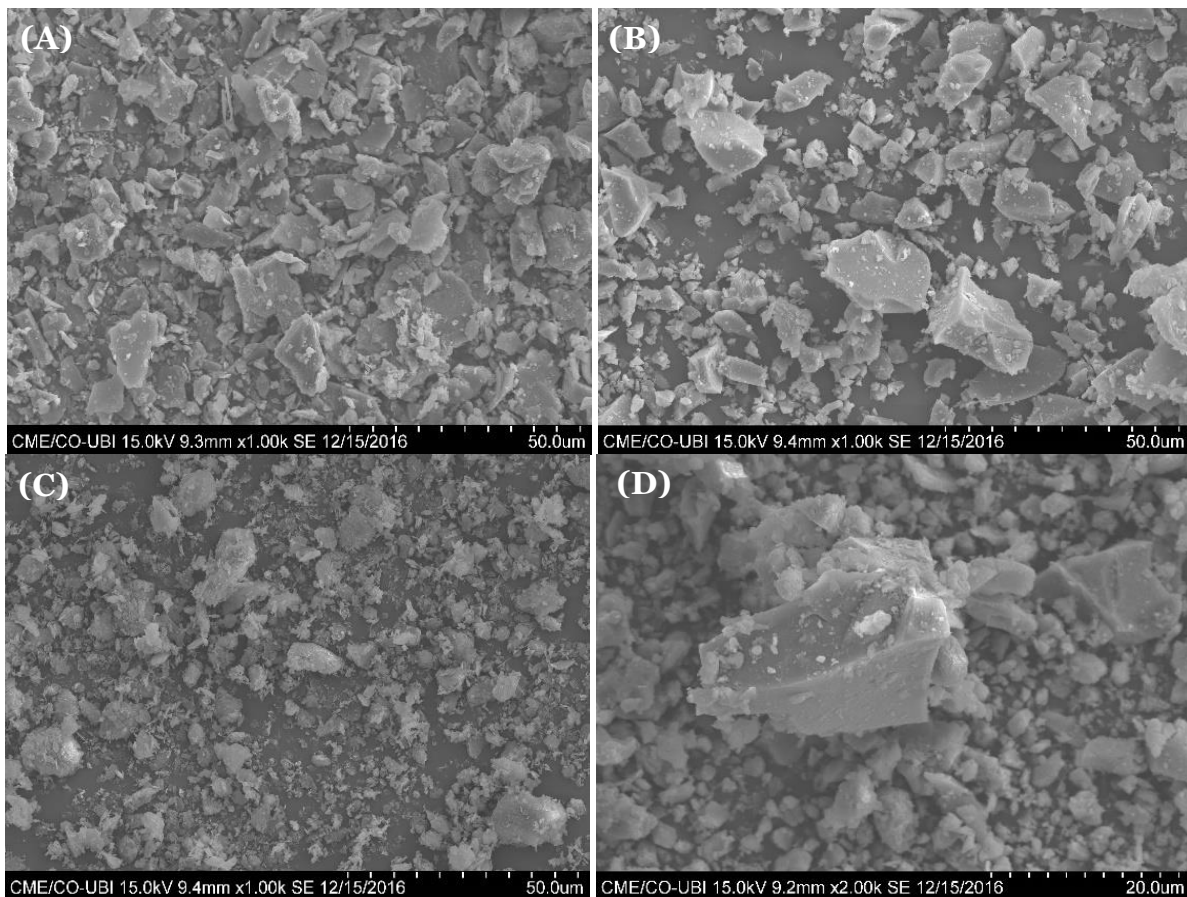
Figure 3.1 - *SEM images of (A); TWM, (B); WG, (C); MK, (D); OP-Cement.*

3.1.1. Precursors

The tungsten waste mud (TWM) was collected from the deposit field of the Panasqueira tungsten mining waste mud in Covilhã, district of Castelo Branco, Portugal. The TWM was used as an aluminosilicate rich precursor. The waste mud was first dried in the oven at a temperature of 60° C for 24h; then, the dried waste mud was mechanically disaggregated using a crushing machine; finally, the mud was sieved to obtain different fractions of particle sizes. It is noticed that the mining tailings are mostly composed of silica and alumina, with a substantial amount of calcium and iron. Furthermore, grain size distribution analysis for the TWM with different maximum particle sizes of powders (150 μm, 300 μm, and 500 μm) was performed by the sedimentation method as demonstrated in Figure 3.6. Additionally, mechanical sieving analysis for the TWM was performed following BS ISO 13320:2009. The mining waste mud was subjected to SEM imaging as shown in Figure 3.1 -A. The SEM micrographs demonstrate that TWM particles have irregular shapes. The Loss on Ignition (LOI) of TWM was determined using simultaneous thermogravimetric and differential scanning calorimetry (TG-DSC) as defined in section 3.2.10.3. thermogravimetric analysis. The TWM lost approximately 11.34 percent of its weight at 1000° C. Regarding the mineralogical composition of TMWM, the X-ray diffraction pattern showed their crystalline nature, which consists mainly of muscovite, quartz (SiO2) and clinochlore; Muscovite is a dioctahedral layered structure made up of two sheets of connected SiO4 tetrahedral with the general formula $KAl2(Si_3Al)O10(OH)_2$. Figure 3.2. shows an example of XRD analysis of TMWM from the Panasqueira mine.
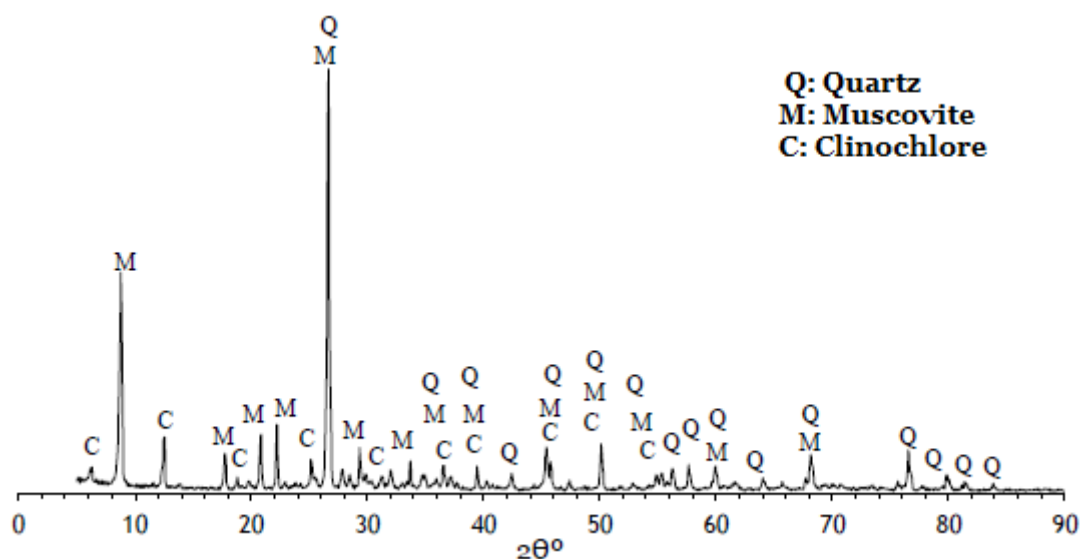
***Figure 3.2** - X-ray diffraction pattern of TMWM from the Panasqueira mine.*

Ground waste glass (WG) was obtained from glass bottles which were crushed and finely milled. The waste glass powder has a light grey colour. It consists mainly of alumina and silica with a substantial amount of calcium and iron and was added to the mixtures as another source of silicate in the matrix. After the bottles' grinding grain size distribution analysis of the WG was similarly made for different maximum particle sizes of powders (150 μm, 300 μm, and 500 μm), was performed by the sedimentation method as demonstrated in Figure 3.7. In addition, the mechanical sieving was

56

similarly performed to TWM. Moreover, SEM imaging was also performed on waste glass powders. As shown in Figure 3.1 -B. SEM micrographs of the milled waste glass (WG) powders have irregular shapes.

Metakaolin (MK) used in this investigation was provided by the German multinational chemical company BASF with a given Specific Gravity of 2.50 (g/cm^3) and a pH = 6 (28% solids). Figure 3.1 - C shows the SEM imaging of metakaolin at 1000x magnification.

Ordinary Portland cement (OPC): The OPC was used in the preliminary phase of this research work for the feasibility of alkali-activated foamed binders to increase the setting time of the produced material. OPC was provided by *Secil* (a business group whose activity is based on the production and sale of cement) Cimento Portland de Calcáirio AN197-1. CEM II/B-L 35.2 N cement type was used in this investigation. SEM image of OPC is presented in Figure 3.1 -D.

Natural expanded granulated cork (EGC): the EGC particles used in this research were kindly provided by (SOFALCA Sociedade Central de Produtos de Cortiça, Lda, Abrantes, Portugal). After being boiled for about 1h and then expanded, flat cork has dried to 20% moisture content, and then it was ready to be used and processed. The interior gas in the cells expands to create a very tight, uniform cell structure. SEM micrographs of the expanded cork cell structure were analysed through high-resolution images using the Scanning Electron Microscope (HITACHI S-3400N) at the University of Beira Interior (UBI) optical centre and are presented in Figure 3.3.
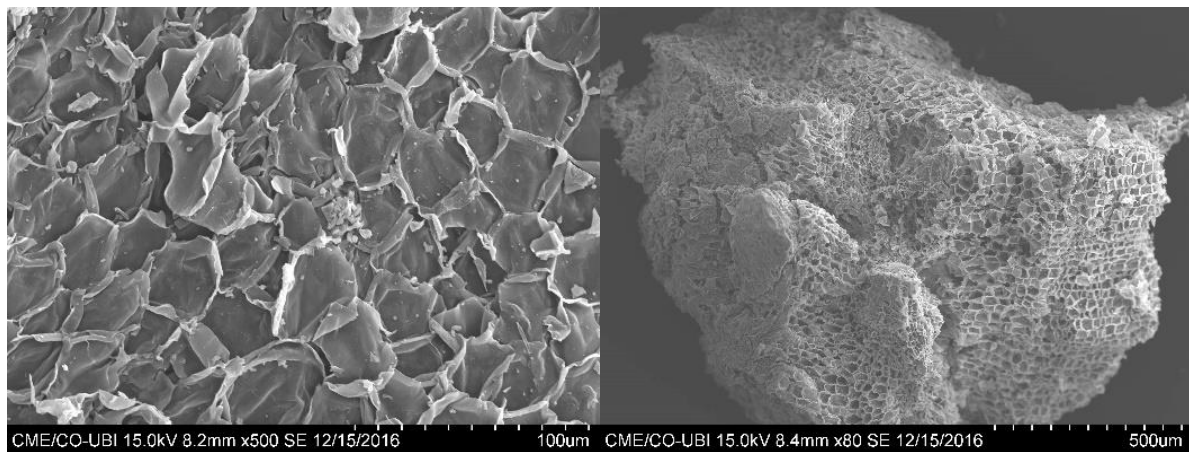
Figure 3.3 - SEM EG-Cork granules at high (left) and low (right) magnification.

Characterization of Cork particles: In this study, cork was used as aggregate. The cork particles are extracted from the outer bark of the cork oak tree (Quercus suber L.) as a natural raw material. Cork particles are shown in Figure 3.4. were provided by Sofalca Lda, Abrantes, Portugal, and present a brown to dark brown colour. The EGC particle sizes ranged from 0 – 2 mm, and density ranges from 70 to 80 kg/m^3.
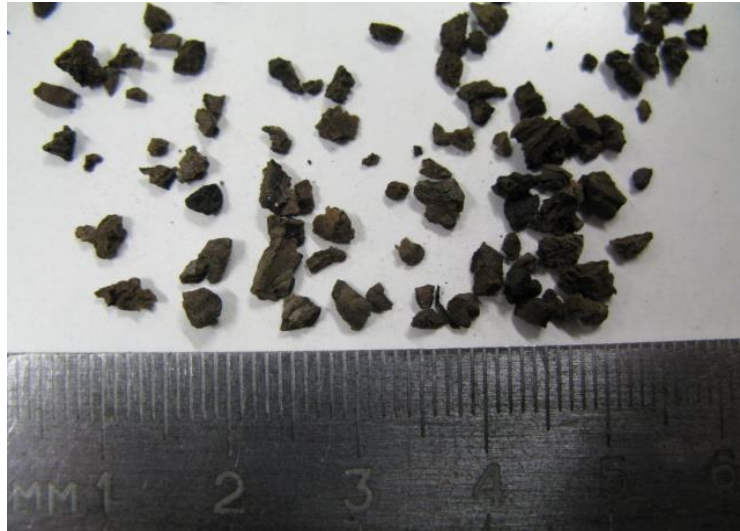
Figure 3.4 - *Natural cork particles.*

The fine aggregate used was obtained by screening natural materials from river dredging marketed by Tabal-Sepor Areias e Argamassas, Lda. The river sand (RS) was also sieved under 2 mm diameter to obtain finer particles for the mortar. Figure 3.5 - shows an image of the river sand used in this investigation. The particle size of RS is shown in addition to TWM and WG in Figures 3.6 and 3.7, respectively.

Figure 3.5 - *River Sand particles (RS).*

3.1.2. Particle sizes of powders

The particles size analysis of the different powders sieved under (150 μm, 300 μm, and 500 μm) of TWM and WG used in this investigation were determined as a result of the sedimentation method, British standard BS 1377-2:1990, using the hydrometer. While the method test for sieving river sand (RS) was determined with the particle size analysis - sieving method NP EN 933-1. Figures 3.6 - and 3.7 - show the particle sizes distribution curves of TWM and WG, respectively.
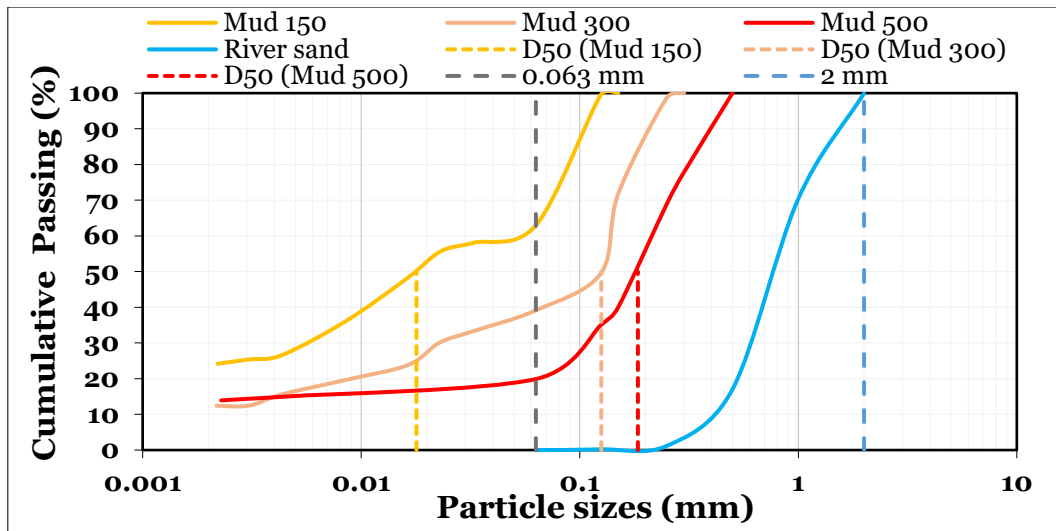
Figure 3.6 - *Particle sizes analysis of the TWM (<150μm), (<300μm), (<500μm), and river sand (RS<2mm).*
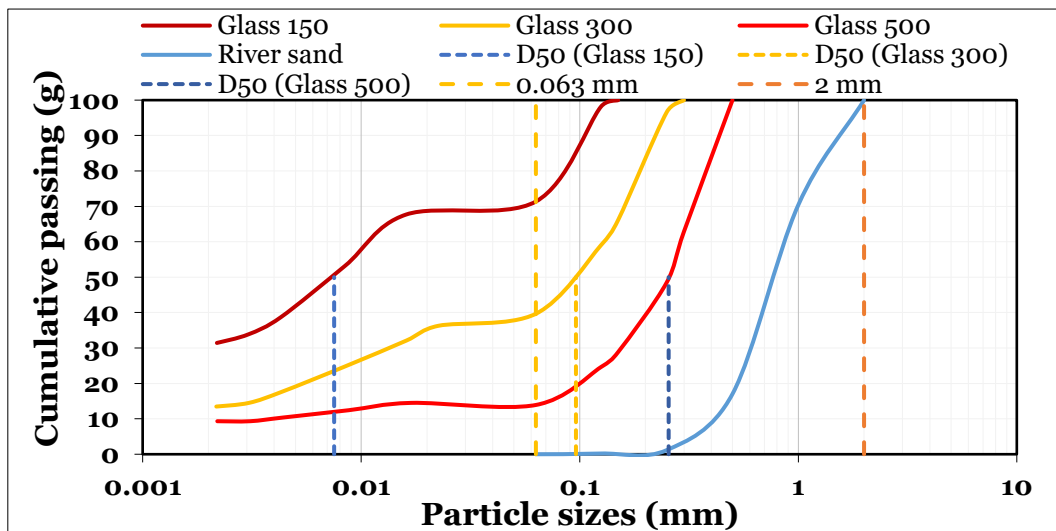
Figure 3.7 - *Particle sizes analysis of the WG (<150μm), (<300μm), (<500μm), and river sand (RS<2mm).*

The typical chemical composition of the powders in which the main oxides are presented in Table 3.1. The composition was determined, in several samples of TWM, MG, metakaolin (MK), and ordinary Portland cement (OPC), through Energy Dispersive Spectroscopy (EDS) technique at the optical centre of the University of Beira Interior (UBI). In the case of TMWM, it consists mainly of silica and alumina with a smaller percentage of iron and potassium. Blaine fineness was performed using ACMEL- Lab device (Model BSA1, 2006) at the construction materials laboratory DECA-UBI. Furthermore, the powders made up of the precursor (TWM, GG, and MK) such as bulk density was determined using a gas displacement pycnometer apparatus (model. AccuPyc1340, Micromeritics, Norcross, Georgia), in addition, the Blain specific surface of the different powders was determined according to EN 196-6, by using Blaine air permeability apparatus (model. ACMEL LABO BSA1). The physical properties of the powders are given in Table 3.2.

Table 3.1 - Oxide chemical composition (weight %) and Blaine specific surface of the powders.

Constituents	Tungsten waste mud (w.%)	Milled waste glass (w.%)	Metakaolin (w.%)*	P. Cement (w.%)*
SiO_2	46.67	68.13	52.28	10.02
Al_2O_3	17.05	2.80	42.99	2.62
TiO_2	0.6	-	-	-
K_2O	4.90	0.86	0.94	1.83
Na_2O	0.85	12.52	0.32	0.09
CaO	0.69	10.52	-	76.79
SO_3	7.90	0.23	-	5.03
Fe_2O_3	15.47	2.90	1.49	2.49
MgO	4.83	2.04	0.47	1.05
ZnO	1.04	-	-	-
Total	100	100	98.49	99.92

* Portland Cement – SECIL CEM II/B-L 35.2N; * Metakaolin – (BASF- the chemical company).

Table 3.2 - Physical properties of the components of the precursors.

Materials	Particle sizes of powders	Blaine fineness	Bulk Density
	<150 µm	1142	3.0048
TWM	<300 µm	896	3.0363
	<500 µm	771	3.2196
	<150 µm	1896	2.5301
WG	<300 µm	1133	2.5254
	<500 µm	824	2.5308
MK	<2 µm	4467	0.2693

3.1.3. Alkaline Activators

The alkaline liquid activators used could react with the silica (Si) and the alumina (Al) in the raw materials of natural minerals or in by-product materials such as waste glass (WG) and metakaolin (MK) to produce alkali-activated binders [260]. The alkaline activation of materials can be defined as a chemical process that provides a rapid change of some specific structures, partial or totally amorphous, into compact cemented frameworks [261]. The used alkaline activators in this research are a mixture of sodium hydroxide (NaOH) with sodium silicate (Na_2SiO_3). Table 3.3 presents the chemical composition of precursors as given by suppliers (José Manuel Gomes dos Santos, Lda., LUXCITANIA, Lda).

Table 3.3 - *Chemical composition of activators.*

Oxide (g) / Materials	Sodium Silicate (SS)	Sodium Hydroxide (SH)
Na_2O	19.37	13.02
SiO_2	62.60	0.000
Al_2O_3	0.90	0.000
H_2O	142.32	43.27
K_2O	-	-
CaO	-	-

Sodium silicate is also known as water glass or liquid glass. This material is available both as an aqueous solution as well as in a solid form. In this research, the aqueous solution with the reference D40 SS was used. Sodium silicate is readily soluble in water, producing an alkaline solution. It is one of several related compounds, which include sodium ortho-silicate, Na_4SiO_4, sodium pyro-silicate, Na_6SiO_2, and others. All the components are glassy, colourless, and soluble in water.

Sodium hydroxide (NaOH), also known as lye and caustic soda, is an inorganic compound. It is a white solid highly caustic metallic base and alkali salt. Sodium hydroxide (SH) in some particular applications is prepared in solutions with water, ethanol, and methanol. Dissolution of solid sodium hydroxide in water is a highly exothermic reaction in which a large amount of heat is liberated, thus posing a threat to safety through the possibility of splashing. The resulting solution is usually colourless and odourless with a slippery feeling upon contact which is a characteristic shared with other alkalis. Sodium hydroxide (10 M) was used in this research work.

3.1.4. Foaming agent

Foaming agents, also known as blowing agents are substances that are capable of producing a cellular structure via a foaming process in a variety of materials that undergo hardening or phase transition, such as polymers, plastics, and metals. They are typically applied when the blown material is in a liquid stage. The cellular structure in a matrix reduces density and increases thermal and acoustic insulation while increasing the relative stiffness of the original polymer.

Aluminium powder (Al) is widely utilized as a foaming agent in alkali-activated and/or geopolymer concretes productions. In this investigation, Al powder was used in the foaming process to create bubbles in the alkali-activated materials (AAMs). The Al powder was provided by ACROS organics and had an average particle size of 75 microns, with a purity and molar mass of 99 % and 26.98 Al, respectively. In this research work, Al powder was introduced by adding different amounts/percentages ranging from 0.1g to 0.5g for the synthesis of the different AALFMs.

Hydrogen peroxide (HP) is a chemical compound with the formula H_2O_2. It is a very pale blue liquid that is somewhat more viscous than water in its purest state. It is used as an oxidant, bleaching agent,

and antiseptic in a weak solution (3 % - 6 % by weight) in water for consumer use, and in larger concentrations for industrial use. When heated, concentrated hydrogen peroxide, or high-test peroxide, decomposes explosively and has been employed as a rocket propellant. In this investigation, HP was used in the preliminary work for the feasibility of making alkali-activated foamed materials by adding different amounts ranging from 1.29 g to 3.87 g.

3.2. Experimental methods

3.2.1. Characterization of the binder

It is essential to tailor the content and composition of the alkali activators as well as aluminosilicate precursor materials, in addition to the aggregate components in an alkali-activated binder/mortar mixture design. The powders that make up the precursor in this research work were first dried at 80 °C for 24 hours. In this investigation, the mixer used is presented in Figure 3.8 as well as the mixing procedures of the dry powders used for the production of tungsten-based waste mud (TWM) alkali-activated materials are as described:

- One minute of low-speed mixing of dry components, including aluminium powder and cork particles (if incorporated);
- Pouring the alkaline solution into the bowl, which contains a composition of SS and SH, and mixing at low speed for 60 seconds;
- Stopping for 60 seconds to hand-mix the mixture to homogenize and eliminate the anhydrous components;
- Mix pastes at high speed for two minutes to get a homogenous fresh paste for casting moulds.

Figure 3.8 - Mixer used for the mixing procedure of the paste.

3.2.2. Mixing of the alkaline solutions

During this research work, the mixing of the alkaline solutions includes in the first step the preparation of 10M sodium hydroxide NaOH (SH) 24 hours before; then they were mixed with liquid sodium silicate Na2SiO3 (SS) (magnetic stirring at a rate of 500 r.p.m. for about 5 minutes). Two different activators ratios of Sodium silicate/Sodium Hydroxide (SS/SH = 3:1 and 4:1) were used in this investigation.

3.2.3. Mixture design procedures

During this research work, the synthesis of the AALFMs includes three steps: (a) preparation of the activation solutions, 10M sodium hydroxide NaOH (SH) mixed with liquid sodium silicate Na_2SiO_3 (SS) (magnetic stirring at a rate of 500 r.p.m. for about 5 minutes); the sodium hydroxide (SH) was first prepared and used in the formula after 24 hours; (b) mixing of the raw materials incorporating cork particles (dry powders and the Al powder). The precursors were prepared by dry mixing the powders: tungsten waste mud (TWM), ground waste glass (WG), and metakaolin (MK) (all dry powders were mixed well for 1 minute at low speed to obtain a homogeneous distribution); and (c) moulding and curing the specimens after mixing the solid components with the alkaline activating solution, for about 2 minutes at a fast speed. The mixer and preparation of the precursors are shown in Figure 3.8.

Several mixtures were produced using the precursor components mainly of tungsten waste mud (TWM) powder, milled waste glass (GG), Ordinary Portland cement (OPC), metakaolin (MK), and natural expanded granulated cork (EGC). Alkali-activated tungsten-based were studied in four phases. In the first phase (A), a preliminary investigation of combination composed of 80% (TWM), 10% (WG), 5% (MK), and 5% (OPC) and the others 70% (TWM), 20% (WG), and 10% (MK).

Table 3.4 - Combinations of precursors and activators.

	Precursors (%)	EGC Particles (%)	River Sand (%)	Activators SS/SH	P/A	Curing
Phase A	80 % TWM + 10 % WG + 5 % MK + 5 % Cement (500 µm)	0 to 40	-	4;1 4;1 4;1 4;1	3.5 3.5 2.8 2.6	60°C For 24h
Phase B	70 % TWM + 20 % WG +10 %MK (150 µm, 300 µm, 500 µm)	-	-	3;1 3;1 3;1	2,5;1 3;1 3;1	60°C For 24h
Phase C	70 % TWM + 20 % WG +10 %MK (150 µm, 300 µm, 500 µm)	- 10 to 40	50 50	3;1 3;1 3;1	2;1 1.5;1 1.5;1	60°C For 24h
Phase D	70 % TWM + 20 % WG +10 %MK (150 µm, 300 µm, 500 µm)	10 to 40	-	3;1 3;1 3;1	2.3 2.6 2.6	60°C For 24h

Figure 3.9. presents an explained diagram of the process to produce the foamed materials by using an alkali-activation system. Table 3.4. presents the detailed combinations of the precursor and activators for the preparation procedures of the different alkali-activated lightweight foamed materials (AALFMs) carried out in this investigation. After mixing, all these fresh mixtures were used to prepare the samples for the different tests which are presented in the next paragraphs. Additionally, throughout the laboratory work, the precursor to activators ratio as well as activators ratio (SS/SH) were used as presented in Table 3.4.
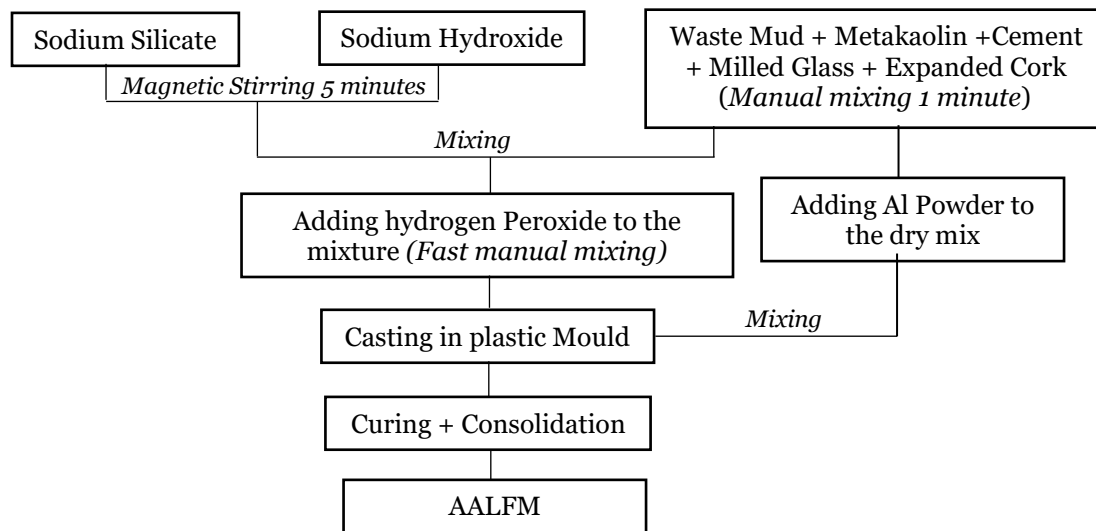
Figure 3. 9 - *Schematic process of the production of alkali-activated lightweight foamed materials (AALFMs).*

3.2.4. Curing conditions

After mixing and moulding, the filled moulds were kept in an oven at a temperature of 60° C for 24 hours. For synthesis and to avoid water evaporation of the AABs during curing, the filled moulds were covered with plastic film during the oven curing synthesis. The specimens were de-moulded after the initial 24 hour oven curing period and were left to cure under laboratory conditions (open-air and at a temperature of about 20° C) in sealed plastic bags, until the testing day (days 7, and 28). The samples were cut to have a cubic dimension using a masonry block saw that has a small disc diameter to avoid micro-cracks, several cubic specimens of (40 x 40 x 40mm^3 and 25 x 25 x 25mm^3) were cut. During the curing process, it was preferred to switch the oven on 30 minutes earlier before putting the moulds.

Oven curing at 60° C: The process of oven curing of the samples began with the oven being preheated at 60°C for 30 minutes. This was to ensure that the oven was at the right temperature when the samples were placed inside and that the samples were not exposed to lower temperatures while the oven was heating up. Otherwise, the samples would have also been subjected to a temperature change. While the oven was heating up, the samples were ready to be placed inside. This preparation process involved sealing the samples into plastic bags to ensure that moisture was retained within the sample. After that, the samples were then left to cure for 24 hours. The samples were removed from

the moulds after 1 day and were allowed to settle at room temperature before testing on days 7, and 28. Additionally, the samples were labelled and identified, and they were secured where they were placed.

Curing at room temperature: Samples were also left curing at room temperature until the testing days in order to gain an insight into how the mixtures will perform in a more practical building application. This is a particularly useful variable since it is most similar to those conditions which would be found on a construction site in which the material would be cast in-situ or even in a precast factory.

3.2.5. Method for hydrogen gas measurement

The volume of the mixtures to be studied and the size of the moulds to adopt were based on the preliminary measurement of the amount of hydrogen released for a specific amount of Al. Equation 3.1 represents the reaction between the Al powder with an alkaline activator solution which results from a significant release of hydrogen (H_2). The total volume of hydrogen released depends on the amount of Al powder added to the solution.

$$2AL + 6NaOH \rightarrow 2Na_3AlO_3 + 3H_2 \qquad (3\text{-}1)$$

The measurement of the total volume of hydrogen released was determined by a simple laboratory setup, as presented in Figure 3.10. For that, several small amounts of Al powder were mixed with a 10M sodium hydroxide (SH) solution, and the H_2 volume produced was determined using a graduated measuring cylinder. It was verified that 1g of Al powder produces about 1.5 l of hydrogen (H_2). It was also confirmed that the reaction occurs very quickly, e.g., when 0.5 g of Al powder is stirred with 20 ml of 10M (NaOH) solution, the reaction lasts about 90 seconds.

Figure 3.10 - *Setup to measure the H_2 volume released of Al powder reaction with a 10 M NaOH solution.*

3.2.6. Expansion volume

The expansion volume of the alkali-activated foamed materials is caused by the foaming process in which the gas released in the mixture changes the shape, area, volume, and density of the material and the mixture expands (increases in size). The method to determine the expansion volume of the specimens in this study was obtained with equation 3.2:

$$Ev = [(Tv-Iv)/Tv] \times 100 \qquad (3.2)$$

- Ev: Expansion volume (%).
- Tv: Total volume (cm^3) - (height of sample at the end of the experiment).
- Iv: Initial volume (cm^3) - (height of sample at the start of the experiment).

3.2.7. Bulk Density

The density of the samples (Foams) was determined by measuring the weight of the specimens with a precision scale and their dimensions with a precision electronic calliper. The density (d) of the samples was computed by dividing the dry mass (m) by the volume (v) (i.e., the so-called geometrical density). Several cubic specimens of 40 x 40 x 40 mm^3 and 25 x 25 x 25 mm^3 size were used for the dry density measurement and calculated through the given equation (3.3):

$$D_{Dry} = M/V \qquad (3.3)$$

3.2.8. Porosity

The porosity of each cube sample was measured accordingly to the EN 12390 − 7: 2009 Standard with some modifications. One specimen from each batch was oven-dried at 60° C ± 5° C for 24h to achieve a constant weight before testing. The samples were then immersed in water for 24 hours to be completely saturated. After that, porosity was determined for LW1 mixes using equation 3.4:

$$Porosity (\%) = [(Ws - Wd) / Wd] \times 100 \qquad (3.4)$$

Where: Ws is the saturated weight (g) and Wd is the oven-dry weight (g).

3.2.9. Methods of image analysis

In this investigation, the analysis of the pores, particle sizes and their distribution within the different foamed materials were determined by the "Image J" open-source software that "understands" most image formats. It allows the characterization of the individual convex particle (size, shape, and surface). To conduct particle analysis efficiently, all images were taken with the same magnification and with similar contrast. The Feret diameter method was adopted. The Feret diameter averaged over all directions (F) is equal to the ratio of the object perimeter (P) and the number pi (constant of Archimedes), i.e. (F) = P/p.

3.2.10. Microstructural characterization

3.2.10.1. Scanning Electron Microscopy (SEM/EDS)

Microstructural studies were examined through high-resolution images using the Scanning Electron Microscope (HITACHI S-3400N) micrographs at the University of Beira Interior (UBI) optical centre. To overcome the major constraint of surface damage, backscattered and secondary electron images were obtained from polished samples. A low-speed saw was used to cut 5 mm thick slices for the polished samples. The samples were polished after being treated with a low viscosity resin.

Figure 3.11 - *Photos of the machine used to take SEM images.*

3.2.10.2. X-ray Diffraction analyses
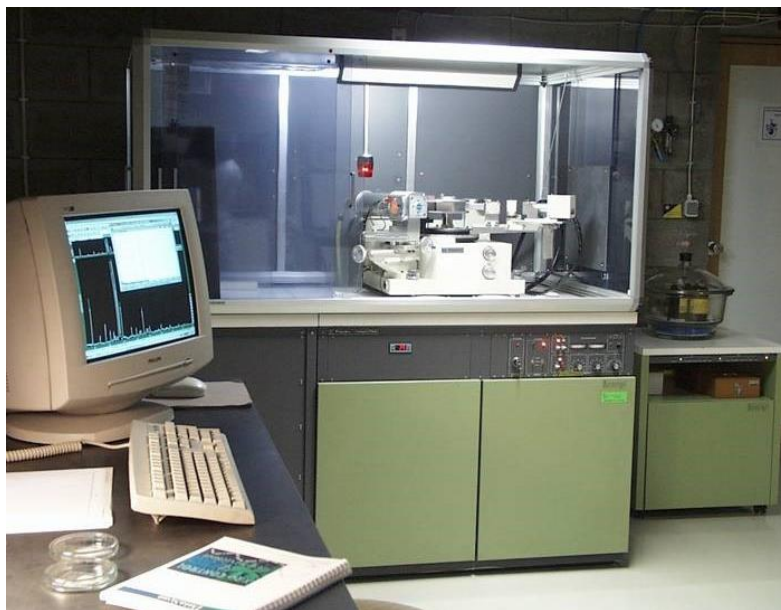
Figure 3.1 *- Machine used to obtain XRD results.*

To assess the crystalline structure of these mixtures, X-ray diffraction (XRD) analysis was used. Powder X-ray diffraction (XRD) was determined using a DMAX III/C Rigaku device with Cu radiation at 1.5405 Å. Figure 3.11 presents the x-ray interferometry device at the Department of Physics, UBI.

3.2.10.3. Thermogravimetric analysis

Thermogravimetric analysis (TGA) is the technique for determining the chemical composition of a sample. TGA (the name is self-explanatory) allows us to examine any weight loss while the sample is subject to an increase in temperature. A relationship can be drawn between temperature and weight loss and therefore it can be used to determine at what temperature weight is lost and how much weight has dropped. TGA is commonly used in research and testing fields to identify the characteristics of materials, such as polymers cement paste and mortars, to determine chemical breaking temperatures, moisture content, as well as the level of inorganic and organic components in materials.

During this research work the apparatus used was a (TG-DSC) TA Instrument SDT Q-50. The TGA apparatus consists mainly of an electro microbalance, a furnace, an operation programmer unit, and a data acquisition unit. The TGA worked with nitrogen gas at maximum temperatures ranging from 0 to 1000° C. Another critical component of this equipment is the cooling box which must be operational before the test can begin. After finishing the TGA, the findings may be visually produced using Universal analysis. The study aimed to use the TGA technique to determine the loss of weight (LOI) present in the TWM component under temperature effect and it is also used to determine bonding H_2O and residual CO_2 levels. Non-calcined TWM was taken from the sieved materials with diameters ranging from 0 and 500 μm.

Figure 3.12 - TGA apparatus series Q50 from TA Instrument Company.

3.2.11. Compressive strength

The compressive strength test was made with (ADR Touch ELE international limited machine, at the construction technology and mechanic test laboratory, DECA-UBI) as presented in Figure 3.13 (a-

right), for non-foamed samples. The compressive load was applied to the cubic specimens with a pace of 0.5 N/s.mm^2 with a low-speed rate based on the test. Whereas foamed samples were tested with (AUTOGRAPH AGS-X, 10KN SHIMADZU machine at the mechanics of materials and mechanical technology laboratory, Centre for Mechanical and Aerospace Science and Technologies C-MAST - UBI) as presented in Figure 3.13 (b-left). The compressive load was applied at 0.10 N/s.mm^2. In order to obtain compressive strength, three 40 x 40 x 40 mm^3 cubes and three 25 x 25 x 25 mm^3 were tested. The cubes were obtained by cutting with a diamond cutting blade from the casted cubic specimens produced. The specimens were tested on day 28 (the results for the compressive strength were obtained on day 28).

*Figure 3.13 - Machines used for the compressive strength test **(left)**: Autograph AGS-X, 10 KN SHIMADZU, **(right):** ADR Touch ELE international limited.*

3.2.12. Thermal conductivity

The tests for the determination of the thermal conductivity were carried out using a NETZSCH HFM 436/3 Lambda flow meter at Sofalca Lda (Estrada Nacional 2, Km 412,2 Bemposta, 2205-213 Abrantes, Portugal). The thermal conductivity tests were carried out in accordance with the European Standard EN 12667: 2001-EN- "Thermal performance of building materials and products - Determination of thermal resistance through guarded hot plate and heat flow meter methods - Products of high and medium thermal resistance". The specimens were preconditioned for a period of 120h, in an environment characterized by an ambient temperature of 23 ± 2° C and relative humidity of 50 ± 5% and the thermal conductivity tests were carried out in the same environment with a temperature of 23 ± 2° C and 50 ± 5 % relative humidity. The specimens were tested in the dry state at a mean temperature of 10 ± 0.3° C and dried in an oven at about 70 ± 2° C. The accuracy of the determination of this thermal parameter is estimated at ± 2.8%. The thermal conductivity values were obtained for the foamed alkali-activated materials (AALFM) from 2 cubic slabs of 100 x 100 x 30 mm^3.

Figure 3.14 - *Machine for the thermal conductivity test at Sofalca Lda.*

3.3. Summary

This chapter presented the materials used in this study, along with the experimental methods. In the first section, the characterization of the raw materials, as well as natural waste cork particles, were described. In the second section, the experimental methods for the manufacture of alkali-activated foamed binders/mortars, incorporating expanded granulated cork (EGC) as lightweight aggregates are explained. These procedures allow for optimizing the content of these mineral raw materials to design alkali-activated foams (AAFs) and lightweight foamed materials (LWFMs) made of tungsten waste mud incorporating EGC, which will be presented in chapter 4. Moreover, the alkaline liquid solution used in this research is presented, as well as the foaming agents introduced. The foaming agent will be used in the foaming process of the alkali-activated foamed materials. The influence of the foaming agent on the properties of the foamed materials will be also presented in chapter 4.

Chapter 4 – Design and characterisation of alkali-activated foamed mixtures

In the first section of this chapter, the mixture design plan for different alkali-activated foamed materials carried out is presented. The properties of the mixtures are also highlighted. Following the mix design procedures, physical and mechanical results are presented and discussed in section 4.2 of this chapter. Microstructure analyses performed by SEM are also presented and highlighted. The mixtures under investigation are described based on the ones presented in the mixture design.

4.1. Mixture design proposals

Different mixtures were made through several combinations of (TWM, WG, MK, and OPC) as well as incorporating EGC for the production of foamed alkali-activated foamed binder/mortar by the chemical foaming method with Al powder are presented in detail in the following four combinations;

- Alkali-activated foamed materials (preliminary investigation);

- Alkali-activated foamed binders;

- Alkali-activated foamed mortar incorporating cork;

- Alkali-activated foamed binders incorporating cork;

The use of precursor/activator ratio was determined with the ease with which AALFMs can be produced, by mixing precursors (incorporating different percentages of cork particles and sand) with activators, and all components can be properly mixed. In the presence of porous aggregate (EGC), it would be expected that the maximum percentage of cork particles added absorbs (needs) a larger quantity of water, which can show a different viscosity behaviour in the mixtures.

4.1.1. Alkali-activated foamed materials; preliminary investigation

In this first phase, four different alkali-activated foamed binders CP, LW1, LW2, and LW3 were produced for the feasibility of alkali-activated lightweight foamed materials tungsten-based mining waste mud and incorporating natural expanded granulated cork (EGC). A percentage of 10 wt.% of the (TWM) was replaced with milled waste glass powder (WG), other 5 wt.% was replaced by metakaolin (MK), and another 5 wt.% was replaced by Ordinary Portland Cement (OPC), in several combinations. Waste glass (WG) and metakaolin (MK) were added to the tungsten waste mud (TWM) to increase alkali-activation reactivity, particularly by adding more quantity of amorphous SiO_2 since TMWM is composed mainly of muscovite and quartz with very low reactivity even after calcination [174]. In this study, TWM used was not calcined, and Ordinary Portland cement (OPC) was added to accelerate the curing time [262].

A total of 11 mixtures were prepared for this study as presented in Table 4.1. Mixture one (CP) was made as a reference and is an alkali-activated material containing only TMWM, MWG, MK and OPC. The mixture (CP) was the control paste mixture. Mixtures LW1 were prepared using a mix CP composition by adding different percentages of (EG-cork) expanded granulated cork (10% to 40% volume of total precursors). Mixtures LW2 and LW3 are foamed mixtures, containing only TWM, WG, and OPC, as well as an aluminium powder (Al) and hydrogen peroxide (H_2O_2), respectively, as foaming agents, with a fixed percentage of 20 vol.% of expanded cork. The precursor consisted of an SS-sodium silicate and 10M SH-sodium hydroxide solution in all mixtures.

Table 4.1 *– Preliminary alkali-activated foamed mixtures formulation.*

	TWM (g)	WG (g)	OPC (g)	Mk (g)	EGC (g) (%)	Activators (g) SS | SH		HP (g)	Al (g)	P/A Ratio	SS/SH Ratio
CP	739.09	75.50	44.62	39.25	-	205.36	51.34	-	-	3.5	4
	665.18	67.95	40.16	35.33	4.03 (10%)	184.82	46.21	-	-	3.5	4
	591.27	60.40	35.70	31.40	8.06 (20%)	164.29	41.07	-	-	3.5	4
LW1	517.36	52.85	31.23	27.48	12.10 (30%)	143.75	35.94	-	-	3.5	4
	443.46	45.30	26.77	23.55	16.13 (40%)	123.21	30.80	-	-	3.5	4
	105.58	10.79	12.75	-	20%	36.89	9.22	1.29	-	2.8	4
LW2	105.58	10.79	12.75	-	20%	36.89	9.22	2.58	-	2.8	4
	105.58	10.79	12.75	-	20%	36.89	9.22	3.87	-	2.8	4
	105.58	10.79	12.75	-	20%	29.79	19.86	-	1.29	2.6	1.5
LW3	105.58	10.79	12.75	-	20%	29.79	19.86	-	2.58	2.6	1.5
	105.58	10.79	12.75	-	20%	29.79	19.86	-	3.87	2.6	1.5

(%) – Percentage of precursors total volume; P- precursors; A- activators

The mixtures were poured into 40 x 40 x 40 mm³ moulds. The mixtures were then placed in the oven at 60° C for 24h to speed up the alkali-activation. After curing in the oven, the samples were demoulded and left to cure under laboratory conditions until testing the compressive strength on days 7 and 28. Before testing, the specimens were weighted to determine their density. The compressive strength of the specimens was performed on cubic samples (40 mm × 40 mm × 40 mm) after the curing process at the ages of 7 and 28 days. The average values from the three specimens were calculated.

4.1.2. Alkali-activated foamed binders

In this phase, we employed precursors from three different particle sizes sieved into (150 μm, 300 μm, and 500 μm) named (P1, P2, and P3) respectively, for the alkali activation of tungsten-based to obtain novel low-cost and more sustainable material. Fifteen AAFs mixtures with all varieties of precursors

(P1, P2, and P3) were produced with different amounts of Al powder ranging from 0.1 to 0.5 g, as presented in Table 4.2. The mixtures were poured into relatively large moulds (100 x 100 x 60 mm³) and left for about 30 minutes to make sure that the expansion process has finished. Then, the filled moulds were covered with plastic film and placed in the oven at 60° C for 24 hours for curing, and to speed up the alkali reaction. After curing in the oven, the samples were removed from the mould and set aside to continue the curing under laboratory conditions over the following days until the testing compressive strength at 28 days.

Table 4.2 – Alkali-activated foamed binders mixture design.

Precursors Particle sizes	Mixtures	Precursors (g)			Al powder (g)	Activators (g)		P/A
		TWM	WG	MK		SS	SH	
	P1-F1	901.49	202.46	107.72	0.1	363.5	121.17	
	P1-F2	901.49	202.46	107.72	0.2	363.5	121.17	
P1	P1-F3	901.49	202.46	107.72	0.3	363.5	121.17	2.5;1
< 150 µm	P1-F4	901.49	202.46	107.72	0.4	363.5	121.17	
	P1-F5	901.49	202.46	107.72	0.5	363.5	121.17	
	P2-F1	850.16	202.46	107.72	0.1	289.79	96.66	
	P2-F2	850.16	202.46	107.72	0.2	289.79	96.66	
P2	P2-F3	850.16	202.46	107.72	0.3	289.79	96.66	3;1
< 300 µm	P2-F4	850.16	202.46	107.72	0.4	289.79	96.66	
	P2-F5	850.16	202.46	107.72	0.5	289.79	96.66	
	P3-F1	841.34	202.41	107.72	0.1	287.86	95.96	
	P3-F2	841.34	202.41	107.72	0.2	287.86	95.96	
P3	P3-F3	841.34	202.41	107.72	0.3	287.86	95.96	3;1
< 500 µm	P3-F4	841.34	202.41	107.72	0.4	287.86	95.96	
	P3-F5	841.34	202.41	107.72	0.5	287.86	95.96	

P/A: precursors to activators ratio

Based on the results of the laboratory to determine the amount of hydrogen gas released, it was decided to adopt a minimum volume of the mixtures to be studied of about 600 cm³ and the minimum size of the moulds of 100 x 200 x 60 mm³, after noting that small amounts of Al powder release a significant volume of H_2.

4.1.3. Alkali-activated foamed mortar incorporating cork

This phase is dedicated to the development of alkali-activated foamed mortar (AAF-Mortar) and lightweight foamed mortar (AALWF-Mortar). The alkali-activated binder (AAB) is a combination of (70 % TWM, 20 % WG, and 10 % MK). A total of 30 mixtures were produced with different amounts of Al powder ranging from 0.1 g to 0.5 g, as presented in Table 4.3. The mixtures were poured into 100 x 100 x 60 mm³ covered acrylic moulds and placed firstly in the oven at 60° C for 24 hours for curing

to speed up the alkali activation. After curing in the oven, the samples were removed from the mould and set aside to continue the curing under laboratory conditions, the samples were then cut and prepared for the tests in the following days as shown in Table 4.4.

Table 4.3 - AAF-Mortar and AALWF-Mortar mixtures proportions.

Mixtures	Precursors (µm)	AAB (%)	River Sand (%)	EG-Cork (%)	Al Powder (g)	P/A
AAF-Mortar	M1 (< 150 µm)	50	50	-	0.1	2;1
					0.2	
					0.3	
					0.4	
					0.5	
	M2 (< 300 µm)	50	50	-	0.1	1.5;1
					0.2	
					0.3	
					0.4	
					0.5	
	M3 (< 500 µm)	50	50	-	0.1	1.5;1
					0.2	
					0.3	
					0.4	
					0.5	
AALWF-Mortar	M1C (< 150 µm)	50		50	0.1	2;1
					0.2	
					0.3	
					0.4	
					0.5	
	M2C (< 300 µm)	50		50	0.1	1.5;1
					0.2	
					0.3	
					0.4	
					0.5	
	M3C (< 500 µm)	50		50	0.1	1.5;1
					0.2	
					0.3	
					0.4	
					0.5	

P/A: Precursor/Activator Ratio; AAB: Alkali-Activated Binder.

Table 4.4 - Tests of the alkali-activated foamed mortar and lightweight foamed mortar carried out.

Mixtures	Compressive strength (MPa)	Density (Kg/m³)	Expansion volume (%)
AAF-Mortar	3 Cubes (25 x 25 x 25) mm³	$D = m/V$	$Ev\,(\%) = [(Tv - Iv)\,/\,Tv] \times 100$
AALWF-Mortar	3 Cubes (40 x 40 x 40) mm³		

4.1.4. Alkali-activated foamed binders incorporating cork

During this phase, Alkali-activated tungsten-based using different precursors' particle size and expanded granulated cork (EGC) were combined for the design and development of alkali-activated lightweight foamed materials (AA-LFM) using aluminium powder (Al) as a foaming agent. Several combinations of AA-LFM with all varieties of precursors (P1, P2, and P3) were prepared by adding different percentages of (EGC) expanded granulated cork (10% to 40% volume of total precursors), with different amounts of Al powder; ranging from 0.1 g to 0.5 g. A total of 60 AA-LFM mixtures were prepared for this study as presented in Table 4.5. The mixtures were poured into relatively large moulds (120 x 200 x 150 mm³) and left to expand for about 30 minutes and afterwards, the filled moulds were covered and placed for curing in the oven at 60° C for 24 hours, to speed up the alkali reaction. After curing in the oven, the samples were removed from the mould and set aside to continue the curing under laboratory conditions over the following days until the testing of compressive strength at 28 days.

Table 4.5 - Detailed composition of alkali-activated lightweight foamed materials (AA-LFM).

Precursors Particle sizes (µm)	Precursors (%)			EG-Cork (vol. %)	Al powder (g)					Activators (g)	(P/A)*
	TWM	WG	MK		0.1	0.2	0.3	0.4	0.5	(SS/SH)*	
P1 (< 150 µm)	70	20	10	10 %	P1F1C1	P1F2C1	P1F3C1	P1F4C1	P1F5C1	3;1	2.3
				20 %	P1F1C2	P1F2C2	P1F3C2	P1F4C2	P1F5C2	3;1	
				30 %	P1F1C3	P1F2C3	P1F3C3	P1F4C3	P1F5C3	3;1	
				40 %	P1F1C4	P1F2C2	P1F3C4	P1F4C4	P1F5C4	3;1	
P2 (< 300 µm)	70	20	10	10 %	P2F1C1	P2F2C1	P2F3C1	P2F4C1	P2F5C1	3;1	2.6
				20 %	P2F1C2	P2F2C2	P2F3C2	P2F4C2	P2F5C2	3;1	
				30 %	P2F1C3	P2F2C3	P2F3C3	P2F4C3	P2F5C3	3;1	
				40 %	P2F1C4	P2F2C2	P2F3C4	P2F4C4	P2F5C4	3;1	
P3 (< 500 µm)	70	20	10	10 %	P3F1C1	P3F2C1	P3F3C1	P3F4C1	P3F5C1	3;1	2.6
				20 %	P3F1C2	P3F2C2	P3F3C2	P3F4C2	P3F5C2	3;1	
				30 %	P3F1C3	P3F2C3	P3F3C3	P3F4C3	P3F5C3	3;1	
				40 %	P3F1C4	P3F2C2	P3F3C4	P3F4C4	P3F5C4	3;1	

*P/A: Precursor/Activator Ratio   *(SS: Sodium Silicate   SH: Sodium hydroxide).

4.2. Characterisation of the mixtures

Physical-mechanical and microstructural results of the produced alkali-activated foamed materials are presented and discussed in this section.

4.2.1. Alkali-activated foamed materials; preliminary investigation

4.2.1.1. Compressive strength

In the first phase (A) of the study, the compressive strength for LW1 with different expanded granulated cork (EGC) content was determined. The results presented in Figure 4.1 - shows that the compressive strength increased from 14.7 MPa at 7 days to 19.5 MPa at 28 days for zero percent of expanded cork (EGC) incorporation. It was observed that for 20 vol.% EG-Cork incorporation compressive strength is about 14 MPa at 28 days while for 40 vol.% EG-cork it decreased up to 11 MPa. This clearly indicates that the increase of EGC particles affects the compressive strength of the AALWM. However, for LW2 and LW3 foamed mixtures incorporating 20 vol.% of EGC particle, it was found that porosity strongly affects the compressive strength since all mixtures present a compressive strength lower than 1 MPa. It was also found out by other authors (Abdollahnejad et al., 2015 [225] and Hlaváček et al., 2015 [201]) that porosity and the pore size distribution greatly influence the properties of the lightweight alkali-activated materials (AALWMs). Alkali-activated foamed materials can be produced with a relatively high compressive strength as is aimed in future research work.

	0%	10%	20%	30%	40%
7 days	14.7	12.67	12.36	10.71	8.93
28days	19.5	15.57	13.93	12.52	10.88

Expanded cork granules (vol,%)
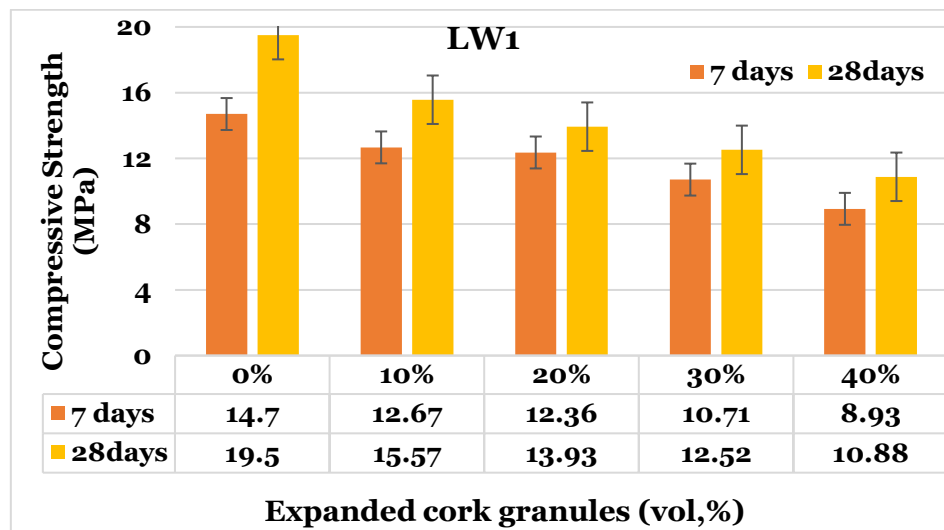
Figure 4.1 - *Compressive strength for LW1 with different (vol.%) of EG-Cork particles.*

4.2.1.2. Bulk density and porosity
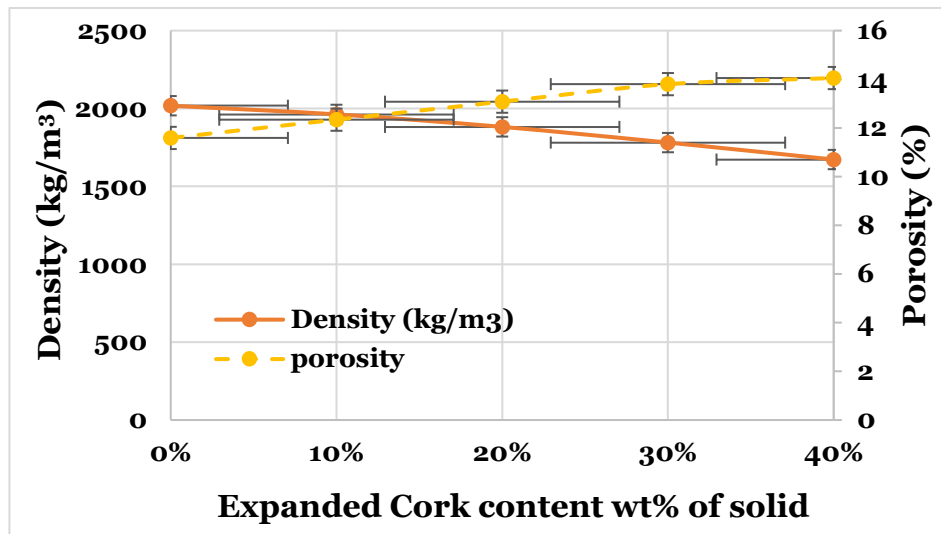
Figure 4.2 - *Change of density and porosity for LW1 as a function of expanded cork particles content; (60° C, 24h).*

The density and porosity of the alkali-activated LW1 produced incorporating the different amounts of expanded granulated cork (EGC) are demonstrated in Figure 4.2. Density is reduced for increasing expanded cork particles content, from about 2000 to 1670 kg/m3. The lowest density was found in the mixture with 40 vol.% expanded cork. In general, an increase in cork particles content led to lower density, as expected. The percentage of porosity of LW1 mixture without cork is about 11,5%, increasing up to 14% for a 40 vol.% of expanded cork content.

4.2.1.3. Microstructural characteristics

Microstructural studies (SEM) analysis for the distribution and size of pores is presented in Figure 5-13. The microstructure of the foams was examined through high-resolution images in the Scanning Electron Microscope (HITACHI S-3400N) micrographs at the University of Beira Interior (UBI) optical centre. The pore size for foamed samples LW2 and LW3 ranged between 42.3 μm small diameter pores to 4 mm diameter large voids, and the distributions of the pores in both samples were found to be relatively uniform. Accordingly, to some authors, the pores are normally closed and almost spherical when the content of H_2O_2 in the paste is low. If the content of H_2O_2 increases coalescence occurs among cells and the cells' geometrical shape changes from spherical to oval (Vaou and Panias 2010). These features were also found in this research work.
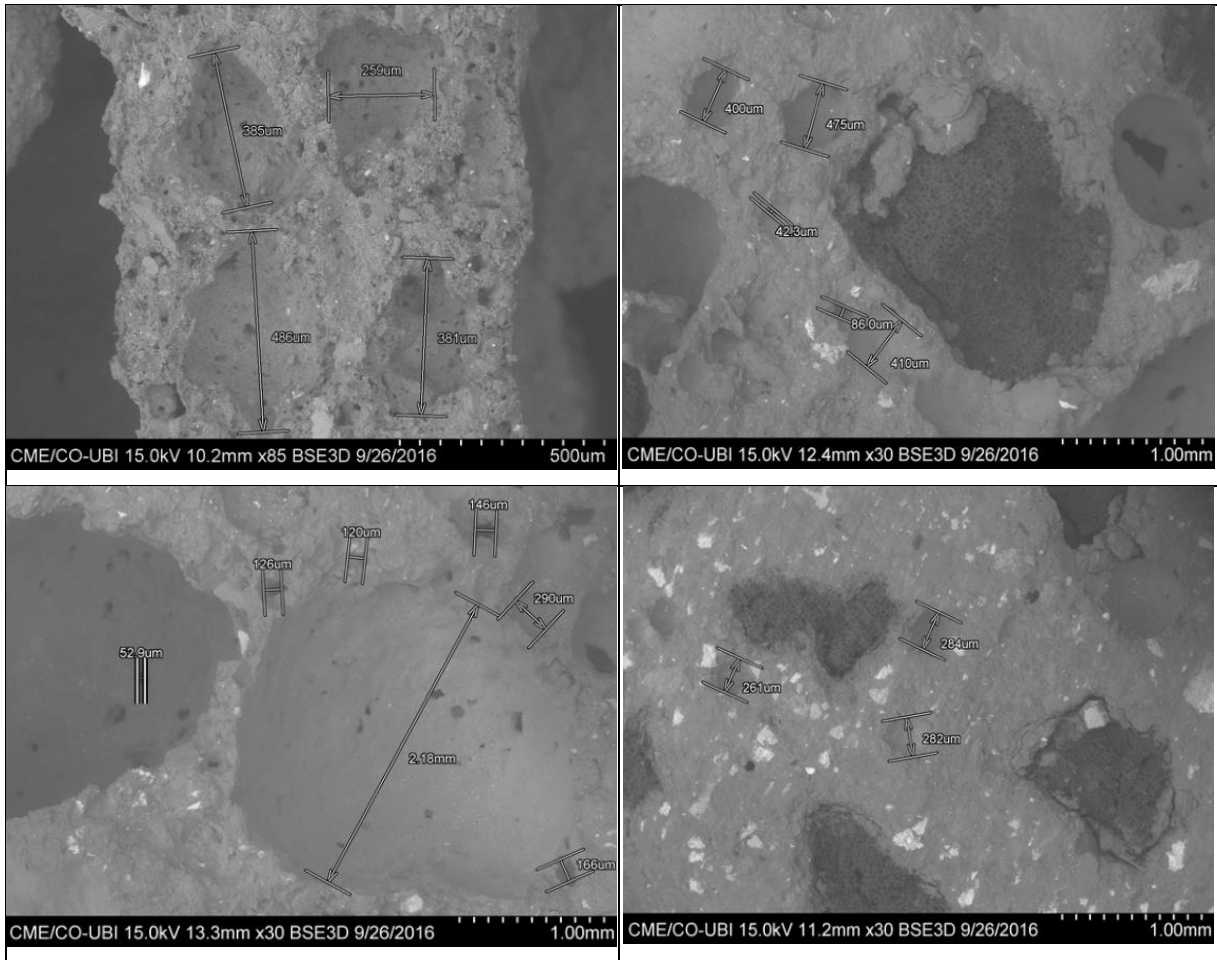
Figure 4.3 - *SEM analysis for distribution and size of pores. Left: LW2 (2 % hydrogen peroxide); Right: LW3 (2 % aluminium powder).*

4.2.2. Alkali-activated foamed binder

4.2.2.1. Compressive strength

The compressive strength results are also presented in Figure 4.4. It is observed that the highest compressive strength values are achieved with specimens made with a lower amount of Al powder, these having the lowest porosity and highest density. Compressive strength results for all samples with diverse amounts of Al powder ranged between 2.28 MPa and 16.10 MPa. Therefore, an increase in the Al powder amount decreases density and increases porosity which results in a gradual decrease in the compressive strength. As expected, the compressive strength is strongly affected by the porosity of the AAFs. It can also be observed that different maximum values of compressive strength were obtained for specimens produced with P1, P2, and P3 maximum particle sizes.

The compressive strength results can be compared with the results obtained by other authors. Laura Dembovska and V. Ducman (2017) developed a highly foamed geopolymer-based product using Al powder as a foaming agent and fly ash as starting material. The compressive strength results of the hardened material obtained were 3.7 MPa, 4.3 MPa, and 3.3 MPa by adding 0.07%, 0.13%, and 0.2% Al powder, having a density of 0.74 g/cm3, 0.64 g/cm3, and 0.73 g/cm3, respectively [263]. Moreover,

A. Hajimohammadi et al. (2017) synthesized geopolymer foams from fly ash with different properties by changing the SS/SH at three different ratios (1.5:1, 1:1, and 0.66:1) using the same amount of Al powder as a foaming agent. The mechanical results showed a compressive strength of 1.590 MPa, 1.129 MPa, and 0.42 MPa for a density of 880 kg/m³, 820 kg/m³, and 650 kg/m³, respectively [205].

AA-Foams	0.1	0.2	0.3	0.4	0.5
P1 (Max 150μm)	16.1	5.92	5.09	3.65	4.25
P2 (Max 300μm)	14.2	4.25	4.28	3.23	3.03
P3 (Max 500μm)	10.97	4.02	3.58	2.45	2.28
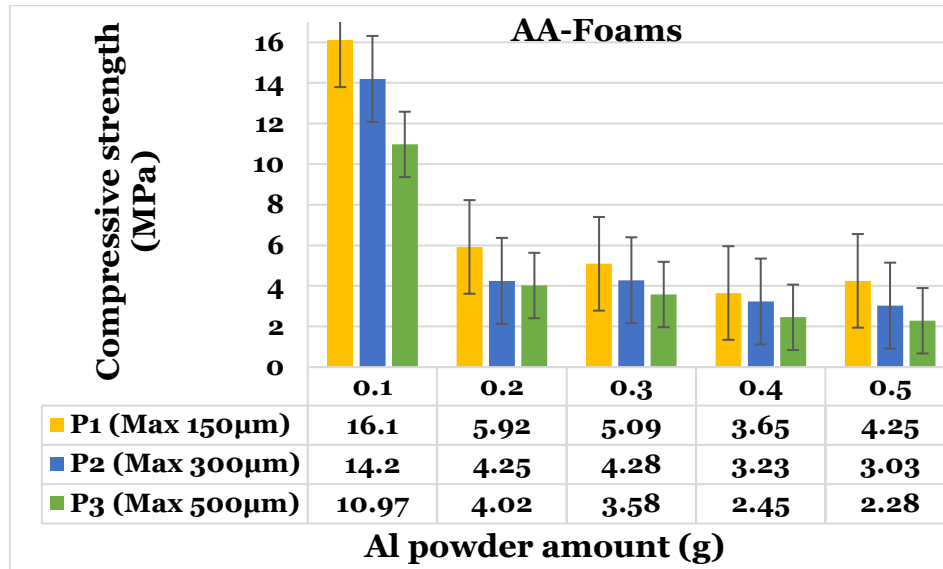
Figure 4.4 - The compressive strength of the AAFs at 28 days.

In comparison with other sub-product and industrial wastes (e.g. fly ash and metakaolin) as starting materials for AAFs [201][23][263] [264]tungsten mining waste mud and waste glass mixtures seem to be beneficial from the point of view of compressive strength showing relatively good compressive strength results of 4.25 MPa, 3.03 MPa, and 2.28 MPa for densities of 1081.62 kg/m³, 1038.09 kg/m³, and 913.26 kg/m³, expansion volume of 42.90%, 48.57%, and 57.56%, for P1, P2 and P3 precursors maximum particle size, respectively. Thus, the compressive strength results obtained using TMW+WG+MK are at the same level or even higher as other research results obtained with fly ash and Mk.

4.2.2.2. Bulk density and porosity

The dry density (bulk density) of the AAFs produced in this investigation is presented in Figure 4.5. The lowest density for P1, P2, and P3 are 1081 kg/m³, 1038 kg/m³, and 913 kg/m³, respectively, when using 0.5g Al powder. It is clearly observed that the lowest density is obtained for precursor P3 with a maximum particle size of 500μm and maximum Al of 0.5g. Furthermore, for any amount of Al the lowest density is found for P3 with the highest maximum particle size.
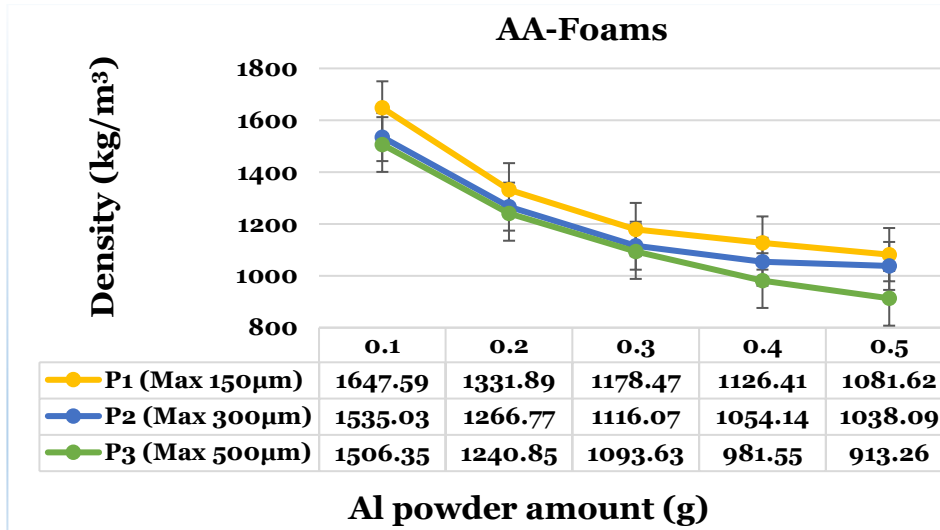
Figure 4.5 - *The relation between AAFs dry density, Al powder and particle size.*

Table 4.6. presents the compressive strength and dry density results of the alkali-activated foams (AAFs), for P1=150 μm, P2=300μm, and P3=500μm maximum particle sizes with the different Al powder amounts.

Table 4.6 - *Compressive strength, density, and expansion volume results of AAFs.*

Samples	Compressive Strength (MPa)	Dry Density (kg/m³)
P1-F1	16.1	1647.59
P1-F2	9.5	1331.89
P1-F3	5.09	1178.47
P1-F4	3.65	1126.41
P1-F5	4.25	1081.62
P2-F1	14.2	1535.03
P2-F2	4.25	1266.77
P2-F3	4.28	1116.07
P2-F4	3.23	1054.14
P2-F5	3.03	1038.09
P3-F1	10.97	1506.35
P3-F2	4.02	1240.85
P3-F3	3.58	1093.63
P3-F4	2.45	981.55
P3-F5	2.28	913.26

4.2.2.3. Microstructural characterisation

***Figure 4.6** - SEM images of the highly porous structure of the alkali-activated foams binder.*

Figure 4.6 shows microstructural studies by SEM for the examination of the size and distribution of the pores. The porous structure of the AAFs samples reveals large voids with pores' size diameter up to -4- mm, and the distributions of the pores in the samples were found to be relatively uniform. As stated before, accordingly to other authors, when the concentration of Al powder foaming agent in the paste is minimal, the pores are generally closed and almost spherical. If the content of Al powder increases coalescence occurs among cells and the cells' geometrical shape changes from spherical to oval. These characteristics of foamed materials were also found in this research work.

As part of this work, foamed alkali-activated tungsten-based is developed, manufactured, and improved. The TWM was utilized in its natural state (non-calcined), cement-free alkali-activated foams were made using aluminium powder as a foaming agent and treated at a temperature below 60° C. The release of hydrogen gas during the foaming process results in a closed-pore network. A laboratory-scale manufacturing method was utilized, and mixture compositions were optimized for pore dispersion and bulk density. Figure 4.7 illustrates typical Cubic TWM-based alkali-activated foams (AAFs) specimens. Moreover, selected components were created in the lab through expansion inside a mould. Architecture students designed moulds for innovative elements used for hollow walls composed of alkali-activated foamed materials of the University of Beira Interior (UBI) for the manufacturing of prefabricated prototypes for facades of buildings. Most hollow elements were structurally stable and had good mechanical qualities, in addition to their creative design. The research improves the possibility of using alkali-activated foamed materials to create individual pieces for hollow walls (see Figure 4.8).

Figure 4.7 - *Typical TWM-based foam specimen.*

Figure 4.8 - *Perforated prototype block (Cobogós) tungsten-based obtained by expansion inside the mould.*

4.2.3. Alkali-activated foamed mortar incorporating cork

4.2.3.1. Compressive strength

For each mixture, three 25 x 25 x 25 mm³, and 40 x 40 x 40 mm³ cubes were tested for the AAF-Mortar and AALWF-Mortar, respectively. The cubes were obtained by cutting the casted 100 x 100 x 60 mm³ with a diamond cutting blade. The compressive strength results of AAF-Mortar and AALWF-Mortar are presented in Figures 4.9 and 4.10 respectively. On one hand, it is clearly observed that the highest compressive strength values are achieved thru samples with less amount of Al powder, that is, with less porosity. It was also observed that for all samples using diverse Al powder amounts for the precursors with the smallest particle sizes of powders (150 µm) presented higher compressive strength results which ranged between 3.13 MPa and 13.23 MPa concerning the AAF-Mortar. On the other

hand, AALWF-Mortar presents relatively good compressive strength for about 4.14 MPa with a small amount of aluminium powder for the precursors with the smallest particle sizes of powders (150 μm). Contrary, precursors with (300 μm and 500 μm) provides relatively good compressive strength for the AAF-Mortar. However, for AALWF-Mortar there is a drop in the compressive strength of less than 2 MPa. As expected, the increase of Al powder amounts decreases the density and high porosity which results in a gradual decrease of the compressive strength. Thus, the compressive strength was strongly affected by the porosity of the AAF-Mortar, whereas porosity and EG-Cork particles influenced the compressive strength of the AALWF-Mortar (Figure 4.10).

AAF-Mortar

	0.1 al	0.2 al	0.3 al	0.4 al	0.5 al
■ AAFM-150	13.23	7.06	4.82	3.24	3.13
■ AAFM-300	3.75	2.08	2.08	2.62	2.45
■ AAFM-500	1.70	0.57	0.89	0.58	0.76

Compressive strength (MPa) — Al powder amount (g)
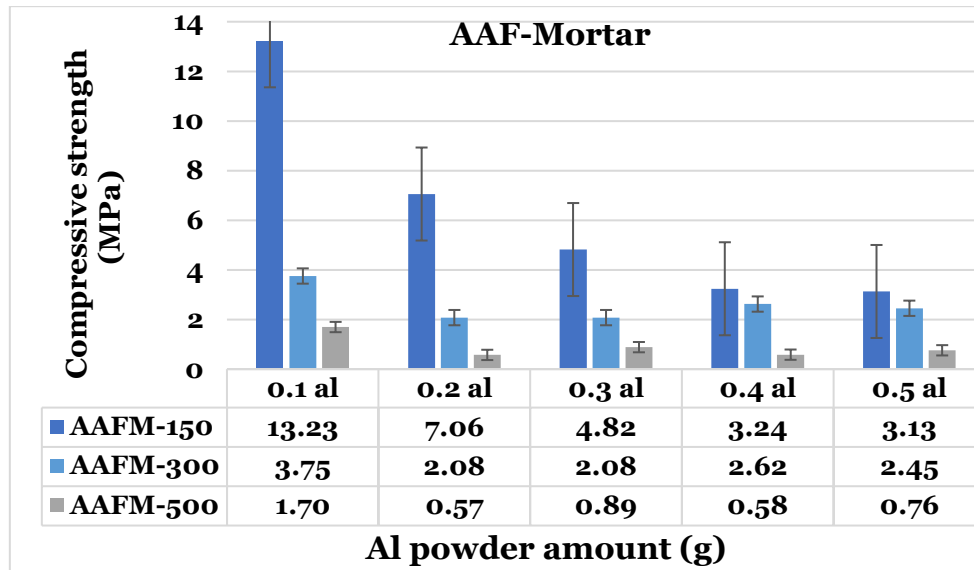
Figure 4.9 - Compressive strength of the AAF-Mortar at 28 days.

AALWF-Mortar

	0.1 al	0.2 al	0.3 al	0.4 al	0.5 al
■ AALWFM-150	4.14	2.72	1.76	1.36	1.31
■ AALWFM-300	2.02	1.00	0.97	0.48	1.06
■ AALWFM-500	1.70	0.57	0.89	0.58	0.76

Compressive strength (MPa) — Al powder amount (g)
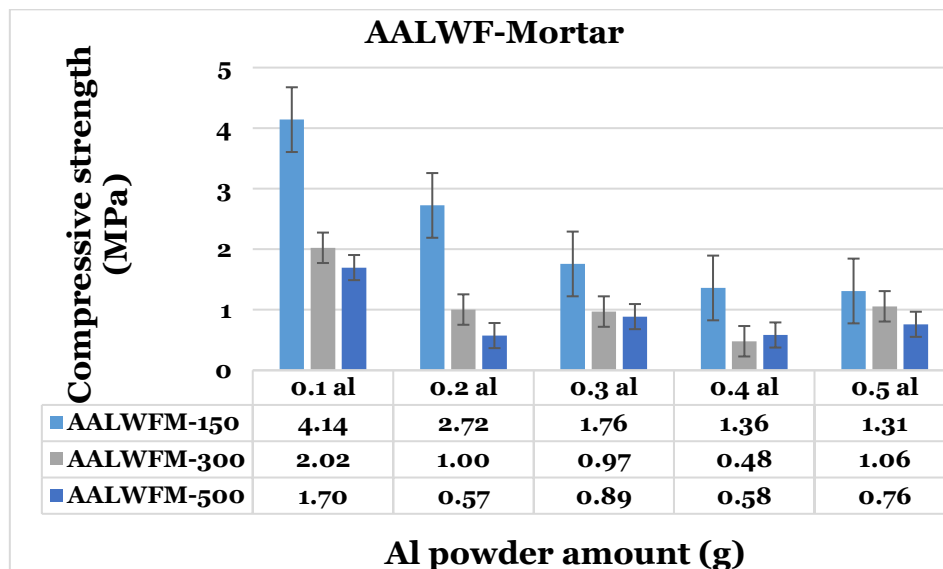
Figure 4.10 - Compressive strength of the AALWF-Mortar at 28 days. Check table for compressive strength

Mixtures using precursors with the smallest particle sizes of the powders show higher compressive strength results of the AAF-Mortar. It can be explained that the powders with the smallest particle sizes (under 150 µm) have more reactivity than that once with particle sizes of (under 300 µm and 500 µm). In addition, the bigger particle sizes of sand (2mm) show less reactivity during the alkali activation reaction. Furthermore, AALF-Mortar presents a decrease of compressive strength results for mixtures with the smallest particle sizes of (150 µm) due to the presence of EGC particles. Besides to the effect of the precursors' maximum particle sizes and the Al powder amounts on the decrease of the compressive strength results, cork particles also play a role on lowering the strength. The presence of natural cork particles that has an inert role in the alkaline activation reaction and due to its honeycomb structure leads to a quantity of water to be kept in the cells of the natural cork aggregate and after the alkaline activation reaction is finished during the curing time and the next days in the atmosphere the water is released, and the samples shows the efflorescence phenomena as it can be seen in the Figure 4.11.

Figure 4.11 - AALWF-Mortar samples under the efflorescence phenomena.

4.2.3.2. Dry density of the mortar

Figures 4.12. and 4.13. show the dry density of the AAF-Mortar and AALWF-Mortar respectively. Cubic specimens (25 x 25 x 25 mm³) were used for the AAF-Mortar and (40 x 40 x 40 mm³) were used for the AALWF-Mortar, for dry density measurements. It is observed that incorporating cork particles (EGC) into the precursors lead to a low density. On the other hand, the increase of porosity, through chemical foaming using Al powder also decreases density. The lowest density for each type of mortar was achieved at about 1337 Kg/m³ and 1077 Kg/m³ for the AA-FM and the AALW-FM, respectively, when adding a large amount of Al powder (0.5g). Furthermore, the increase of the Al powder amount enlarges the pore size of the samples and several voids inside the material filled with air could be generated, thus resulting in the reduction of density.
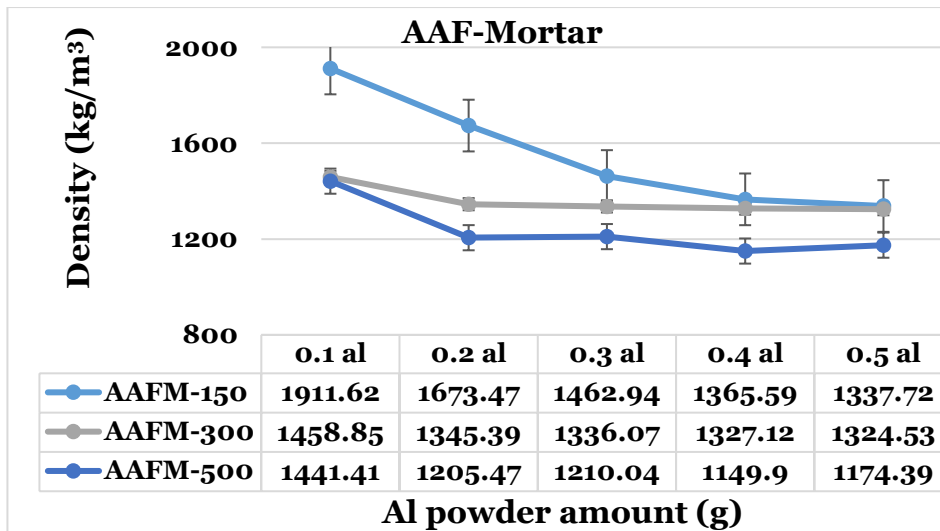
Figure 4.12 - *The relation between density and the Al powder amounts of the AAF-Mortar.*

	0.1 al	0.2 al	0.3 al	0.4 al	0.5 al
AAFM-150	1911.62	1673.47	1462.94	1365.59	1337.72
AAFM-300	1458.85	1345.39	1336.07	1327.12	1324.53
AAFM-500	1441.41	1205.47	1210.04	1149.9	1174.39
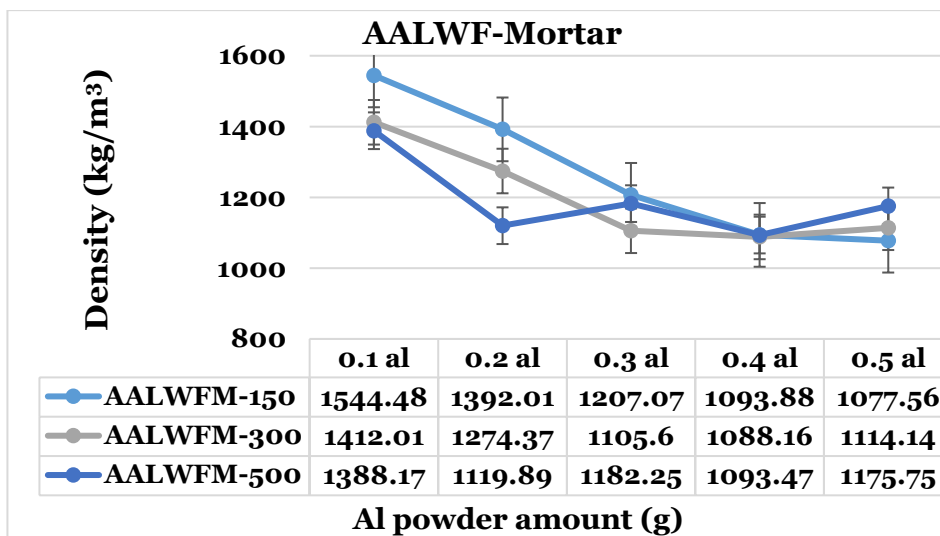
Figure 4.13 - *The relation between density and the Al powder amounts of the AALW-FM.*

	0.1 al	0.2 al	0.3 al	0.4 al	0.5 al
AALWFM-150	1544.48	1392.01	1207.07	1093.88	1077.56
AALWFM-300	1412.01	1274.37	1105.6	1088.16	1114.14
AALWFM-500	1388.17	1119.89	1182.25	1093.47	1175.75

4.2.4. Alkali-activated foamed binders incorporating cork

4.2.4.1. Compressive strength

Compressive strengths of the alkali-activated lightweight foamed materials (AA-LFM) containing different percentages of expanded granulated cork (EGC) particles for all different precursors' particle sizes at 28 days are presented in Figure 4.14. It was reported that the compressive strength of the AA-LFM relatively increases with the change of the precursor particles size; in other words, by reducing the size of the powders, the percentage of the reactants of the precursor increases On the other hand, the compressive strength is strongly affected by the porosity created with the foaming agent and cork particles added to the mixtures.

P1 (< 150 μm)

	10% Cork	20% Cork	30% Cork	40% Cork
0.1 al	6.29	5.77	4.33	3.47
0.2 al	4.38	4.34	3.86	2.28
0.3 al	3.88	2.99	2.58	2.04
0.4 al	2.32	2.73	2.18	1.89
0.5 al	2.92	3.34	3.33	2.24

Cork particles (vol.%)

(i)

P2 (< 300 μm)

	10% Cork	20% Cork	30% Cork	40% Cork
0.1 al	4.80	3.88	3.18	2.48
0.2 al	3.49	2.89	2.81	2.08
0.3 al	2.28	2.50	2.31	1.98
0.4 al	3.03	2.75	2.45	2.09
0.5 al	2.90	2.65	2.33	2.30

Cork particles (vol.%)

(ii)

P3 (< 500 μm)

	10% Cork	20% Cork	30% Cork	40% Cork
0.1 al	4.56	3.83	2.86	2.56
0.2 al	3.15	2.58	2.10	1.90
0.3 al	2.25	1.94	1.50	1.31
0.4 al	2.09	2.10	1.57	1.60
0.5 al	1.93	1.89	1.38	1.66

Cork particles (vol.%)

(iii)

Figure 4.14 - *Compressive strength results versus cork particles percentage with different amounts of Al powder at 28 days;* ***(i)*** *P1 (<150 μm),* ***(ii)*** *P2 (<300 μm), and* ***(iii)*** *P3 (<500 μm).*

As expected, the compressive strength decreases with the change of the foaming agent and cork particles content of the alkali-activated lightweight foamed materials (AA-LFM). The highest values of compressive strength achieved for each precursor particle size were obtained when adding a small amount (0.1g) of Al powder incorporating different percentages of cork particles. Precursor P1 (<150 µm) shows a high compressive strength value of (6.29 MPa, 5.77 MPa, 4.33 MPa and 3.47 MPa) using 0.1g of Al powder when adding (10 vol.%, 20 vol.%, 30 vol.%, and 40 vol.%) of expanded granulated cork (EGC), respectively (as presented in Figure 4.14. (i)). For precursor P2 (<300 µm) the highest compressive strength results obtained using 0.1g Al powder were (4.80 MPa, 3.88 MPa, 3.18 MPa and 2.48 MPa) for samples containing (10 vol.%, 20 vol.%, 30 vol.%, and 40 vol.%) expanded cork (EGC), respectively, as shown in Figure 4.14. (ii). The highest compressive strength values obtained for precursor P3 (<500 µm) using 0.1 Al powder were of (4.56 MPa, 3.83 MPa, 2.86 MPa and 2.56 MPa) with different percentages of cork particles at 10 vol.%, 20 vol.%, 30 vol.%, and 40 vol.%, respectively, as presented in Figure 4.14. (iii). In addition, with the decrease of the density (the increase of cork particles content) compressive strength also decrease gradually.

Strength loss/gain

In previous investigations using mining waste mud, I. Beghoura et al. [165] studied alkali-activated foams using different precursor particle sizes stating that lower strengths were due to the increase of porosity which results in a gradual decrease in the compressive strength. In other words, alkali-activated foamed binders with high porosity leads to the loss of strength. A strong decline in the sample compressive strength was observed when adding a higher amount of 0.5g Al powder and the strength further decreases with the increase of Al powder. Nevertheless, the higher porosity foams (produced with 0.5 g Al powder) has a compressive strength of 4.25 MPa, 3.03 MPa, and 2.28 MPa for P1, P2, and P3, respectively. These results can be compared with the results obtained by others [23][205][201][220] using other sub-product and industrial wastes as starting materials (e.g., metakaolin, fly ash, etc.).

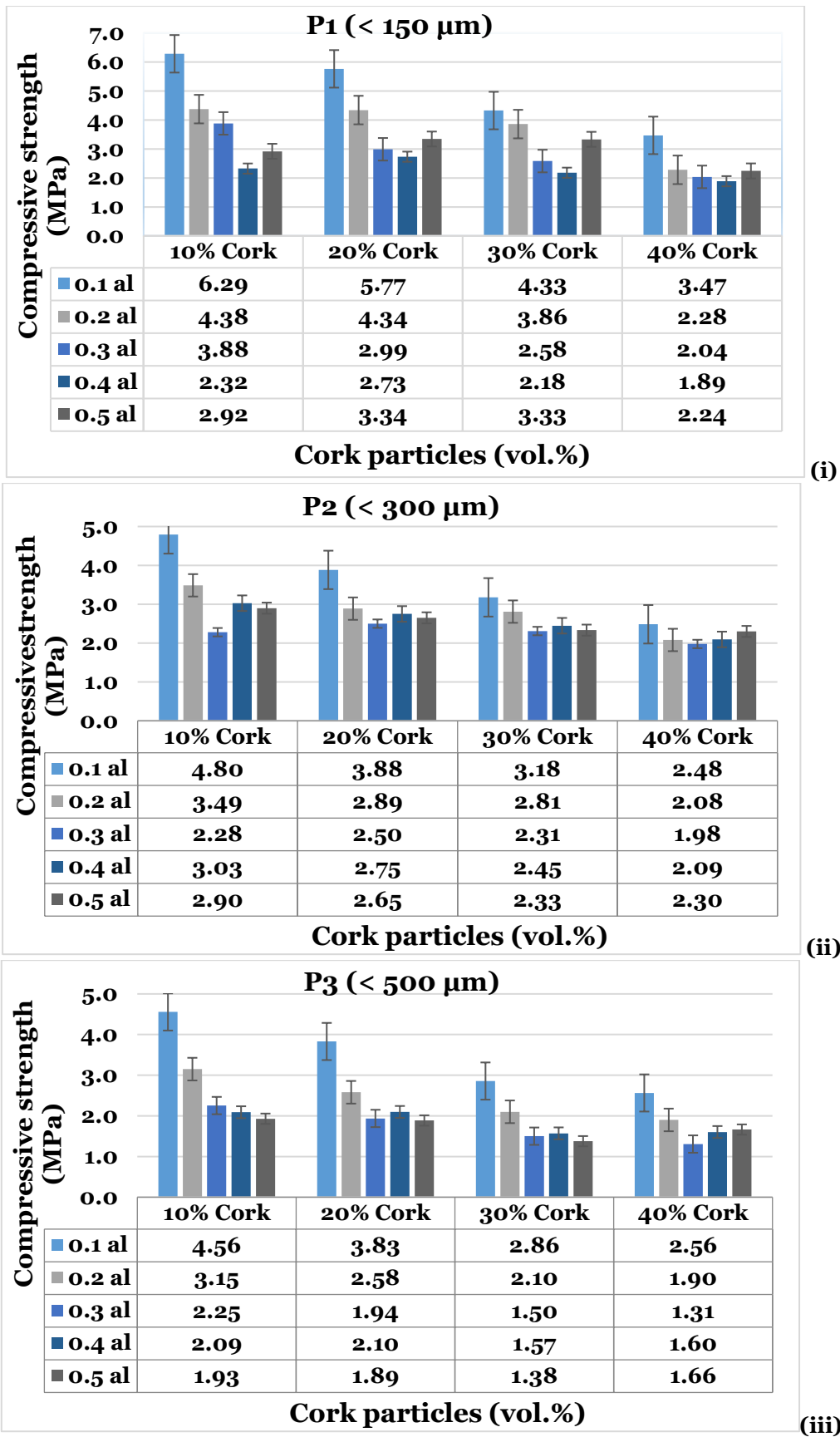AA-LFM seem to be beneficial from the point of view of compressive strength showing relatively good compressive strength results of 2.04 MPa, 1.98 MPa, and 1.31 MPa for densities of 664 kg/m^3, 722 kg/m^3, and 753 kg/m^3, with expansion volume of 58.73%, 56.87%, and 54.16% for P1, P2 and P3 precursors' maximum particle size incorporating 40 vol.% of cork particles, respectively. However, it is interesting that the collapsed samples present an increase in the compressive strength while the porosity decreased through the failure of the expansion process of the samples. AA-LFM prepared using higher Al powder amount incorporating 40 vol.% cork particles have a compressive strength of 2.24 MPa, 2.30 MPa, and 1.66 MPa for P1, P2, and P3, respectively with this being roughly 10%, 16%, and 22% higher than samples prepared with a large amount of Al powder and does not show the failure in the expansion process, which can explain that compressive strength is strongly affected by the porosity of the alkali-activated foams. Thus, the compressive strength results obtained using tungsten-based alkali-activated foams incorporating expanded cork particles are at the same or even higher level as other research results obtained with fly ash and MK.

4.2.4.2. Dry density

The density of the samples was measured by dividing the dry mass by the volume (i.e., so-called geometrical density). The average of 3 cubic specimens (40 x 40 x 40 mm^3) was used for dry density measurements. The dry densities of the AA-LFM are presented in Figure 4.15. It was observed that the density was affected by two parameters: pores created by the foaming process with different amount of Al powder and the changes of the cork particles in the mixtures. The lowest density obtained for precursors P1, P2 and P3 is 664 kg/m^3, 722 kg/m^3, 753 kg/m^3, respectively, using 0.4g Al powder in case of the precursor P1 and 0.3g Al powder for precursors P2 and P3. It is clearly noticed that the lowest density is obtained through the changes of Al powder amount as a result of adding cork particles at 40 vol.% for all different precursor's particle sizes. Furthermore, the density showed superior values when adding 0.5 Al powder as in the case of P1 and 0.4g to 0.5g Al powder added in the cases of P2 and P3 because the AA-LFM mixtures show a collapse of the simples.

Figure 4.16. demonstrate further the differences between the various AA-LFM mixtures by projecting their compressive strength versus dry density. Expectedly, the density reduction of the AA-LFM samples achieved by using Al powder as a foaming agent, and incorporating cork particles, has a significant effect on the decrease of the compressive strength. It has been found that samples with lower porosity show higher compressive strength and densities. As expected, and in comparison, with results found by I. Beghoura et al. [114] density reduces for increasing expanded cork particles content (below 900 Kg/m^3). The lowest density was found in the mixture with 40 vol.% expanded cork particles 664 kg/m^3, 722 kg/m^3, and 753 kg/m^3, for precursors P1, P2 and P3, respectively. Overall, an increase in cork particles content led to lower density.
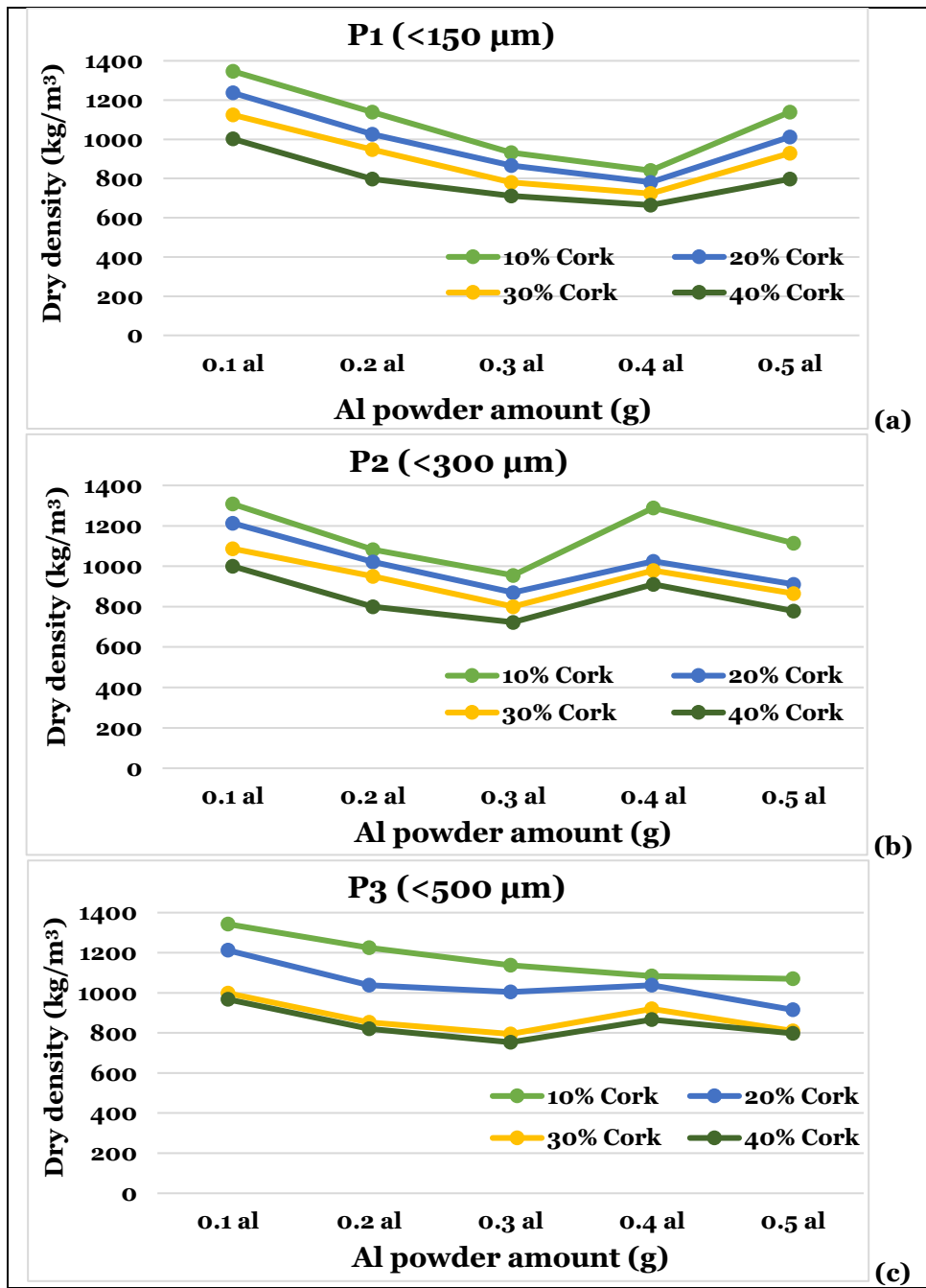
Figure 4.15 - *Dry density versus Al powder amount changes for samples with different percentages of cork particles; **(a)**; P1 (<150 μm), **(b)**; P2 (<300 μm), and **(c)**; P3 (<500 μm).*
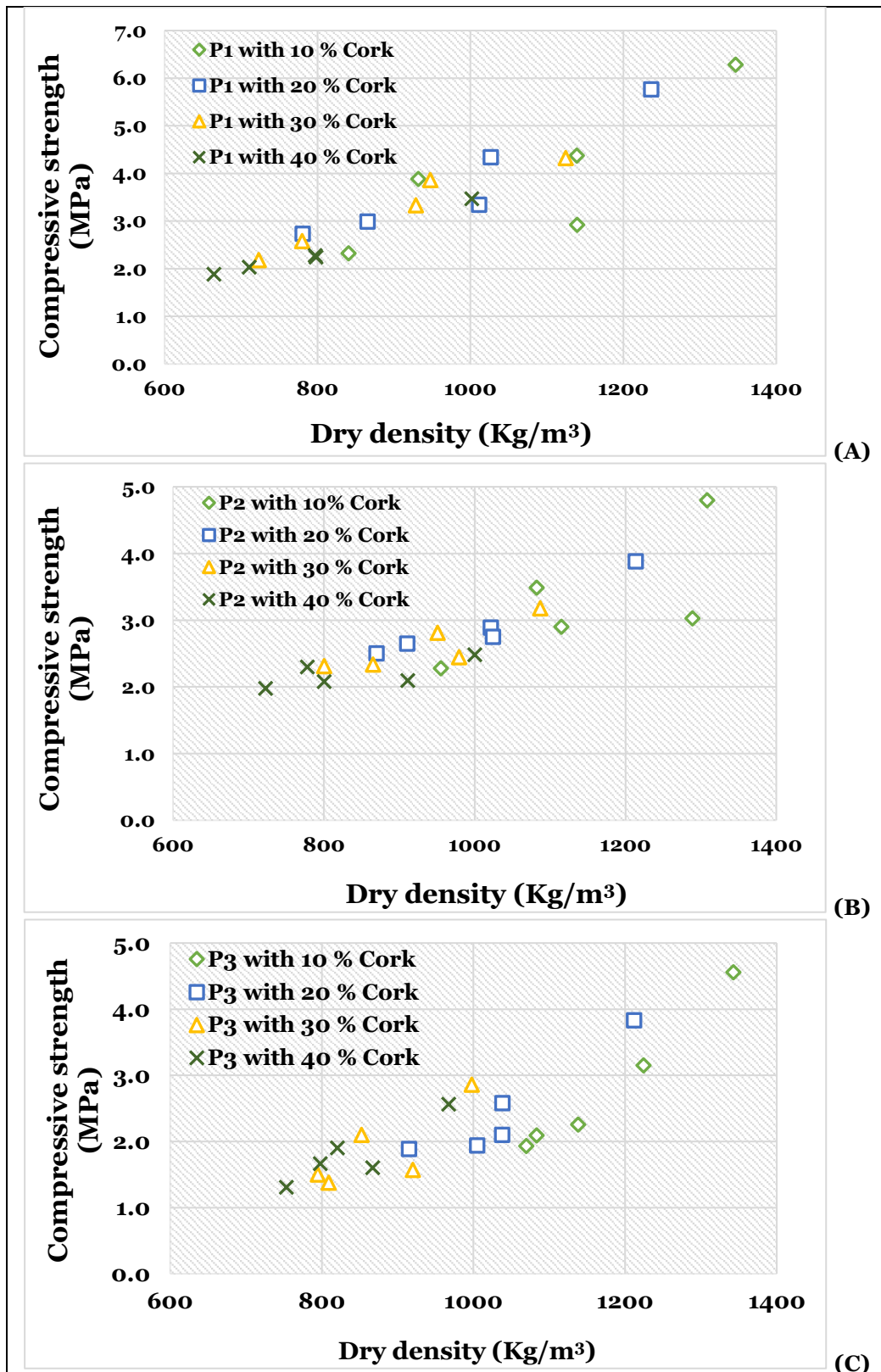
Figure 4.16 - *Correlation between the dry density and compressive strength in the AA-LFM; **(A):** P1 (<150 μm), **(B):** P2 (<300 μm), and **(C):** P3 (<500 μm).*

4.3. Summary

This chapter presents in detail the mixture design and properties of the several AALFMs investigated during this research work. Then, microstructure, physical, and mechanical properties such as compressive strength and density results of each phase in this research work, are presented and discussed. The TWM binder-based alkali-activated foamed materials have not only relatively high mechanical performance but can also be a better eco-friendly material when incorporating EG-Cork particles. The following findings were made:

• An increase of the Al powder amount decreases the AALFMs density and increases porosity which results in a gradual decrease of the compressive strength. Moreover, for any amount of Al (between 0.1 g to 0.5 g) the lowest density was found out for samples made with the precursors' highest maximum particle size (P3 > 500 µm).

• The lowest density obtained for P1, P2 and P3 is 664 kg/m³, 722 kg/m³, 753 kg/m³, respectively, using 0.04 w.% Al powder in the case of precursor P1 and 0.03 w.% Al powder for precursors P2 and P3. Additionally, it was found that the density decreases as expanded granulated cork (EGC) particles content increases due to the low density of cork particles.

• The compressive strength results of the AALFMs obtained with 70 % of TMW amount are at the same level or even higher as other research results obtained with fly ash and MK. The compressive strength results in the case of the high amount of Al powder added were 2.04 MPa, 1.98 MPa, and 1.31 MPa for densities of 664 kg/m3, 722 kg/m3, and 753 kg/m3, with expansion volumes of 58.73%, 56.87%, and 54.16% for P1, P2 and P3 precursors' maximum particle size incorporating 40 vol.% of cork particles, respectively. Furthermore, the compressive strength of the AA-LFM is strongly affected by the increase of Al powder amount and slightly with the change of cork particles content.

• The quantity of the foaming agent used strongly affects the density results; when the amount of foaming agent increases, the density of the specimen decreases.

Chapter 5 - Expansion process of foams

In this chapter, the expansion process is presented and discussed. The different parameters affecting the expansion process (i.e., particles size of the powders, foaming agent amount, and cork particles) are shown to be the main parameters that influence the expansion volume. This chapter will present the main results as follows:

- Expansion volume;
- Expansion time;
- Pore sizes and cork particles distributions;
- Image analysis of the foams;

5.1. Expansion process

In this investigation, the expansion process of different alkali-activated tungsten-based was studied. The method for the measurement of the total volume of hydrogen (H_2) released was used to prepare foamed mixtures to obtain a uniform air-void distribution. The results demonstrate that during the reaction of the foaming agent, the expansion process is affected by several factors. The results of the four phases to produce alkali-activated foamed binder and mortar incorporating cork particles are presented and discussed.

5.2. Characterisation of the foams

5.2.1. Alkali-activated foamed materials; preliminary investigation

5.2.1.1. Expansion volume

Figures 5.1 and 5.2 shows a typical expansion volume in alkali-activated LW2 and LW3 mixtures using hydrogen peroxide (HP) and aluminium powder (Al), respectively. For LW3 the expansion volume increases changes by 150%, 250% and 358% with adding 1%, 2% and 3% aluminium powder content respectively. While, for LW2 the expansion volume increases changes by about 84%, 137% and 141% with the addition 1%, 2% and 3% hydrogen peroxide content respectively. Due to the fast reaction between the hydrogen peroxide and the aqueous solution in the mixture, it decomposes very quickly and produces oxygen gas. In this preliminary phase, it was observed that the expansion process was very short for the mixtures LW2 and LW3 along with the release of hydrogen gas due to the quick reaction between the foaming agents (H_2O_2 and Al powder) and the catalyser NaOH (SH) in the alkali activator solution. Furthermore, the expansion time was very fast, and the reaction of the hydrogen peroxide (HP) starts immediately when added it to LW2, while the LW3 took about 3 minutes from the start of the reaction to the end of the expansion.

a)   1% HP. Before and after expanding.

b)   2% HP. Before and after expanding.

c) 3% HP. Before and after expanding.
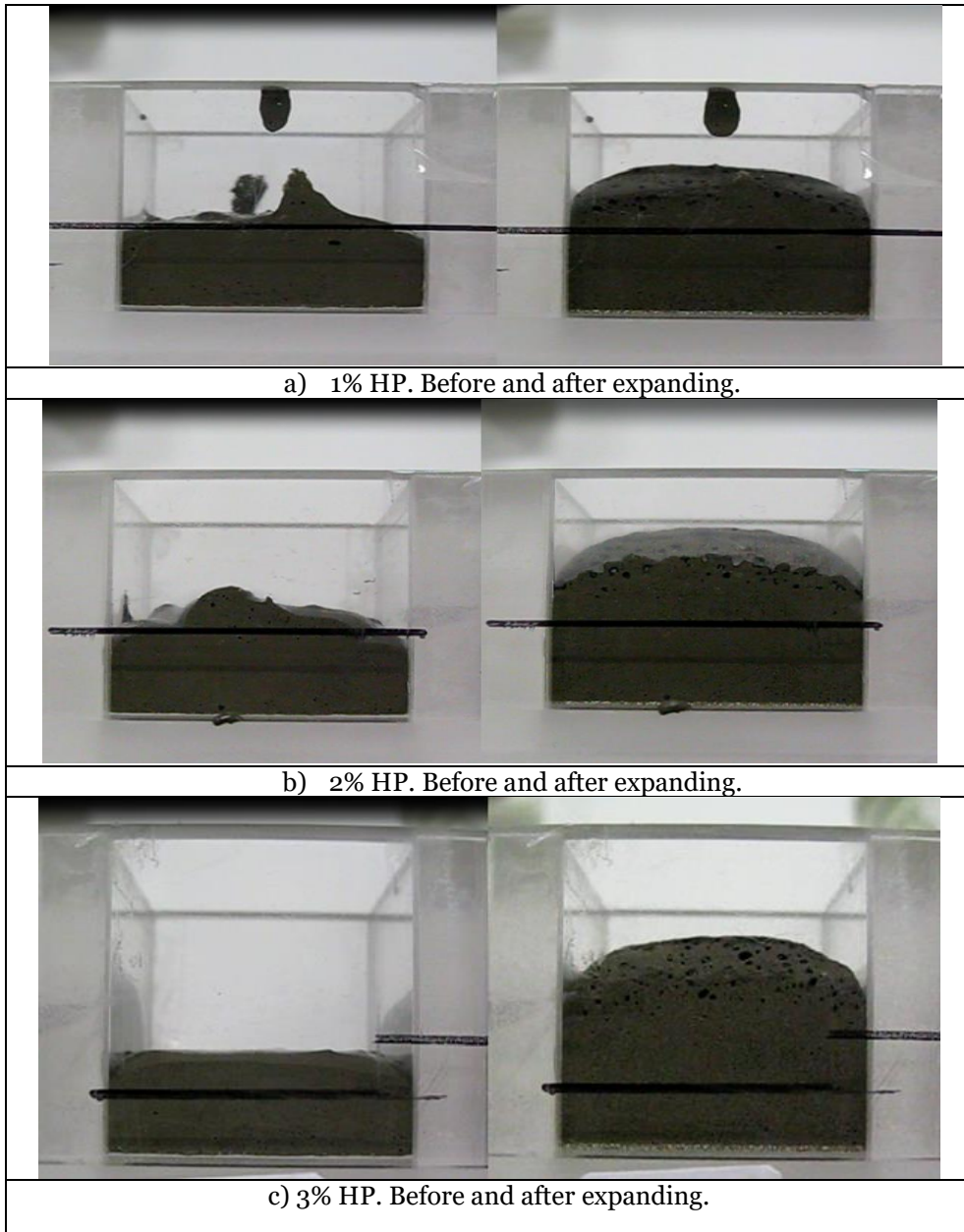
Figure 5.1 - *Expansion inside the mould of LW2 using hydrogen peroxide (HP).*

b) 2% Al. Before and after expanding.

c) 3% Al. Before and after expanding.
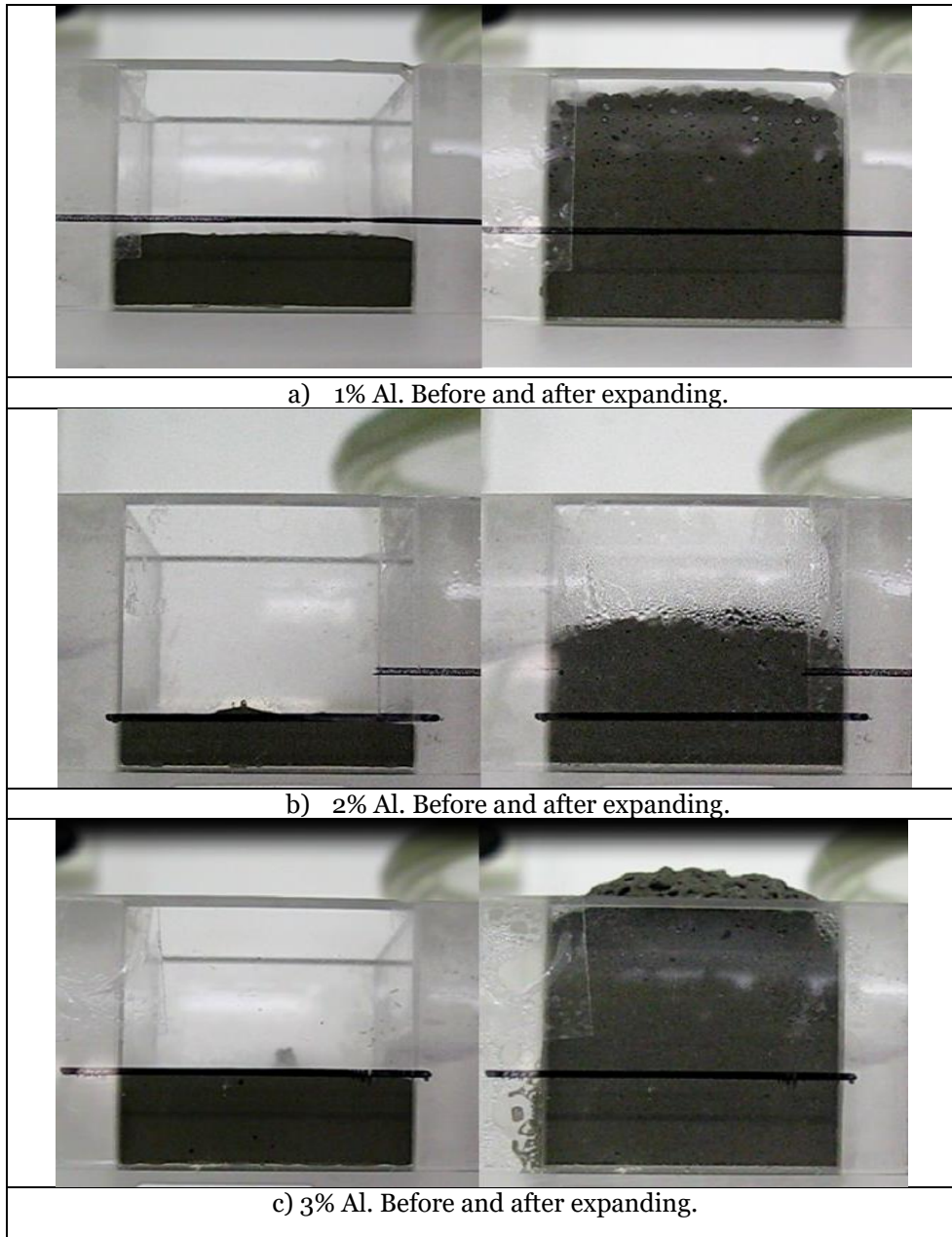
Figure 5.2 - *Expansion inside the mould of LW3 using aluminium powder (Al).*

5.2.1.2. Central section of the AAFMs

Figure 5.3 displays images of the preliminary alkali-activated foamed materials with cement mixtures foamed using different amounts of Al powder.

Figure 5.3 *– Photograph of the preliminary alkali-activated binders with cement mixtures foamed with Al powder.*

5.2.2. Alkali-activated foamed binders

5.2.2.1. Expansion volume

Figures 5.4 and 5.5 shows a cross-section and the expansion volume of different AAFs specimens obtained with various amounts of Al and different precursors particle sizes respectively. The highest expansions volume obtained by adding 0.5g Al powder were about (43%, 49%, and 58%) when using precursors' particle sizes of 150 μm, 300 μm, and 500 μm, respectively. The overall results were presented earlier in table 5.1. It can be observed that the expansion volume during the foaming process is directly proportional to the increase in the dosage of Al powder. The expansion volume is also affected by the fineness of the precursor (P1, P2, or P3), which can be noted since the same amount of Al powder does not lead to the same expansion volume for P1, P2, and P3. AAFs obtained using smaller size particle powders (P1 < 150 μm) showed significantly smaller maximal expansion volume when compared with AAFs obtained with medium and larger size particle powders (P2 < 300 μm), and (P3 < 500 μm). On one hand, the results can be considered surprising, as smaller sized powders will have a higher surface area something that should accelerate the dissolution and synthesis reaction and somehow increase the speed of hydrogen release which, in turn, should cause a higher volume expansion. On the other hand, pastes made with smaller size particles are more viscous and thus more difficult to be expanded by hydrogen gas release, than pastes made with slightly larger size particle powders (P2 and P3).
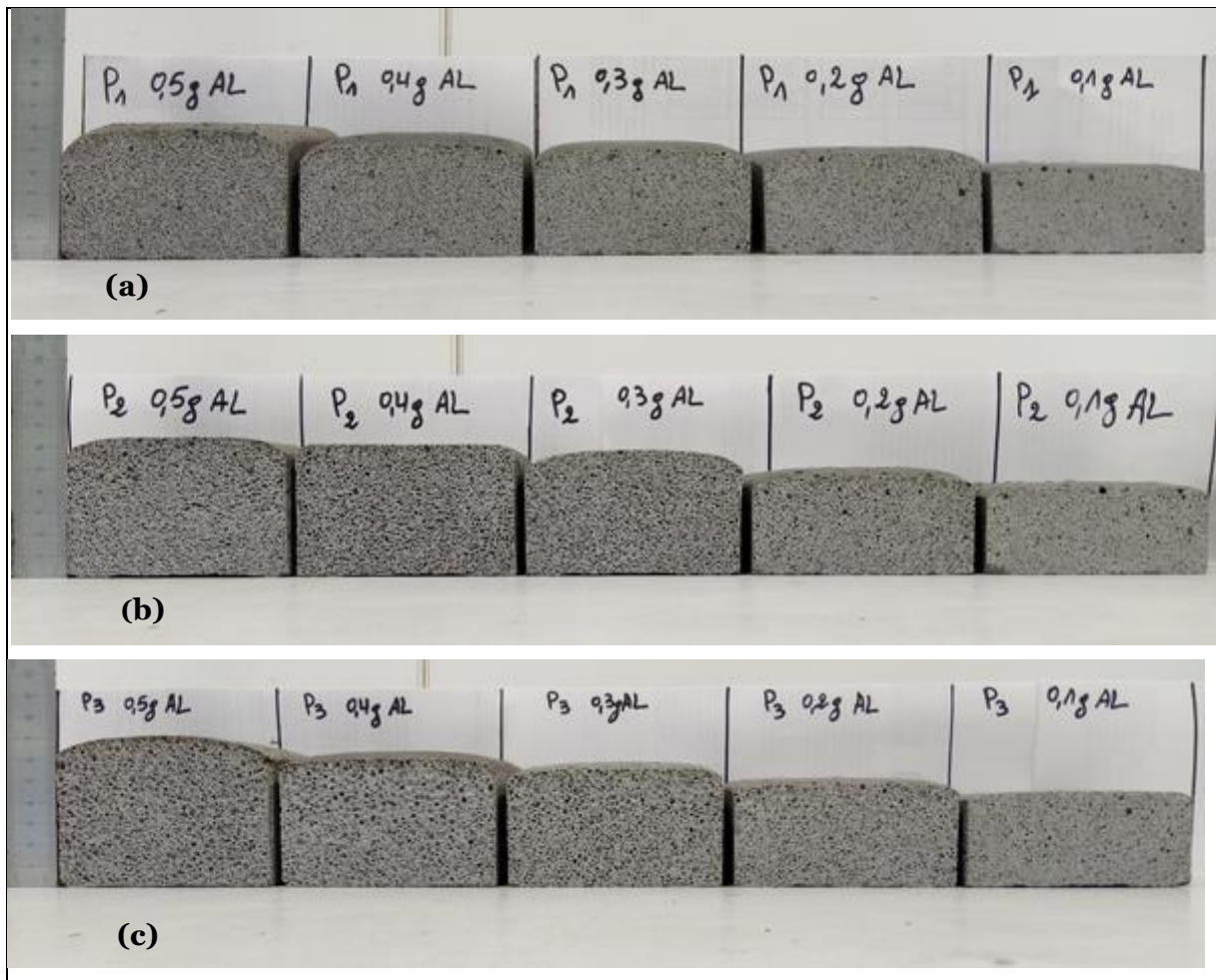
Figure 5.4 - *Cross section of AAFs versus Al powder content and maximum precursors' particle size. (a) 150 μm, (b) 300 μm and (c) 500 μm.*

	0.1	0.2	0.3	0.4	0.5
■ P1 (Max 150μm)	11.5	29.63	39.81	41.21	42.9
■ P2 (Max 300μm)	19.05	36.2	41.46	45.31	48.57
■ P3 (Max 500μm)	23.86	40.84	44.26	50.37	57.56

Al powder amount (g)
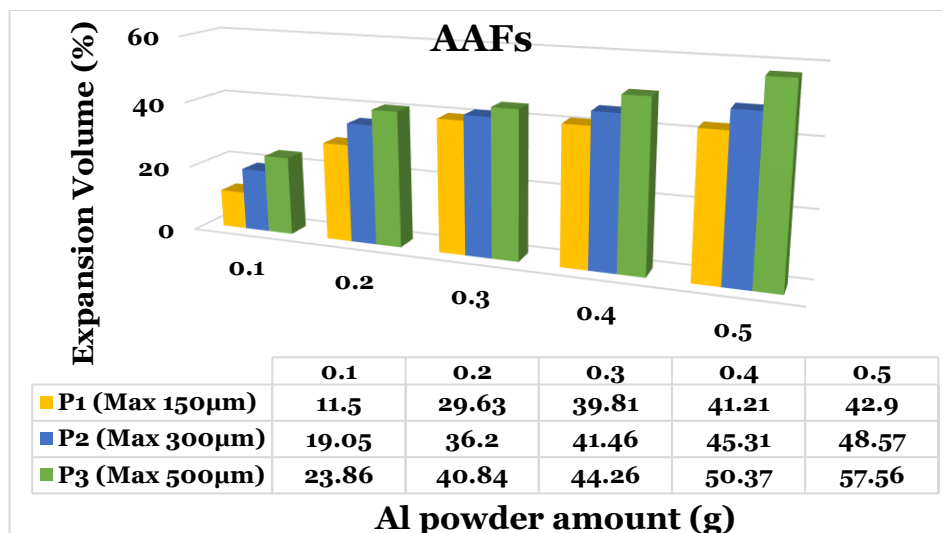
Figure 5.5 - *AAFs expansion volume versus Al content (g) for P1, P2 and P3.*

In addition, it was also observed that when increasing the Al powder mass, the expansion time decreases due to the faster reaction between the Al powder and the catalyser (NaOH) present in the alkaline liquid activator, as presented in Table 5.1.

Table 5.1 - *Expansion time of AAFs specimens.*

Precursors' particle sizes	Specimens	Expansion time (Minutes)
P1 **< 150 μm**	P1-F1	26 min
	P1-F2	23 min
	P1-F3	20 min
	P1-F4	19 min
	P1-F5	16 min
P2 **< 300 μm**	P2-F1	24 min
	P2-F2	22 min
	P2-F3	18 min
	P2-F4	17 min
	P2-F5	15 min
P3 **< 500 μm**	P3-F1	21 min
	P3-F2	19 min
	P3-F3	16 min
	P3-F4	15 min
	P3-F5	14 min

5.2.2.2. Central section of the AAFs

Figure 5.6. present images of the central foam section of random AAFs specimens obtained with precursors (P1, P2, and P3). It shows that they have a macrostructure with irregular spherical macrospores derived from the foaming process. In other words, it can be seen that the increase of Al powder content from 0.1g to 0.5g enlarges the pore size of the samples of the different precursors (P1, P2, and P3). The amount of Al powder and the particle size of the precursor affected the morphology of the pores (shape and diameter) and their distribution (regularity). In addition, we can observe that mixtures with the larger particle size powders (500μm) present more porosity and larger pores than mixtures with finer powders (150μm and 300μm).
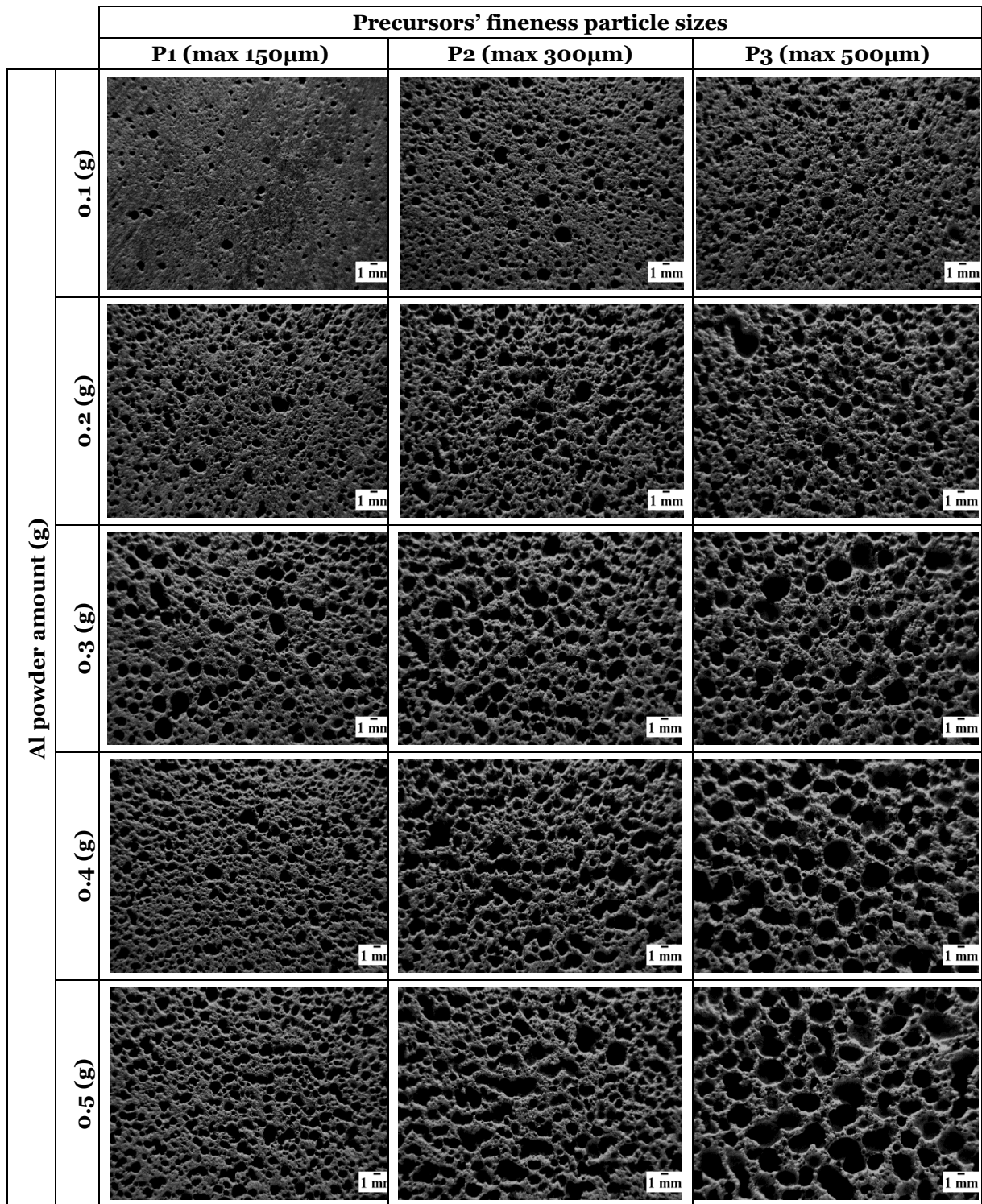
Figure 5.6 - *AAFs porous structure for different Al amounts and of different precursors' fineness.*

5.2.2.3. Image analysis of the foamed materials

Figures 5.7 - highlights the AAFs pore size distribution (pore diameter obtained by image J) for maximum particles sizes P1 (max 150 µm), P2 (max 300 m), and P3 (max 500 µm), respectively. The pore size distribution for different AAFs specimens seems almost identical, as expected. Table 5-3 presents the average percentage of AAFs pore diameter.

(P1) 150 μm

0.1 Al	0 - 1.0	1.0 - 2.0	2.0 - 3.0	more
0.1 Al	98.20	1.68	0.13	0.00
0.2 Al	92.15	6.93	0.87	0.06
0.3 Al	84.73	11.43	2.86	0.99
0.4 Al	87.56	9.05	2.90	0.48
0.5Al	82.66	13.38	3.04	0.92

Pore diameter (mm)

(P1) 300 μm

	0 - 1.0	1.0 - 2.0	2.0 - 3.0	more
0.1 Al	94.13	5.49	0.39	0.00
0.2 Al	85.84	10.24	2.56	1.36
0.3 Al	80.74	11.30	5.65	2.31
0.4 Al	84.30	9.63	3.14	2.94
0.5Al	82.43	8.91	5.32	3.34

Pore diameter (mm)

(P3) 500 μm

	0 - 1.0	1.0 - 2.0	2.0 - 3.0	more
0.1 Al	92.27	6.84	0.82	0.07
0.2 Al	86.52	10.56	2.66	0.26
0.3 Al	84.73	10.11	3.30	1.87
0.4 Al	86.39	5.93	3.37	4.31
0.5Al	85.96	6.08	3.91	4.05

Pore diameter (mm)

***Figure 5.7 -** Pore size distribution for the AAFs with precursors' maximum particle sizes of (P1); 150 μm, (P2); 300 μm, (P3); 500 μm.*

For all AAFs, it can be observed that pores with size <1mm are more than 85% of the total porosity. On average the percentage of pores with sizes between 1 to 2mm is about 8%. While for the larger pores (with a size larger than 3mm pore diameter), it is observed that AAFs specimens with precursors

maximum particle sizes (P3< 500 μm) present the highest percentage (2.11%) when compared with AAFs made of precursors maximum size P2< 300 μm, and P1< 150 μm (with a lower percentage of 1.99 %, and 0.49%, respectively). From Figure 5.6, it can also be concluded that AAFs made with a small amount of Al powder, in the case of 0.1g Al and 0.2g Al, present a more homogenous structure and smaller sized pores.

Table 5.2 - AAFs percentage of average pores diameter.

Pores diameter (mm)	Precursors' particle sizes		
	150 μm (%)	300 μm (%)	500 μm (%)
0 - 1.0	89.1	85.5	87.2
1.0 - 2.0	8.5	9.1	7.9
2.0 − 3.0	1.7	3.4	2.8
More	0.5	2	2.1

From the results of Table 5.2, it can be concluded that the percentage of pores formed with a size of more than 3 mm increases with the increase of precursor particle sizes from 150μm to 500μm. While the percentage of medium size pores increases from 1mm to 3mm when using precursors' particle size from 150μm to 300μm but decreases for 500μm precursor particle size. Thus, it looks like that by increasing the particle size of the precursor from 300μm to 500μm there is no significant effect on the increase of medium size pores (between 1mm to 3mm). It could be that H2 is released from the paste more readily when the precursor particle size is larger, thus not causing a further increase in the size of the pores. Regarding the small pores (< 1mm), it is verified that the increase of the Al powder from 0.1g to 0.5g does not significantly change their percentage (differed from 85% to 89%). Thus, it can be concluded that the formation of small pores (up to 1mm diameter) is more dependent on the precursors' particle size, while the formation of large pores (from 1 to 3mm) appears to be more dependent on the amount of aluminium powder added to the mixtures.

5.2.3. Alkali-activated foamed mortar incorporating cork

5.2.3.1. Expansion volume

As shown in the Figures 5.8 and 5.9, the highest expansions volume of the AA-FM and the AALW-FM, obtained by adding 0.5 g of Al powder, was about 81.54%, and 40.45% respectively. It is clearly observed that expansion volume during the foaming process is directly proportional to the increase of the dosage of the Al powder. The expansion volume is also affected by the expanded granulated cork (EGC) particles which can be noted since the same amount of Al powder does not lead to the same expansion volume for the AA-FM and AALW-FM. Moreover, the increase of the particle sizes of the powders leads to the decrease of the maximum expansion volume percentage when using large amounts of Al powder (0.4 and 0.5 g) which can be explained by the bigger particle size of the precursor and sand with the presence of EG-Cork particles, the hydrogen gas released from the

reaction can easily escape out of the mixture. Additionally, it was also observed that when increasing the mass of the Al powder, the expansion time decreases due to the faster reaction between the Al powder and the catalyser (NaOH) present in the alkaline liquid activator.

AAF-Mortar

	0.1 al	0.2 al	0.3 al	0.4 al	0.5 al
■ AAFM-150	12.16	23.70	46.47	64.74	81.54
■ AAFM-300	34.24	53.35	61.98	62.75	63.66
■ AAFM-500	29.15	32.01	34.86	40.09	44.54

Al powder amount (g)
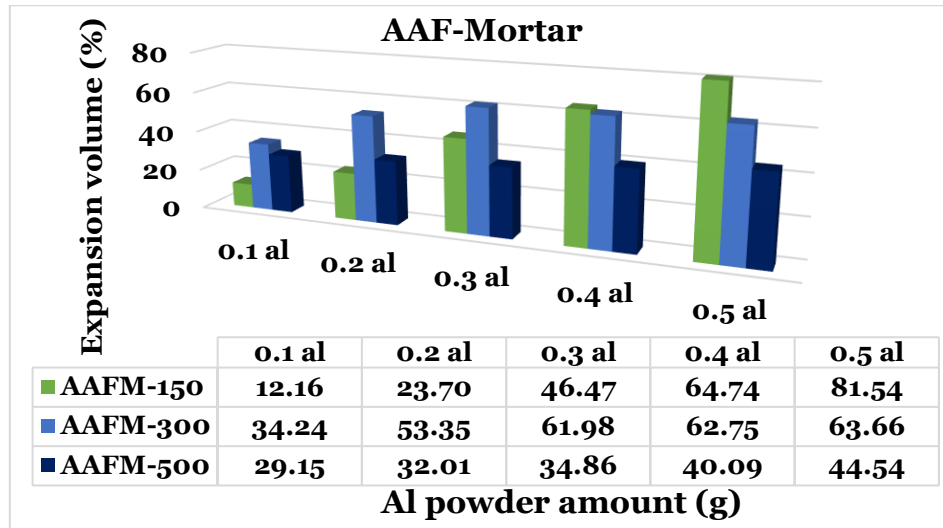
Figure 5.8 - Expansion volume versus Al powder content of the AAF-Mortar.

AALWF-Mortar

	0.1 al	0.2 al	0.3 al	0.4 al	0.5 al
■ AALWFM150	4.38	19.62	22.94	31.53	40.45
■ AALWFM300	16.71	44.00	48.44	49.65	65.41
■ AALWFM500	21.48	36.93	27.49	51.54	40.57
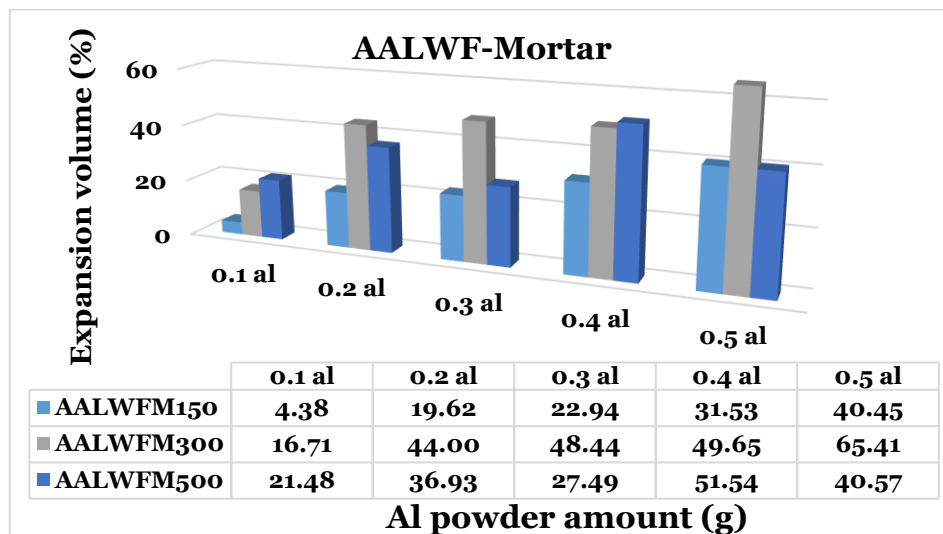
Al powder amount (g)

Figure 5.9 - Expansion volume versus Al powder content of the AALWF-Mortar.

5.2.3.2. Central section of the AAF-Mortar

Figures 5.10 and 5.11 – illustrates a cross-section of the AAF-Mortar and AALW-FM specimens obtained with different amounts of Al powder as well as the photographs of the central foam section of the samples with a small and large amount of Al powder.

Figure 5.10 - *Cross-section image of the AA-FM versus Al powder content.*

(a)

(b)
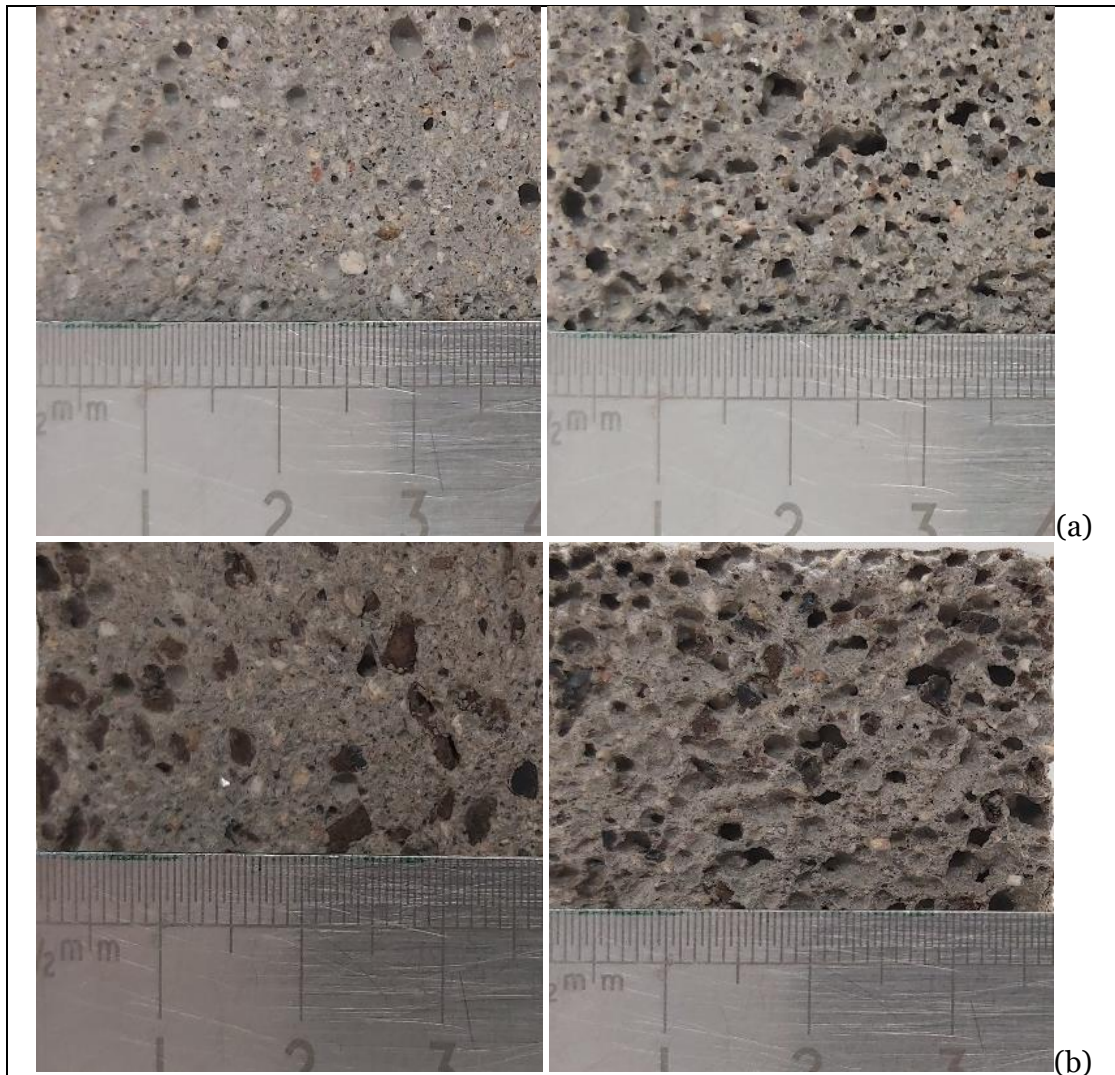
Figure 5.11 - *Photographs of the central foam section of the samples with small and large amounts of Al powder, (a) AA-FM, (b) AALW-FM.*

It is also observed in Figure 5.10 that the formation of large pores appears to be more dependent on the amount of Al. The amount of Al powder affects the morphology of the pores and several small pores formed (up to 1- mm or 2-mm diameter) appeared when using a little amount of Al powder, while large pores (more than 2 mm diameter) appeared when using a large amount of Al powder.

5.2.4. Alkali-activated foamed binders incorporating cork

5.2.4.1. Expansion volume

It was reported that the expansion of the AA-LFM mixtures for all samples with the different precursors' particle sizes using Al powder mainly took place within the first 1 h. As expected, the increase of aluminium powder (Al) amounts leads to the increase of the expansion volume percentage which means that the amount of foaming agent enhances the number and the pore sizes of the AA-LFM produced as presented in Figure 5.12. Precursor (P1) shows a typical expansion volume for all the samples when adding Al powder from 0.1 g to 0.4g, with a higher expansion volume of 55.90%, 53.84%, 59.42%, and 58.73% when adding 10 vol.%, 20 vol.%, 30 vol.%, and 40 vol.% of expanded granulated cork (EGC), respectively, presented in Figure 5.12 (I). On the other hand, precursor P1 shows a collapse of the samples when adding 0.5g of Al powder to the mixtures as indicated with an arrow in Figure 5.13 (a). For precursor P2 the expansion volume increases changes by 51.94%, 52.29%, 47.82%, and 56.87% for all samples containing 10 vol.%, 20 vol.%, 30 vol.%, and 40 vol.% expanded cork (EGC), respectively, when adding Al powder from 0.1g to 0.3g as outlined in Figure 5.12 (II). Precursor P2 also shows a collapse of the samples when adding 0.4g and 0.5g of Al powder in the mixtures (see Figure 5.13 (b)). For P3 the expansion volume when adding Al powder from 0.1 g to 0.3g increases changes as a result of 43.45%, 52.43%, 56.62%, and 54.16% when adding (10 vol.%, 20 vol.%, 30 vol.%, and 40 vol.%) of expanded granulated cork (EGC), respectively as reported in Figure 5.12 (III). However, precursor P3 shows a collapse (as referred to with arrows) of the samples when adding 0.4g and 0.5g of Al powder to the mixtures (as presented in Figure 5.13 (c)).

P1 (<150 µm)

Expansion volume (%)

	10%	20%	30%	40%
0.1 al	30.06	34.72	37.49	40.85
0.2 al	41.09	43.78	45.30	48.13
0.3 al	51.09	51.69	55.60	55.46
0.4 al	55.90	53.84	59.42	58.73
0.5 al	44.16	49.39	45.79	45.83

Cork particles (vol.%) (I)

P2 (<300 µm)

Expansion volume (%)

	10%	20%	30%	40%
0.1 al	38.85	45.97	37.05	44.25
0.2 al	47.62	46.53	44.02	54.03
0.3 al	51.94	52.29	47.82	56.87
0.4 al	40.82	46.93	47.55	51.36
0.5 al	46.95	50.77	54.06	56.08

Cork particles (Vol %) (II)

P3 (<500 µm)

Expansion volume (%)

	10%	20%	30%	40%
0.1 al	29.53	36.25	42.23	43.34
0.2 al	37.07	44.84	50.23	50.61
0.3 al	43.45	52.43	56.62	54.16
0.4 al	50.02	48.87	48.44	44.35
0.5 al	48.48	50.20	50.46	46.85

Cork particles (Vol %) (III)

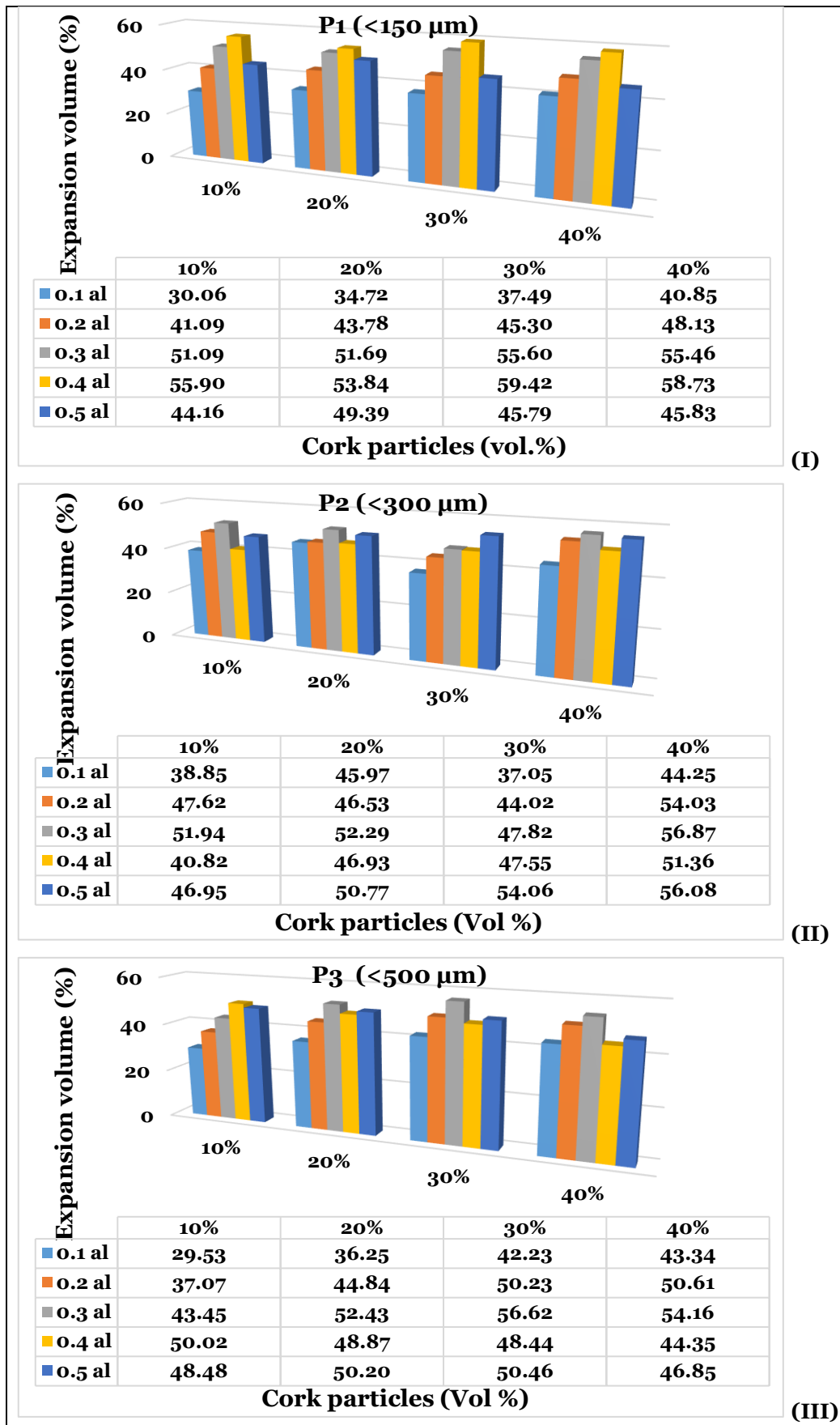*Figure 5. 12 - Expansion volume versus cork particles using a different amount of Al powder; (I); P1 (<150 µm), (II); P2 (<300 µm), and (III); P3 (<500 µm).*

The failure modes (collapse behaviour) of the expansion of AA-LFM can be explained by three main reasons: (1) the viscosity of the mixtures changed since fine powders were replaced with a percentage of cork particles and this last one has a porous structure that could absorb or (keep/catch) a quantity of water and release it then during the curing time. It can be seen that mixtures made using precursor P1 with the smaller particle size of powders are more viscous and shows a typical expansion with Al powder when changed from 0.1 g to 0.4g while using precursor P2 and P3, with a slightly bigger particle size of powders shows expansion when adding Al powder from 0.1g to 0.3g: (2) the aggressively (violent reaction) of the foaming agent due to the high amount used in the mixtures, which shows a fast expansion period and more volume of gas generated; (3) The aggregation of cork particles to the surface of the samples could be the reason of the collapse behaviour since the gas generated during the Al powder reaction with the NaOH make the lightweight particles of cork rise up in the direction of the expansion to the top of the AA-LFM samples.

5.2.4.2. Central section of the AA-LFM

The cross-section of the different AA-LFM specimens with all varieties of precursors (P1, P2, and P3), was obtained using different amounts of Al powder, as well as the different percentages of cork particles presented in Figure 5.13. It is clearly observed that during the expansion process the increase in the Al powder dosage leads to the increase of the volume of the samples. Moreover, the fast expansion period ends earlier when adding a bigger amount of the foaming agent Al powder due to the faster reaction between Al powder and the catalyser NaOH. On the other hand, the expansion volume is also affected by the fineness of the precursor (P1, P2, or P3) and the incorporation of cork particles, which can be noted since the same amount of Al powder does not lead to the same expansion volume for the samples when using different precursors' particle sizes incorporating the same percentage of cork particles.
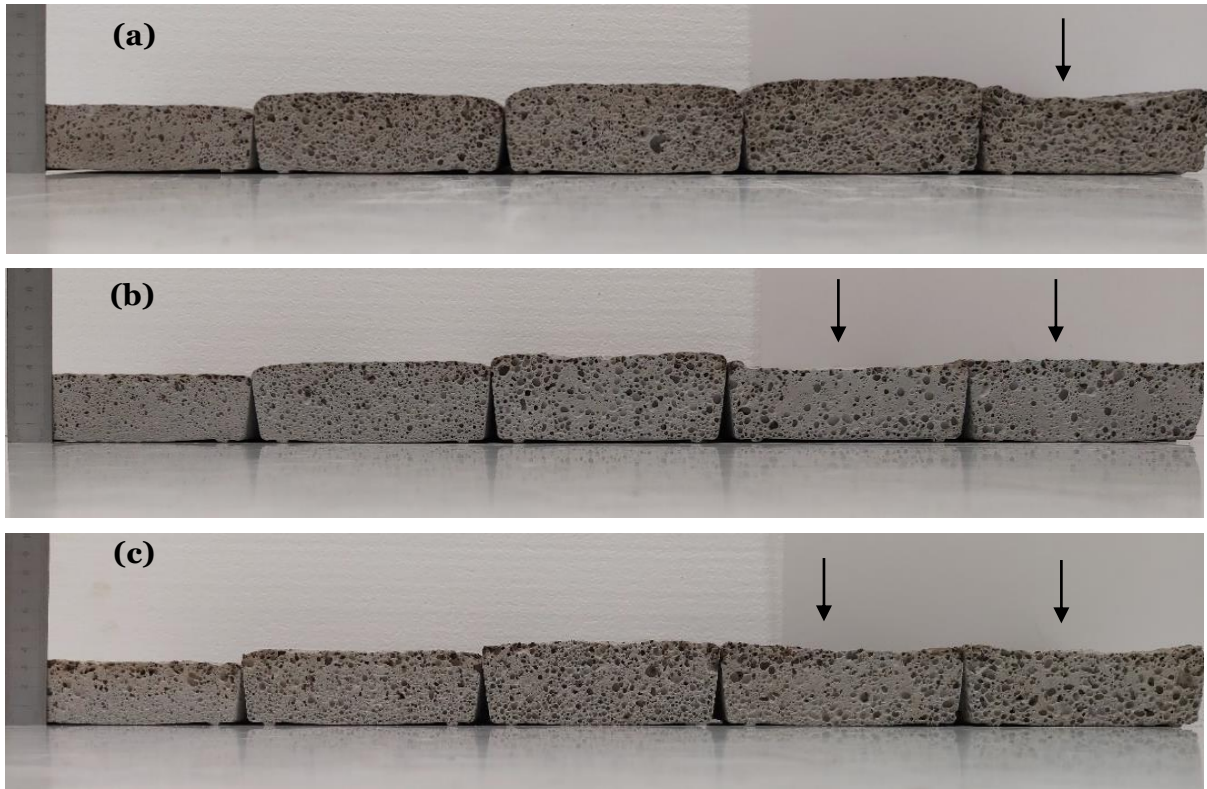
*Figure 5.13 - Expansion mode with Al powder content from (0.1g, left) to (0.5g, right); **(a)** P1 with 40 vol.% cork, **(b)** P2 with 10 vol.% cork and **(c)** P3 with 10 vol.% cork.*

Furthermore, it was observed that cork particles rise in the direction of the expansion, and it was also observed the dense aggregation of many cork grains in the top part of the specimens due to the extremely light density of the cork, as indicated with red lines in Figure 5.14 (i), (ii), and (iii).

| (i) | (ii) | (iii) |
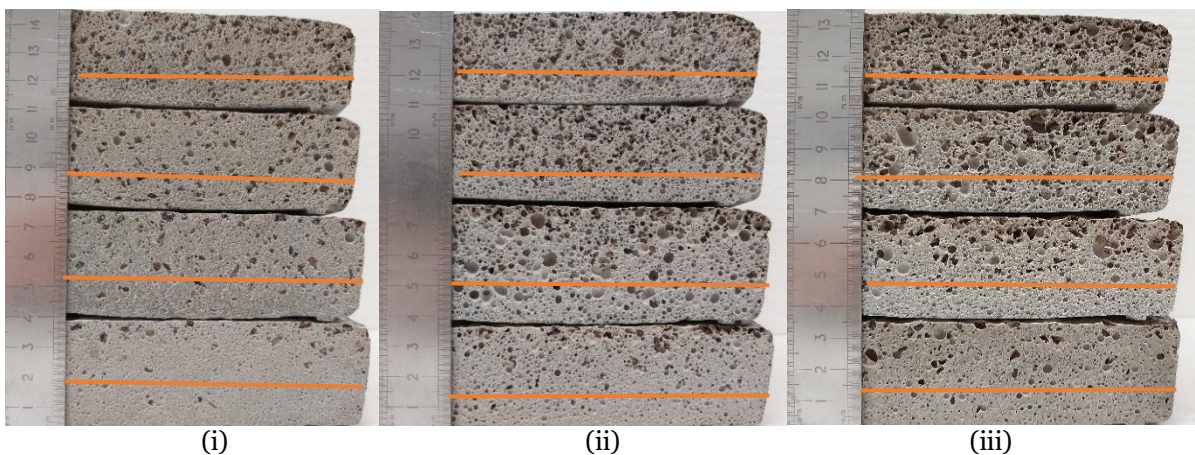
Figure 5.14 - Cross section of AAFM versus cork particles content using 0.1g Al; (i) P1, (ii) P2 and (iii) P3.

5.2.4.3. Pore sizes and cork particles distributions

Figure 5.15 presents images of the central foam section of random AA-LFM specimens obtained with all different precursors' (P1, P2, and P3) particle sizes using different amounts of Al powder (small

and large amount) and incorporating expanded granulated cork (EGC) with different percentages (10 vol.% and 40 vol.% volume of total precursors). It was observed that the formation of large pores appears to be more dependent on the amount of Al powder. The morphology of the pores is influenced by the amount of Al powder used in the foaming reaction. Several pores with a diameter up to 1 mm or 2 mm were formed when using a small amount of Al powder, while large pores with sizes over 2 mm in diameter were formed when using a large amount of Al powder. It clearly shows that they have a macrostructure with irregular spherical macrospores derived from the foaming process. In other words, it can be seen that the increase of Al powder content enlarges the pore size of the samples of the AA-LFM. It is obvious that cork particles are randomly distributed in the samples and the percentage of cork particles incorporated and the amount of Al powder affects the morphology of the pores (shape and diameter) and their distribution (regularity).

- Effect of Al powder addition

It can be observed that the increase of Al powder amount enlarges the pore size of the samples of the AA-LFM. Moreover, the reaction between the Al metal powder and the alkaline activator (NaOH) takes place very fast when significant quantities of the foaming agent are added, and for that reason, the expansion time decreases. On one hand, the hydrogen gas released from the reaction of Al powder with the catalyser in the mixtures presents a volume depending on the amount of Al powder added in other words, a specific amount of Al powder generates a specific hydrogen gas volume. The dissolution and synthesis reaction should be accelerated and somehow it increased the speed of hydrogen release, and this resulted from a violent reaction which, in turn, caused a higher volume expansion. On the other hand, mixtures made by incorporating different cork particles show different viscosity and it slightly changed with the alteration of the percentage of cork particles from 10 vol.% to 40 vol.%.

- Effect of Cork addition

It was observed that the expansion behaviour of AA-LFM is different in some specific conditions. It is obvious that the incorporation of cork particles by eliminating a part of fine powders in the precursor (replacement of these powders with cork particles ranges from 0 to 2 mm), reduces the volume of the powders that are often responsible for keeping the gas emitted during the reaction with Al powder. Furthermore, during the foaming reaction besides the expansion, the volume of gas produced with a large amount of Al powder creates a lot of bubbles inside the mixtures and is followed by the collapse of the samples when adding 0.5g Al powder in the case of precursor P1 and when adding an amount of 0.4g and 0.5g of Al powder in the cases of the precursors P2 and P3. On the other hand, the accumulation of many cork particles on the surface of the AA-LFM samples as a result of their rise during the release of gas generated from the reaction of Al powder has also an influence and is followed by the collapse of the samples.

P1 <150 μm	 **P1F1C1**	 **P1F4C1**
	 P1F1C4	 **P1F4C4**
P2 <300 μm	 **P2F1C1**	 **P2F3C1**
	 P2F1C4	 **P2F3C4**
P3 <500 μm	 **P3F1C1**	 **P3F4C1**

| | P3F1C4 | P3F3C4 |
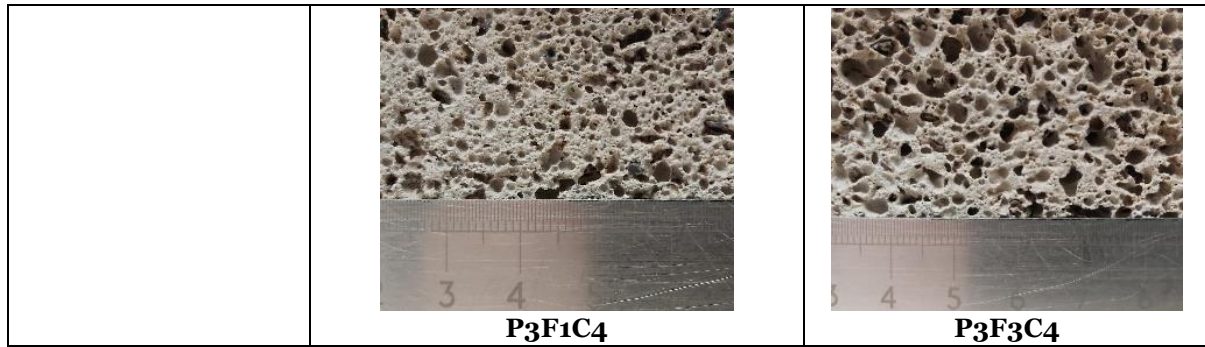
Figure 5.15 - *Photographs of the central foam section of the samples with small and large amounts of Al powder AA-LFM.*

5.3. Summary

• The fineness of the precursor's particles size plays a significant role during the expansion process, and it influences the total expansion volume. The highest expansion volume was obtained with 0.5 g Al powder of about 43%, 49%, and 58% when using precursor particle sizes of 150 µm, 300 µm, and 500 µm, respectively.

• Typical self-foaming (chemical foaming) was observed in alkali-activation of different precursors' particles size when incorporating different cork particles' percentages under 2 mm.

• Highly porous foams were produced when using the Al powder as a blowing agent. The amount of Al powder and the precursors' particle size affected the morphology of the pores. While the formation of large pores (from 1 to 3 mm) appears to be more dependent on the amount of Al, the number of small pores formed (up to 1 mm diameter) are more dependent on the precursors' particle size.

• The expansion volume obtained from Al powder catalysed by NaOH with the ratio SS; SH = 3.1 is about 55.90%, 53.84%, 59.42%, and 58.73% for precursor P1 (<150 m), 51.94%, 52.29%, 47.82%, and 56.87% for precursor P2 (<300 m) and 43.45%, 52.43%, 56.62%, and 54.16 % for precursor P3 (<150 m) when incorporating 10 vol.%, 20 vol.%, 30 vol.%, and 40 vol.%, respectively.

• Adding a large amount of Al powder was followed by the collapse of the samples when adding 0.05 w.% Al powder in the case of precursor P1 and when adding 0.04 w.% and 0.05 w.% of Al powder in the case of precursors P2 and P3. Consequently, for each precursors' particle size, the density obtained through the changes in the amount of Al powder and as a result of adding cork particles at 40 vol.% showed superior values when adding 0.05 w.% Al powder as in P1 and 0.04 w.% Al powder as in P2 and P3; the collapsed samples present an increase in the compressive strength because of the decrease of the porosity through the failure of the samples expansion process.

• The foaming process was extremely quick in the high bubbling specimens, preventing full alkali activation of the geopolymers, and hence many unreacted particles remain [23].

Chapter 6 - Thermal conductivity of the foamed materials

In this chapter, the focus is to investigate the thermal insulation properties of tungsten-based alkali-activated binder and alkali-activated binder incorporating cork particles. Results are presented and a comparative study of the alkali-activated foamed materials produced during the combination of the (alkali-activated foamed binders (AAFs) and alkali-activated foamed binders incorporating cork (AA-LFMs)), as well as discussions are highlighted. Furthermore, findings that have been published or accepted for publication are also presented. The results demonstrate that produced materials throughout the different combinations show significantly influence final binder mechanical properties.

6.1. Thermal conductivity of the AAFs

The average thermal conductivity values obtained for the foams are presented in Figure 6.1. The alkali-activated foamed (AAFs) mixture P3-F5 have the lowest thermal conductivity value, equal to 0.21 W/m K, while P1-F1 foams display the highest one 0.33 W/m K. Thermal conductivity depends, for a large part, on the total pore volume achieved after the foaming process. In fact, the thermal conductivity decreases by increasing the total porosity, as demonstrated in Figure 6.1. The higher the porosity, the lower the thermal conductivity. This is because a higher porosity means more voids and the thermal conductivity of air within the voids is much lower than that of solid substance, as consequence, an overall lowering of the thermal conductivity of the material since the thermal conductivity of air within the voids is much lower than that of solid substance [265] [266].
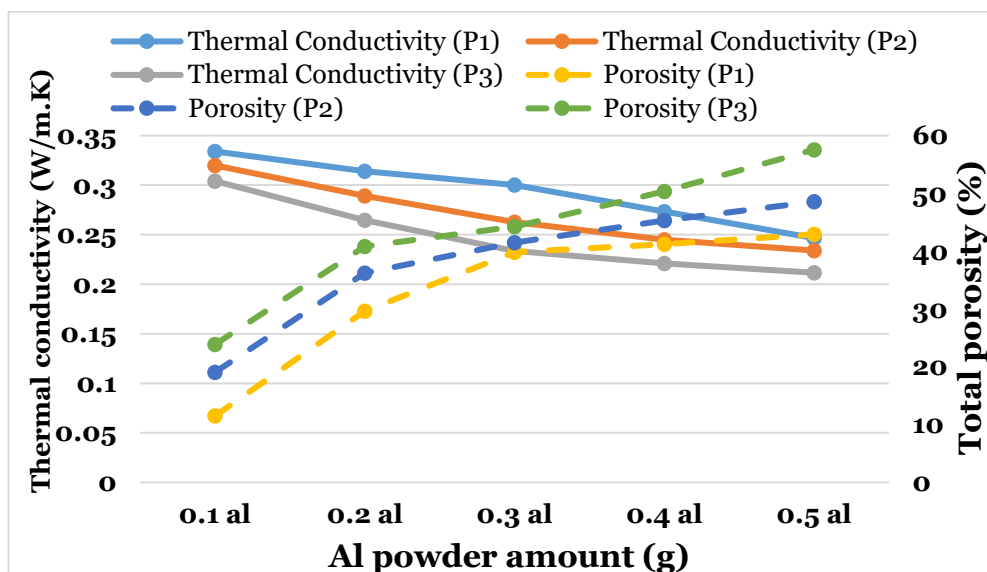
Figure 6.1 - Relationship between total porosity and thermal conductivity of the AAFs as a function of Al powder content.

The porosity in the graph is the higher expansion volume of the samples

6.2. Thermal conductivity of the AA-LFMs

Figure 6.2 shows the average thermal conductivity values obtained for the alkali-activated lightweight foamed material (AA-LFMs) comprising cork particles. It was reported that thermal conductivity of the AA-LFM mixtures for all samples with the different precursors' particle sizes using several amounts of Al powder and incorporating different percentages of cork particles depends, for a large part, on the total pore volume achieved after the foaming process. The lowest thermal conductivity value, equal to 0.13 W/m K, was obtained by the mixture P3F3C3, while P1F1C1 foams display the highest one 0.26 W/m K. As expected, the increase of the Al powder amounts leads to lower thermal conductivity results which means that the amount of foaming agent enhances the number and the pore sizes of the AA-LFM produced. It is obvious that the increase of the overall porosity lowers the thermal conductivity. Thus, the lower the heat conductivity, the bigger the porosity since the thermal conductivity of air within the voids is much lower than that of solid matter, a higher porosity means more voids, and the thermal conductivity of air within the voids is much lower than that of solid matter, resulting in an overall reduction in the thermal conductivity of the material.

Precursor (P1) shows a relatively hight thermal conductivity results for the samples that shows a typical expansion as presented in Figure 6.2 (A) while precursors (P2 and P3) show lower thermal conductivity of the AA-LFMs as presented in Figure 6.2 (B) and (C), respectively. However, the samples that collapsed presented an increase of the thermal conductivity results which confirm that the porosity plays an important role for the thermal conductivity properties of the materials. Additionally, it was observed that the maximum thermal conductivity results for the AA-LFM incorporating cork particles was lower than the AAFs without cork. Thus, cork particles enhance the thermal conductivity properties of the alkali-activated foamed materials, moreover, the addition of cork can benefit for a good fire resistance.

P1 (<150 µm)

	0.1 al	0.2 al	0.3 al	0.4 al	0.5 al
■ 10%	0.269060	0.200605	0.178503	0.180775	0.198604
■ 20%	0.225603	0.206708	0.178785	0.171548	0.163537
■ 30%	0.202863	0.189512	0.163641	0.166260	0.161644
■ 40%	0.180171	0.162139	0.156942	0.148310	0.151986

Al powder amount (g)

(A)

P2 (<300 µm)

	0.1 al	0.2 al	0.3 al	0.4 al	0.5 al
■ 10%	0.247392	0.191119	0.167997	0.212071	0.190510
■ 20%	0.195324	0.201004	0.142502	0.179985	0.177938
■ 30%	0.201015	0.197030	0.201600	0.188035	0.151690
■ 40%	0.196275	0.161071	0.148703	0.171972	0.149429

Al powder amount (g)

(B)

P3 (<500 µm)

	0.1 al	0.2 al	0.3 al	0.4 al	0.5 al
■ 10%	0.225921	0.205984	0.215052	0.174860	0.171373
■ 20%	0.186025	0.176709	0.163136	0.172996	0.166249
■ 30%	0.187581	0.167266	0.139327	0.161981	0.160968
■ 40%	0.199841	0.160246	0.142138	0.159123	0.148060

Al powder amount (g)

(C)

Figure 6. 2 - *Thermal conductivity of the AA-LFMs as a function of Al powder amounts and cork particles content.*

Table 6.1 - presents the characteristics of the AAFs and AA-LFMs tungsten-based which are non-flammable and whose maximum application temperature is up to 1000° C.

Table 6.1 - *Physical characteristics of tungsten-based alkali-activated foamed materials.*

Bulk density of the AAFs (kg/m³)	913 – 1647	Lightweight
Bulk density of the AA-LFMs (kg/m³)	664 - 1346	Lightweight
Max. temperature of application of the AAFs (° C)	*1000*	*High*
Max. temperature of application of the AA-LFMs (° C)	1000	High
Thermal conductivity of the AAFs (W/(m.K))	*0.21 – 0.33*	Medium
Thermal conductivity of the AA-LFMs (W/(m.K))	0.13 – 0.26	Medium
Compressive strength of the AAFs (N/mm²)	*2.28 – 16.1*	Medium
Compressive strength of the AA-LFMs (N/mm²)	*1.38 – 6.29*	Medium

6.3. Summary

This chapter was focused on the thermal conductivity of the produced AAFs and AA-LFMs. Results and discussions of the investigated innovative foamed materials based on tungsten mining waste mud (TWM) and incorporating expanded granulated cork (EGC) through a chemical foaming method using aluminium powder (Al) indicate that AAFs and AALFMs have appropriate thermal insulation properties for buildings application. Furthermore, this chapter demonstrated the great importance of EGC particles on the density reduction by incorporating them as lightweight aggregates, as well as the enhancement of the thermal conductivity properties of the manufactured tungsten-based alkali-activated foamed materials with the remaining relatively high compressive strength.

Chapter 7 - Conclusions and recommendations

7.1. Conclusions

Overall, the objective of this study was to develop new alkali-activated lightweight foamed materials composed of a valorised tungsten mining waste mud binder (TMWM) and natural expanded granulated cork (EGC), which meets the criteria of eco-friendly material. The work within the framework of this study is divided into three main parts: development of new alkali-activated foamed materials and the investigation of the foaming process, as well as study thermal insulation properties.

In the chapter of the literature review, the notion of sustainable development was discussed. This chapter illustrated how important it is to replace conventional building materials with eco-materials from a construction perspective. It was also suggested that alkali-activated foamed tungsten mining waste mud by the incorporation of EGC to be used for thermal insulation wall since it has good thermal properties, is low in cost and therefore is environmentally friendly. For the precursors, this chapter stated that mining wastes are one of the greatest eco-materials since their manufacture requires significantly less energy than Portland cement and produces a small amount of CO_2. Furthermore, the valorisation of TWM, natural cork waste, and waste glass is considered as eco-materials when compared to Portland cement. As a result, tungsten mining waste mud, natural expanded granulated cork particles, and other components to develop alkali-activated foamed materials were chosen. On the other hand, metakaolin was used to increase the reactivity of these binders. Additionally, these materials combine several environmental benefits: they are local and renewable resources, they are carbon neutral, and their embodied energy is usually low. Previous works permitted us to select waste cork because it is an eco-material and available in Portugal (in our case). Moreover, it had a low cost and a good thermal insulation properties. This chapter also indicated that it is necessary to incorporate expanded granulated cork as lightweight aggregate, so that it is not only used as cork-boards in the building, but also has favourable effect on reducing the density of the alkali-activated composites.

In the third chapter, the precursor and natural cork particles were characterized, and the methods used in this study were described. The method for the measurement of gas released in the reaction of the foaming agent catalysed by the NaOH was illustrated. For raw materials, the chemical composition of tungsten waste mud, waste glass, metakaolin, and cement were characterized through SEM analyses. These analyses allowed us to calculate the content of SiO_3 and Al_2O_3 contained in TWM. Additionally, the chemical characteristics of the alkaline solution Sodium Silicate and Sodium Hydroxide used were introduced. Furthermore, Cork is a multifunctional material that was used in this study to produce alkali-activated tungsten mining waste composites as a sustainable material to enhance the buildings' energy and acoustic performance.

Chapter four was divided into two parts: in the first part, mix design for different alkali-activated materials was presented and in the second part, the physical-mechanical and microstructural results for new tungsten-based alkali-activated foamed materials were described.

Furthermore, chapter five was dedicated to studying the expansion process and it was found that the amounts of the Al powder in addition to the fineness of the precursor's particles size as well as cork particles play a significant role during the expansion process, and it influences the total expansion volume. In this chapter also the pore size distribution of the AAFs was also highlighted (pore diameter obtained by image J). For the different maximum particles sizes of powders which constitute the precursor it can be concluded that the size of the precursor particle has a significant impact on the formation of small pores (up to 1mm in diameter), while the amount of aluminium powder added to the combinations were found to have a significant impact on the formation of large pores (from 1 to 3mm).

In the last chapter, the thermal conductivity of different alkali-activated tungsten-based binder as well as the alkali-activated cork composite were presented and compared. According to our findings, the thermal conductivity of alkali-activated cork composites was directly influenced by porosity and cork incorporation.

Finally, alkali-activated foamed binders (AAFs) and alkali-activated lightweight foamed materials (AALFMs) were developed in this study through the chemical foaming method with Al powder. Enhancement of the mechanical strength and reducing density by reducing precursor particle sizes. These binders/mortars can be considered eco-binders thanks to the high contents of tungsten mining waste mud. This alkali-activated tungsten-based presents fairly good mechanical and thermal properties in comparison to other raw materials.

7.2. Recommendations

Alkali-activated foamed materials from tungsten mining waste mud (TWM) incorporating expanded granulated cork presented relatively good mechanical and thermal properties when compared to other raw materials. In order to enhance the manufacture of alkali-activated foamed materials as well as to develop a deeper and more thorough controlling of the foam manufacturing process and remain good mechanical properties (compressive strength) of the produced material, there are still several areas of future research that need to be investigated:

- Study the potential applications in artistic, architectural, and historical heritage restoration of these material;

- Develop light-weighted but highly energy-efficient alkali-activated foamed composites for buildings;

- Study different approaches of the expansion process using other foaming agents (hydrogen peroxide, sodium perborate);

7.3. Summary of Publications and Conferences

Imed BEGHOURA

University of Beira Interior;

Calçada Fonte do Lameiro Edifício II das Engenharias, 6201-001 Covilhã, Portugal

E-mail : beghoura.imed@ubi.pt

Phone: +351 910 566 053

Published Articles in International Refereed Journals

Imed Beghoura., João Castro-Gomes, Haroon Ihsan, Nuno Estrada, (2017). Feasibility of alkali-activated mining waste foamed materials incorporating expanded granulated cork. *Journal of Mining Science.*

Imed Beghoura, João Castro-Gomes, (2019). Design of alkali-activated aluminium powder foamed materials for precursors with different particle sizes. *Journal of Construction and Building Materials.*

Imed Beghoura, João Castro-Gomes, (2021). Enhancing Density-Based Mining Waste Alkali-Activated Foamed Materials Incorporating Expanded Cork. *Journal of civileng.*

Presentations at International Conferences

Imed Beghoura., João Castro-Gomes, Haroon Ihsan, John Pickstone, Nuno Estrada, (2019). Expansion volume of alkali activated foamed cork composites from tungsten mining mud waste with aluminium. *Paper presented at the REMINE International Conference & Brokerage Event (RICON17) from 25th to 27th of October 2017, University of Beira Interior, Covilhã, Portugal.*

Joao Castro-Gomes, Manuel Magrinho, Naim Sedira, **Imed Beghoura,** Pedro Humbert, Maria Manso, Ana Fernandes, Rafael Silva, (2017). Alkali-activation of tungsten mining waste mud blended with waste glass: reactivity, performance, and innovative applications. *Paper presented at the International Congress on Engineering, A Vision For the Future December 5th, 6th, and 7th ICEUBI 2017, University of Beira Interior, Covilhã, Portugal.*

Imed Beghoura., João Castro-Gomes, (2019). Development of porous tungsten mud waste-based alkali-activated foams with low thermal conductivity". *Paper presented at the International Doctorate Students Conference + Lab Workshop in Civil Engineering (STARTCON19) from 26th to 28th of June 2019, University of Beira Interior, Covilhã, Portugal.*

Imed Beghoura., João Castro-Gomes, (2019). Development of Alkali-activated Foamed Lightweight Mortar Tungsten Mining Waste Mud-based Incorporating Expanded Cork. *Paper presented at the REMINE International Conference on Valorisation of mining and industrial wastes into construction materials by alkali-activation (RICON19) from 11th to 13th December 2019, University of Beira Interior, Covilhã, Portugal.*

7.4. References

[1]   J. Davidovits, "Global warming impact on the cement and aggregates industries," *World Resour. Rev.*, vol. 6, no. 2, pp. 263–278, 1994.
[2]   M. C. G. Juenger, F. Winnefeld, J. L. Provis, and J. H. Ideker, "Advances in alternative cementitious binders," *Cem. Concr. Res.*, vol. 41, no. 12, pp. 1232–1243, 2011.
[3]   Y. M. Liew, H. Kamarudin, A. M. Mustafa Al Bakri, M. Luqman, I. Khairul Nizar, and C. Y. Heah, "Investigating the possibility of utilization of kaolin and the potential of metakaolin to produce green cement for construction purposes-A review," *Aust. J. Basic Appl. Sci.*, vol. 5, no. 9, pp. 441–449, 2011.
[4]   J. Davidovits, "Transfer and exploitation of scientific and technical information," *Transf. Exploit. Sci. Tech. Inf.*, no. June, pp. 316–320, 1981.
[5]   J. Davidovits, "Geopolymer Cement, a review: Geopolymer Institute," *Geopolymer Inst.*, no. 0, pp. 1–11, 2013.
[6]   P. Hlavacek, "Engineering properties of alkali activated composites," pp. 1–88, 2014.
[7]   N. Neithalath and J. Hicks, *Advances in Green Binder Systems*. .
[8]   European Commission, "A healthy and sustainable environment for present and future generations Environment," p. 16 pp., 2014.
[9]   C. Ferone, F. Colangelo, F. Messina, L. Santoro, and R. Cioffi, "Recycling of pre-washed municipal solid waste incinerator fly ash in the manufacturing of low temperature setting geopolymer materials," *Materials (Basel).*, vol. 6, no. 8, pp. 3420–3437, 2013.
[10]   F. Pacheco-Torgal, J. P. Castro-Games, and S. Jalali, "Alkali activated geopolymeric binder using Tungsten mine waste: preliminary investigation," *Geopolymer, Green Chem. Sustain. Dev. Solut.*, pp. 93–98, 2005.
[11]   J. P. Castro-gomes, A. P. Silva, R. P. Cano, J. D. Suarez, and A. Albuquerque, "Potential for reuse of tungsten mining waste-rock in technical-artistic value added products," *J. Clean. Prod.*, vol. 25, pp. 34–41, 2012.
[12]   L. Gil, "New cork-based materials and applications," *Materials (Basel).*, vol. 8, no. 2, pp. 625–637, 2015.
[13]   A. M. Matos, S. Nunes, and J. Sousa-coutinho, "Cork waste in cement based materials," *JMADE*, vol. 85, pp. 230–239, 2015.
[14]   European commission, "Closing the loop : Commission adopts ambitious new Circular Economy Package to boost competitiveness , create jobs and generate sustainable," no. December 2015, 2015.
[15]   "DGEG Direção-Geral de Energia e Geologia, Caraterização Energética Nacional 2019, http://www.dgeg.gov.pt/, last accessed 2021/12/ 15." .
[16]   L. Zhang, S. Ahmari, and J. Zhang, "Synthesis and characterization of fly ash modified mine tailings-based geopolymers," *Constr. Build. Mater.*, vol. 25, no. 9, pp. 3773–3781, 2011.
[17]   Pacheco-torgal, "Utilization of mining wastes to produce geopolymeric binders book chapter," 2009.
[18]   Z. Zhang, J. L. Provis, A. Reid, and H. Wang, "Geopolymer foam concrete: An emerging material for sustainable construction," *Constr. Build. Mater.*, vol. 56, pp. 113–127, 2014.
[19]   N. Narayanan and K. Ramamurthy, "Structure and properties of aerated concrete : a review," vol. 22, pp. 321–329, 2000.
[20]   E. P. Kearsley and P. J. Wainwright, "The effect of high fly ash content on the compressive strength of foamed concrete," vol. 31, pp. 0–7, 2001.
[21]   J. Davidovits, *Geopolymer Chemistry and Applications 3rd edition*. 2011.
[22]   R. A. Aguilar, O. B. Díaz, and J. I. E. García, "Lightweight concretes of activated metakaolin-fly ash binders , with blast furnace slag aggregates," *Constr. Build. Mater.*, vol. 24, no. 7, pp. 1166–1175, 2010.
[23]   J. G. et al. Sanjayan, "Physical and mechanical properties of lightweight aerated geopolymer," *Constr. Build. Mater.*, vol. 79, pp. 236–244, 2015.
[24]   F. Zulkarnain and M. Ramli, "'Performance of foamed concrete mix design with silica fume for general housing construction,'" *Eur. J. Technol. Adv. Eng. Res.*, vol. 1, pp. 18–28, 2011.
[25]   M. M. Al Bakri Abdullah, K. Hussin, M. Bnhussain, K. N. Ismail, Z. Yahya, and R. A. Razak, "Fly ash-based geopolymer lightweight concrete using foaming agent," *Int. J. Mol. Sci.*, vol. 13, no. 6, pp. 7186–7198, 2012.
[26]   D. K. Panesar and B. Shindman, "The mechanical , transport and thermal properties of mortar and concrete containing waste cork," *Cem. Concr. Compos.*, vol. 34, no. 9, pp. 982–992, 2012.

[27]   S. R. Karade, M. Irle, and K. Maher, "Influence of granule properties and concentration on cork-cement compatibility," pp. 281–286, 2006.

[28]   F. Pacheco-Torgal, J. P. Castro-Gomes, and S. Jalali, "Investigations of tungsten mine waste geopolymeric binder: Strength and microstructure," *Constr. Build. Mater.*, vol. 22, no. 11, pp. 2212–2219, 2008.

[29]   F. Pacheco-torgal, "Tungsten mine waste geopolymeric binder : Preliminary hydration products investigations," vol. 23, pp. 200–209, 2009.

[30]   F. Pacheco-Torgal, J. P. Castro-Gomes, and S. Jalali, "Adhesion characterization of tungsten mine waste geopolymeric binder. Influence of OPC concrete substrate surface treatment," *Constr. Build. Mater.*, vol. 22, no. 3, pp. 154–161, 2008.

[31]   G. Kastiukas, X. Zhou, and J. Castro-gomes, "Development and optimisation of phase change material-impregnated lightweight aggregates for geopolymer composites made from aluminosilicate rich mud and milled glass powder," *Constr. Build. Mater.*, vol. 110, pp. 201–210, 2016.

[32]   M. Manso, J. Castro-Gomes, and P. Silva, "Modular system design for vegetated surfaces: a proposal for energy-efficient buildings," *BESS-SB13 Calif. Adv. Towar. Net Zero. Pomona, California, USA.*, no. June, pp. 1–6, 2013.

[33]   N. Sedira, "Novel waste-based alkali-activated binders by combining mining and other mineral waste," 2021.

[34]   B. C. McLellan, R. P. Williams, J. Lay, A. Van Riessen, and G. D. Corder, "Costs and carbon emissions for geopolymer pastes in comparison to ordinary portland cement," *J. Clean. Prod.*, vol. 19, no. 9–10, pp. 1080–1090, 2011.

[35]   L. K. Turner and F. G. Collins, "Carbon dioxide equivalent (CO2-e) emissions: A comparison between geopolymer and OPC cement concrete," *Constr. Build. Mater.*, vol. 43, pp. 125–130, 2013.

[36]   C. Shi, A. F. Jiménez, and A. Palomo, "New cements for the 21st century : The pursuit of an alternative to Portland cement," *Cem. Concr. Res.*, vol. 41, no. 7, pp. 750–763, 2011.

[37]   D. M. Roy, "Alkali-activated cements Opportunities and challenges," vol. 29, pp. 249–254, 1999.

[38]   C. Li, H. Sun, and L. Li, "A review: The comparison between alkali-activated slag (Si + Ca) and metakaolin (Si + Al) cements," *Cem. Concr. Res.*, vol. 40, no. 9, pp. 1341–1349, 2010.

[39]   John L. Provis and S. A. Bernal, "Milestones in the Analysis of Alkali-Activated," *White rose Res.*, vol. 4, pp. 74–84, 2014.

[40]   A. Fernández-Jiménez and F. Puertas, "alkali-activated slag cements: Kinetic studies," *Cem. Concr. Res.*, vol. 27, no. 3, pp. 359–368, 1997.

[41]   P. R. Jochens, "Utilisation of slags for the manufacture cement," *J. South African Inst. Min. Metall.*, pp. 464–474, 1969.

[42]   J. L. Provis, *Geopolymers - Structure, processing, properties and industrial applications Jhon L. Provis.pdf.* 2009.

[43]   J. L. Provis and J. S. J. van Deventer, *Alkali avtivated materials: State of Art Report.* 2014.

[44]   P. R. Jochens, "Utilisation of slags for the manufacture of cement," *J. South Africain Inst. Min. Metall.*, pp. 464–474, 1969.

[45]   K. Komnitsas and D. Zaharaki, "Geopolymerisation: A review and prospects for the minerals industry," *Miner. Eng.*, vol. 20, no. 14, pp. 1261–1277, 2007.

[46]   J. Davidovits and M. Davidovics, "Geopolymer. Ultra-high temperature tooling material for the manufacture of advanced composites," *Int. SAMPE Symp. Exhib.*, vol. 36, no. pt 2, pp. 1939–1949, 1991.

[47]   J. Davidovits, "Mineral Polymer and Methods of Making Them," *United States Pat.*, pp. 1–6, 1982.

[48]   J. Davidovits, "Geopolymers; Inorganic polymeric new materials," *J. Therm. Anal.*, vol. 37, pp. 1633–1656, 1991.

[49]   N. R. Rakhimova and R. Z. Rakhimov, "A review on alkali-activated slag cements incorporated with supplementary materials," *J. Sustain. Cem. Mater.*, vol. 3, no. 1, pp. 61–74, 2014.

[50]   C. S. Della.Roy, Pavel V. Krivenko, "Alkali activated cements and concretes." 2006.

[51]   Krivenko et al., "Directed synthesis of alkaline aluminosilicate minerals in a geocement matrix," pp. 2944–2952, 2007.

[52]   František Škvára and Department, "Alkali Activated Material – Geopolymer," *ICT Prague*, no. 02, pp. 68–72, 2011.

[53]   A. Palomo, M. W. Grutzeck, and M. T. Blanco, "Alkali-activated fly ashes A cement for the future," vol. 29, pp. 1323–1329, 1999.

[54]   A. Palomo, P. Krivenko, I. Garcia-Lodeiro, E. Kavalerova, O. Maltseva, and A. Fernández-

Jiménez, "A review on alkaline activation: New analytical perspectives," *Mater. Constr.*, vol. 64, no. 315, 2014.

[55] P. Kryvenko, H. Cao, O. Petropavlovskii, L. Weng, and O. Kovalchuk, "Efficiency of alkali activated hybrid cements for immobilization of low-level radioactive anion-exchange resins," *Eastern-European J. Enterp. Technol.*, vol. 5, no. 10–83, pp. 38–43, 2016.

[56] J. Davidovits and J. L. Sawyer, "Early high-strength mineral polymer," *United States Pat.*, pp. 1–12, 1985.

[57] K. H, "Kühl, H. (1930) Zementchemie. Berlin, Germany. Verlag Technik, Band III; 1958 or Zement 19. IN; A. Palomo et al. 'A review on alkaline activation: New analytical perspectives,' Mater. Constr., vol. 64, no. 315, 2014. doi: http://dx.doi.org/10.3989/mc.2014," 1930.

[58] R. Feret, "Slags for the manufacture of cement. IN; A. Palomo et al. 'A review on alkaline activation: New analytical perspectives,' Mater. Constr., vol. 64, no. 315, 2014. doi: http://dx.doi.org/10.3989/mc.2014.," *Rev. Mater. Constr. Tr. Publ.*, pp. 1–145, 1939.

[59] A. Purdon, "The action of alkalis on blast furnace slag. IN; A. Palomo et al. 'A review on alkaline activation: New analytical perspectives,' Mater. Constr., vol. 64, no. 315, 2014. doi: http://dx.doi.org/10.3989/mc.2014.," *J. Soc. Chem. Ind.*, vol. 59, pp. 191–202.

[60] V. D. Glukhovsky, "Ancient, Modern and Future Concretes. IN; A. Palomo et al. 'A review on alkaline activation: New analytical perspectives,' Mater. Constr., vol. 64, no. 315, 2014. doi: http://dx.doi.org/10.3989/mc.2014.," *Proceed. 2nd Int. Semin. (Gothenburg, Sweden).*, pp. 53–62.

[61] Glukhovsky V.D., "'Slag-alkali concretes produced from fine-grained aggregate'. In; Z. Abdollahnejad, 'Development of Foam One-Part Geopolymers.,' PhD thesis. p. 132, July, 2016.," *Kiev VishchaShkolay;*, 1981.

[62] Joseph Davidovits, "Geopolymer chemestry & applications." 2008.

[63] Malinowski, "Ancient aqueducts characterized. In; Z. Abdollahnejad, 'Development of Foam One-Part Geopolymers.,' PhD thesis. p. 132, July, 2016.," 1979.

[64] P. J. Davidovits, "30 Years of Successes and Failures in Geopolymer Applications . Market Trends and Potential Breakthroughs .," *Geopolymer 2002 Conf.*, pp. 1–16, 2002.

[65] Forss, "F-cement (Slag-alkali-superplasticizer). In; Z. Abdollahnejad, 'Development of Foam One-Part Geopolymers.,' PhD thesis. p. 132, July, 2016."

[66] J. Davidovits, "Application of Ca-based geopolymer with blast furnace slag , a review," *Proceeding Second Int. Slag Valoris. Symp.*, pp. 33–49, 2011.

[67] D. M. Roy and C. A. Langton, "Studies of Ancient Concrete as Analogs of Cementitious Sealing Materials for a Repository in Tuff," *La-11527-Ms*, no. March, 1989.

[68] Philip G. Malone *et al.*, "Potential applications of alkali-activated alumino-silicate binders in millitary operations," *Misccellaneous Pap. GL-85- 15.*, no. 4, pp. 1–37, 1985.

[69] P. Krivenko, "DSc thesis, R2O-RO-SiO2-H2O. In; Z. Abdollahnejad, 'Development of Foam One-Part Geopolymers.,' PhD thesis. p. 132, July, 2016.," 1986.

[70] Malolepsy and Petri, "Activation of synthetic melilite slags. In; Z. Abdollahnejad, 'Development of Foam One-Part Geopolymers.,' PhD thesis. p. 132, July, 2016." 1986.

[71] Malek et al., "Slag cement-low level radioactive wastes forms. In; Z. Abdollahnejad, 'Development of Foam One-Part Geopolymers.,' PhD thesis. p. 132, July, 2016." 1986.

[72] J. Davidovits, "Geopolymeric Reactions in Archaeological Cements and in Modern Blended Cements," *Concr. Int.*, vol. 9, no. December 1987, pp. 23–29, 1987.

[73] Deja and Malolepsy, "Resistance to chlorides shown. In; Z. Abdollahnejad, 'Development of Foam One-Part Geopolymers.,' PhD thesis. p. 132, July, 2016." 1989.

[74] Kaushal et al., "Adiabatic cured nuclear wastes from alkaline mixtures. In; Z. Abdollahnejad, 'Development of Foam One-Part Geopolymers.,' PhD thesis. p. 132, July, 2016." 1989.

[75] Majundar et al., "C12A7-slag activation. In; Z. Abdollahnejad, 'Development of Foam One-Part Geopolymers.,' PhD thesis. p. 132, July, 2016." 1989.

[76] Talling and Brandstetr, "Alkali-activated slag. In; Z. Abdollahnejad, 'Development of Foam One-Part Geopolymers.,' PhD thesis. p. 132, July, 2016." vol. 1989.

[77] D. W.-C. D.M. Roy, M.R. Silsbee, "New rapid setting alkali activated cement compositions. In D. M. Roy, 'Alkali-activated cements Opportunities and challenges,' vol. 29, pp. 249–254, 1999.," *MRS Proceedings.*, vol. 179, pp. 203– 220.

[78] W. et Al., "Activation of slag cement. In; Z. Abdollahnejad, 'Development of Foam One-Part Geopolymers.,' PhD thesis. p. 132, July, 2016.," 1990.

[79] M. R. S. D.M. Roy, "Alkali-activated materials: an overview. In D. M. Roy, 'Alkali-activated cements Opportunities and challenges,' vol. 29, pp. 249–254, 1999.," *MRS Proceedings,* vol. 245, pp. 153–164., 1992.

[80] palomo and glasser, "CBC with metakaolin. In; Z. Abdollahnejad, 'Development of Foam One-

Part Geopolymers.,' PhD thesis. p. 132, July, 2016.," 1992.

[81]   Roy and Malek, "Slag cement. In; Z. Abdollahnejad, 'Development of Foam One-Part Geopolymers.,' PhD thesis. p. 132, July, 2016.," 1993.

[82]   V. D. Glukhovsky, "Ancient, modern and future concretes. In: Proceedings of the 2nd International Seminar, Gothenburg, Sweden, 53 – 62, (1989); In: P. Krivenko, 'Why alkaline activation - 60 years of the theory and practice of alkali-activated materials,' J. Ceram. Sci. Tec," 1994.

[83]   P.V. Krivenko, "Alkaline cements, in: P.V. Krivenko (Ed.), Alkaline Cements and Concretes, Proceedings of the 1st International Conference, VIPOL Stock Co., Kiev, Ukraine, 1994, pp. 11–130. In D. M. Roy, 'Alkali-activated cements Opportunities and challenges,' vol. 29, p," 1994.

[84]   S. Wang and K. L. Scrivener, "Hydration products of alkali-activated slag cement," vol. 25, no. 3, pp. 561–571, 1995.

[85]   C. Shi, "Strength, pore structure and permeability of alkali-activated slag," *Cem. Concr. Res.*, vol. 26, no. 12, pp. 1789–1799, 1996.

[86]   A. Katz, "Microstructure of alkali-activated fly ash," *Cem. Concr. Res.*, vol. 28, no. 2, pp. 197–208, 1998.

[87]   Joseph Davidovits, "Chemistry of geopolymeric systems, technology. In; Z. Abdollahnejad, 'Development of Foam One-Part Geopolymers.,' PhD thesis. p. 132, July, 2016.," *Geopolymer*, vol. 99, no. 292, pp. 9–39, 1999.

[88]   M.D. Roy, "Alkali-activated cements Opportunities and challenges," vol. 29, pp. 249–254, 1999.

[89]   C. Gong and N. Yang, "Effect of phosphate on the hydration of alkali-activated red mud slag cementitious material," vol. 30, pp. 3–6, 2000.

[90]   F. Puertas, S. Martínez-Ramírez, S. Alonso, and T. Vázquez, "Alkali-activated fly ash/slag cements. Strength behaviour and hydration products," *Cem. Concr. Res.*, vol. 30, no. 10, pp. 1625–1632, 2000.

[91]   T. Bakharev, J. G. Sanjayan, and Y. Cheng, "Resistance of alkali-activated slag concrete to alkali ± aggregate reaction," vol. 31, pp. 331–334, 2001.

[92]   A. Palomo and M. Palacios, "Alkali-activated cementitious materials: Alternative matrices for the immobilisation of hazardous wastes - Part II. Stabilisation of chromium and lead," *Cem. Concr. Res.*, vol. 33, no. 2, pp. 289–295, 2003.

[93]   M. Grutzeck, S. Kwan, and M. DiCola, "Zeolite formation in alkali-activated cementitious systems," *Cem. Concr. Res.*, vol. 34, no. 6, pp. 949–955, 2004.

[94]   H. Sun, R. Jain, K. Nguyen, and J. Zuckerman, "Sialite technology - Sustainable alternative to portland cement," *Clean Technol. Environ. Policy*, vol. 12, no. 5, pp. 503–516, 2010.

[95]   C. et al Shi, *alkali activated cements and concretes*. 2006.

[96]   P. Duxon et al, "Geopolymer technology : the current state of the art," no. 4, pp. 2917–2933, 2007.

[97]   A. Hajimohammadi, J. L. Provis, and J. S. J. Van Deventer, "One-part geopolymer mixes from geothermal silica and sodium aluminate," *AIChE Annu. Meet. Conf. Proc.*, pp. 9396–9405, 2008.

[98]   L. A. Pereira-De-Oliveira, J. P. Castro-Gomes, and P. M. S. Santos, "The potential pozzolanic activity of glass and red-clay ceramic waste as cement mortars components," *Constr. Build. Mater.*, vol. 31, pp. 197–203, 2012.

[99]   R. Ghosh et al., "Fly-ash Geopolymer Concrete as Future Concrete," vol. 6, no. 3, pp. 260–271, 2013.

[100] J. L. Provis, *Alkali Activated Materials state of the art report*. 2014.

[101] B. Singh, G. Ishwarya, M. Gupta, and S. K. Bhattacharyya, "Geopolymer concrete: A review of some recent developments," *Constr. Build. Mater.*, vol. 85, pp. 78–90, 2015.

[102] J. L. Provis, A. Palomo, and C. Shi, "Advances in understanding alkali-activated materials," *Cem. Concr. Res.*, vol. 78, pp. 110–125, 2015.

[103] W. K. Part, M. Ramli, and C. B. Cheah, "An overview on the influence of various factors on the properties of geopolymer concrete derived from industrial by-products," *Constr. Build. Mater.*, vol. 77, pp. 370–395, 2015.

[104] P. Krivenko, "Why alkaline activation - 60 years of the theory and practice of alkali-activated materials," *J. Ceram. Sci. Technol.*, vol. 8, no. 3, pp. 323–333, 2017.

[105] J. L. Provis, "Alkali-activated materials," *Cem. Concr. Res.*, vol. 114, pp. 40–48, 2018.

[106] A. Wang *et al.*, "The Durability of Alkali-Activated Materials in Comparison with Ordinary Portland Cements and Concretes: A Review," *Engineering*, vol. 6, no. 6, pp. 695–706, 2020.

[107] F. Farooq *et al.*, "Geopolymer concrete as sustainable material: A state of the art review," *Constr. Build. Mater.*, vol. 306, no. September, p. 124762, 2021.

[108] J. Davidovits, "False Values on CO2 Emission for Geopolymer Cement/Concrete published In Scientific Papers," *Geopolymer Inst. Libr. Tech. Pap.*, vol. 24, pp. 1–9, 2015.

[109] P. Duxson, J. L. Provis, G. C. Lukey, and J. S. J. van Deventer, "The role of inorganic polymer technology in the development of 'green concrete,'" *Cem. Concr. Res.*, vol. 37, no. 12, pp. 1590–1597, 2007.

[110] D. Panias, I. P. Giannopoulou, and T. Perraki, "Effect of synthesis parameters on the mechanical properties of fly ash-based geopolymers," *Colloids Surfaces A Physicochem. Eng. Asp.*, vol. 301, no. 1–3, pp. 246–254, 2007.

[111] S. Schiavoni, F. D'Alessandro, F. Bianchi, and F. Asdrubali, "Insulation materials for the building sector: A review and comparative analysis," *Renew. Sustain. Energy Rev.*, vol. 62, pp. 988–1011, 2016.

[112] M. Amin, N. Putra, E. A. Kosasih, E. Prawiro, R. A. Luanto, and T. M. I. Mahlia, "Thermal properties of beeswax/graphene phase change material as energy storage for building applications," *Appl. Therm. Eng.*, vol. 112, pp. 273–280, 2017.

[113] R. R. Lloyd, J. L. Provis, and J. S. J. Van Deventer, "Microscopy and microanalysis of inorganic polymer cements. 1: Remnant fly ash particles," *J. Mater. Sci.*, vol. 44, no. 2, pp. 608–619, 2009.

[114] I. Beghoura, J. Castro-Gomes1, H. Ihsan, and N. Estrada, "Feasibility of alkali-activated mining waste foamed materials incorporating expanded granulated cork," *Min. Sci.*, vol. 24, pp. 7–28, 2017.

[115] F. Pacheco-Torgal, J. Castro-Gomes, and S. Jalali, "Alkali-activated binders: A review. Part 1. Historical background, terminology, reaction mechanisms and hydration products," *Constr. Build. Mater.*, vol. 22, no. 7, pp. 1305–1314, 2008.

[116] M. OlivierMuntean and J. A. H. W. Peters, "Trends im global CO2 emissions; 2015 Report," *PBL Netherlands Environ. Assess. Agency Eur. Comm. Jt. Res. Cent.*, pp. 1–78, 2015.

[117] A. Talaei, D. Pier, A. V. Iyer, M. Ahiduzzaman, and A. Kumar, "Assessment of long-term energy efficiency improvement and greenhouse gas emissions mitigation options for the cement industry," *Energy*, vol. 170, pp. 1051–1066, 2019.

[118] F. Pacheco-Torgal, J. Castro-Gomes, and S. Jalali, "Investigations about the effect of aggregates on strength and microstructure of geopolymeric mine waste mud binders," *Cem. Concr. Res.*, vol. 37, no. 6, pp. 933–941, 2007.

[119] A. Palomo, O. Maltseva, I. Garcia-Lodeiro, and A. Fernández-Jiménez, "Portland Versus Alkaline Cement: Continuity or Clean Break: 'A Key Decision for Global Sustainability,'" *Front. Chem.*, vol. 9, no. October, pp. 1–28, 2021.

[120] "Wagners (2021) Wagners Earth Friendly Concrete. Available at: https://goo.gl/LquYyF (Accessed: 01 September 2017)." .

[121] "VicRoads: VicRoads Standard Specifi cations. In: Section 620 – Precast Concrete Units, VicRoads, Melbourne (2009). In: J. L. Provis, Alkali Activated Materials state of the art report. 2014."

[122] "No TitleVicRoads: VicRoads Standard Specifi cations. In: Section 703 – General Concrete Paving, VicRoads, Melbourne (2010). In: J. L. Provis, Alkali Activated Materials state of the art report. 2014."."

[123] D. Khale and R. Chaudhary, "Mechanism of geopolymerization and factors influencing its development: A review," *J. Mater. Sci.*, vol. 42, no. 3, pp. 729–746, 2007.

[124] F. Eurostat *et al.*, "Waste statistics Main statistical findings Total waste generation," vol. 2012, no. September, 2016.

[125] H. Hebhoub, H. Aoun, M. Belachia, H. Houari, and E. Ghorbel, "Use of waste marble aggregates in concrete," *Constr. Build. Mater.*, vol. 25, no. 3, pp. 1167–1171, 2011.

[126] F. Raupp-Pereira, R. J. Ball, J. Rocha, J. A. Labrincha, and G. C. Allen, "New waste based clinkers: Belite and lime formulations," *Cem. Concr. Res.*, vol. 38, no. 4, pp. 511–521, 2008.

[127] J. P. Castro-Gomes, A. P. Silva, R. P. Cano, J. Durán Suarez, and A. Albuquerque, "Potential for reuse of tungsten mining waste-rock in technical-artistic value added products," *J. Clean. Prod.*, vol. 25, pp. 34–41, 2012.

[128] D. Hardjito, S. E. Wallah, D. M. J. Sumajouw, and B. V. Rangan, "On the development of fly ash-based geopolymer concrete," *ACI Mater. J.*, vol. 101, no. 6, pp. 467–472, 2004.

[129] P. Duxson and J. L. Provis, "Designing precursors for geopolymer cements," *J. Am. Ceram. Soc.*, vol. 91, no. 12, pp. 3864–3869, 2008.

[130] B. Varela, P. B. Tavares, A. T. Pinto, and J. P. Castro-Gomes, "Chemical composition correction of aluminosilicate materials to enhance their conditions as precursors for alkaline activation," *J. Mater. Sci. Eng. with Adv. Technol.*, vol. 7, no. 1, pp. 17–33, 2013.

[131] A. Palomo, M. T. Blanco-Varela, M. L. Granizo, F. Puertas, T. Vazquez, and M. W. Grutzeck,

"Chemical stability of cementitious materials based on metakaolin - Isothermal conduction calorimetry study," *Cem. Concr. Res.*, vol. 29, pp. 997–1004, 1999.

[132] M. L. Granizo, S. Alonso, M. T. Blanco-Varela, and A. Palomo, "Alkaline activation of metakaolin: Effect of calcium hydroxide in the products of reaction," *J. Am. Ceram. Soc.*, vol. 85, no. 1, pp. 225–231, 2002.

[133] B. Sabir, S. Wild, and J. Bai, "Metakaolin and calcined clays as pozzolans for concrete: A review," *Cem. Concr. Compos.*, vol. 23, no. 6, pp. 441–454, 2001.

[134] "(2021, November 01) Retrieved from https://gccassociation.org/cement-and-concrete-innovation/clinker-substitutes/calcined-clays/." .

[135] I. Külaots, A. Hsu, R. H. Hurt, and E. M. Suuberg, "Adsorption of surfactants on unburned carbon in fly ash and development of a standardized foam index test," *Cem. Concr. Res.*, vol. 33, no. 12, pp. 2091–2099, 2003.

[136] M. Mustafa, A. Bakri, K. Hussin, and M. Bnhussain, "Fly Ash-based Geopolymer Lightweight Concrete Using Foaming Agent," pp. 7186–7198, 2012.

[137] W. D. A. Rickard and A. Van Riessen, "Performance of solid and cellular structured fly ash geopolymers exposed to a simulated fire," *Cem. Concr. Compos.*, vol. 48, pp. 75–82, 2014.

[138] G. Habert, J. B. D'Espinose De Lacaillerie, and N. Roussel, "An environmental evaluation of geopolymer based concrete production: Reviewing current research trends," *J. Clean. Prod.*, vol. 19, no. 11, pp. 1229–1238, 2011.

[139] N. R. Rakhimova and R. Z. Rakhimov, "Alkali-activated cements and mortars based on blast furnace slag and red clay brick waste," *Mater. Des.*, vol. 85, pp. 324–331, 2015.

[140] A. Fernández-Jiménez, J. G. Palomo, and F. Puertas, "Alkali-activated slag mortars: Mechanical strength behaviour," *Cem. Concr. Res.*, vol. 29, no. 8, pp. 1313–1321, 1999.

[141] P. Duxson, A. Fernández-Jiménez, J. L. Provis, G. C. Lukey, A. Palomo, and J. S. J. Van Deventer, "Geopolymer technology: The current state of the art," *J. Mater. Sci.*, vol. 42, no. 9, pp. 2917–2933, 2007.

[142] H. Xu and J. S. J. Van Deventer, "The geopolymerisation of alumino-silicate minerals," *Int. J. Miner. Process.*, vol. 59, no. 3, pp. 247–266, 2000.

[143] P. Chindaprasirt, S. Homwuttiwong, and C. Jaturapitakkul, "Strength and water permeability of concrete containing palm oil fuel ash and rice husk-bark ash," *Constr. Build. Mater.*, vol. 21, no. 7, pp. 1492–1499, 2007.

[144] A. Kusbiantoro, M. F. Nuruddin, N. Shafiq, and S. A. Qazi, "The effect of microwave incinerated rice husk ash on the compressive and bond strength of fly ash based geopolymer concrete," *Constr. Build. Mater.*, vol. 36, pp. 695–703, 2012.

[145] E. A. Azimi *et al.*, "Processing and Properties of Geopolymers As Thermal Insulating Materials : a Review," *Rev. Adv. Mater. Sci.*, vol. 44, pp. 273–285, 2016.

[146] D. R. Yixin Shao, Thibaut Lefort, Shylesh Moras, "Studies on concrete containing ground waste glass," *Cem. Concr. Res.*, vol. 30, pp. 91–100, 2000.

[147] C. Shi and K. Zheng, "A review on the use of waste glasses in the production of cement and concrete," *Resour. Conserv. Recycl.*, vol. 52, no. 2, pp. 234–247, 2007.

[148] J. W. Figg, "Reaction between cement and artificial glass in concrete," *Society*, 1981.

[149] A. Karamberi and A. Moutsatsou, "Participation of coloured glass cullet in cementitious materials," *Cem. Concr. Compos.*, vol. 27, no. 2, pp. 319–327, 2005.

[150] Eurostat, *Energy, transport and environment statistics 2020 edition*. 2020.

[151] F. Pacheco-torgal, "Investigations on mix design of tungsten mine waste geopolymeric binder," vol. 22, pp. 1939–1949, 2008.

[152] Castro-Gomes et al., "2006 (Castro-Gomes) Valorizacao de residuos de minas em pavimento de baixo custo.pdf." 2006.

[153] H. Akbulut and C. Gürer, "Use of aggregates produced from marble quarry waste in asphalt pavements," *Build. Environ.*, vol. 42, no. 5, pp. 1921–1930, 2007.

[154] M. Yellishetty, V. Karpe, E. H. Reddy, K. N. Subhash, and P. G. Ranjith, "Reuse of iron ore mineral wastes in civil engineering constructions: A case study," *Resour. Conserv. Recycl.*, vol. 52, no. 11, pp. 1283–1289, 2008.

[155] S. Ahmari and L. Zhang, "Production of eco-friendly bricks from copper mine tailings through geopolymerization," *Constr. Build. Mater.*, vol. 29, pp. 323–331, 2012.

[156] L. Zhang, S. Ahmari, and J. Zhang, "Synthesis and characterization of fly ash modified mine tailings-based geopolymers," *Constr. Build. Mater.*, vol. 25, no. 9, pp. 3773–3781, 2011.

[157] F. A. Kuranchie and S. K. Shukla, "Utilisation of iron ore mine tailings for the production of geopolymer bricks," *Int. J. Mining, Reclam. Environ.*, no. May, 2014.

[158] A. R. Mwesigye, S. D. Young, E. H. Bailey, and S. B. Tumwebaze, "Population exposure to trace elements in the Kilembe copper mine area , Western Uganda : A pilot study," *Sci. Total*

Environ., vol. 573, pp. 366–375, 2016.

[159] T. Sun, J. Chen, X. Lei, and C. Zhou, "Detoxification and immobilization of chromite ore processing residue with metakaolin-based geopolymer," *J. Environ. Chem. Eng.*, vol. 2, no. 1, pp. 304–309, 2014.

[160] X. Jiao, Y. Zhang, and T. Chen, "Thermal stability of a silica-rich vanadium tailing based geopolymer," *Constr. Build. Mater.*, vol. 38, pp. 43–47, 2013.

[161] L. Vickers, A. van Riessen, and W. Rickard, *Fire-resistant Geopolymers: Role of Fibres and Fillers to Enhance Thermal Properties*. 2015.

[162] A. Silva *et al.*, "The effects of Na 2 O / SiO 2 molar ratio , curing temperature and age on compressive strength , morphology and microstructure of alkali-activated fly ash-based geopolymers," *Cem. Concr. Compos.*, vol. 33, no. 6, pp. 653–660, 2011.

[163] P. Duxson, J. L. Provis, G. C. Lukey, S. W. Mallicoat, W. M. Kriven, and J. S. J. Van Deventer, "Understanding the relationship between geopolymer composition, microstructure and mechanical properties," *Colloids Surfaces A Physicochem. Eng. Asp.*, vol. 269, no. 1–3, pp. 47–58, 2005.

[164] M. Komljenović, Z. Baščarević, and V. Bradić, "Mechanical and microstructural properties of alkali-activated fly ash geopolymers," *J. Hazard. Mater.*, vol. 181, no. 1–3, pp. 35–42, 2010.

[165] I. Beghoura and J. Castro-gomes, "Design of alkali-activated aluminium powder foamed materials for precursors with different particle sizes," *Constr. Build. Mater.*, vol. 224, pp. 682–690, 2019.

[166] U. S. E. P. Agency, "Report to Congress: Wastes from the Extraction and Beneficiation of Metallic Ores, Phosphate Rock, Asbestos, Overburden from Uranium Mining and Oil Shale," no. December, 1985.

[167] European Commission, "A Roadmap for moving to a competitive low carbon economy in 2050," 2011.

[168] F. Pacheco-Torgal, J. P. Castro-Gomes, and S. Jalali, "Adhesion characterization of tungsten mine waste geopolymeric binder. Influence of OPC concrete substrate surface treatment," *Constr. Build. Mater.*, vol. 22, no. 3, pp. 154–161, 2008.

[169] G. Kastiukas and X. Zhou, "Effects of waste glass on alkali-activated tungsten mining waste : composition and mechanical properties," *Mater. Struct.*, 2017.

[170] S. Dawczyński, P. Cieśla, M. Górski, and R. Krzywoń, "Research on strength properties of geopolymer based on tungsten mine waste and recycled ground glass," *Millenium - Journal of Education, Technologies, and Health*, no. 8. pp. 13–20, 2019.

[171] A. Franco, R. Vieira, C. Geologist, R. Bunting, and N. Executive, "The Panasqueira Mine at a Glance," vol. 3, no. June, 2014.

[172] F. Adam Wheeler, B.Sc, M.Sc, C. Eng, "Technical report on the mineral resources and reserves of the Panasqueira mine, Portugal," no. 20th November, 2015.

[173] M. Zhu, R. Ji, Z. Li, H. Wang, L. L. Liu, and Z. Zhang, "Preparation of glass ceramic foams for thermal insulation applications from coal fly ash and waste glass," *Constr. Build. Mater.*, vol. 112, pp. 398–405, 2016.

[174] F. Pacheco-Torgal, J. Castro-Gomes, and S. Jalali, "Properties of tungsten mine waste geopolymeric binder," *Constr. Build. Mater.*, vol. 22, no. 6, pp. 1201–1211, 2008.

[175] F. Pacheco-Torgal, J. P. Castro-Gomes, and S. Jalali, "Alkali-activated tungsten mine waste mud binder versus OPC concrete : acid and abrasion resistance.," *2007 - Int. Conf. Alkali Act. Mater. – Res. Prod. Util.*, p. 18, 2007.

[176] Pacheco. Torgal, "Desenvolvimento de ligantes obtidos por activacao alcalina de lamas residuais das minas da panasqueira," 2006.

[177] J. Centeio, "Propriedades físicas de argamassa geopolimérica de lamas residuais das minas da panasqueira," 2011.

[178] N. Sedira, J. Castro-Gomes, and M. Magrinho, "Red clay brick and tungsten mining waste-based alkali-activated binder: Microstructural and mechanical properties," *Constr. Build. Mater.*, vol. 190, pp. 1034–1048, 2018.

[179] M. A. Longhi, E. D. Rodríguez, S. A. Bernal, J. L. Provis, and A. P. Kirchheim, "Valorisation of a kaolin mining waste for the production of geopolymers," *J. Clean. Prod.*, vol. 115, pp. 265–272, 2016.

[180] A. I. Badanoiu, T. H. A. Al Saadi, S. Stoleriu, and G. Voicu, "Preparation and characterization of foamed geopolymers from waste glass and red mud," *Constr. Build. Mater.*, vol. 84, pp. 284–293, 2015.

[181] Z. Liu *et al.*, "Fabrication and properties of foam geopolymer using circulating fluidized bed combustion fly ash," vol. 21, no. 1, pp. 89–94, 2014.

[182] K. H. Yang, C. W. Lo, and J. S. Huang, "Production and properties of foamed reservoir sludge

inorganic polymers," *Cem. Concr. Compos.*, vol. 38, pp. 50–56, 2013.

[183] Z. Zhang, J. L. Provis, A. Reid, and H. Wang, "Fly ash-based geopolymers: The relationship between composition, pore structure and efflorescence," *Cem. Concr. Res.*, vol. 64, pp. 30–41, 2014.

[184] N. Narayanan and K. Ramamurthy, "Structure and properties of aerated concrete: a review," *Cem. Concr. Compos.*, vol. 22, pp. 321–329, 2000.

[185] A. Othuman and Y. C. Wang, "Elevated-temperature thermal properties of lightweight foamed concrete," *Constr. Build. Mater.*, vol. 25, no. 2, pp. 705–716, 2011.

[186] S. Kang, C. Siang, O. Yuan, and Y. Ling, "Fresh and hardened properties of lightweight foamed concrete with palm oil fuel ash as filler," *Constr. Build. Mater.*, vol. 46, pp. 39–47, 2013.

[187] D. Castañeda *et al.*, "Production of a lightweight masonry block using alkaline activated natural pozzolana and natural fibers," vol. 253, 2020.

[188] P. Krivenko and G. Kovalchuk, "Achieving a heat resistance of cellular concrete based on alkali activated fly ash cements," pp. 599–606, 2015.

[189] E. Prud'homme *et al.*, "Silica fume as porogent agent in geo-materials at low temperature," *J. Eur. Ceram. Soc.*, vol. 30, no. 7, pp. 1641–1648, 2010.

[190] E. Prud'homme, P. Michaud, E. Joussein, C. Peyratout, A. Smith, and S. Rossignol, "In situ inorganic foams prepared from various clays at low temperature," *Appl. Clay Sci.*, vol. 51, no. 1–2, pp. 15–22, 2011.

[191] M. M. Al-Bakri Abdullah, L. Jamaludin, K. Hussin, M. Bnhussain, C. M. R. Ghazali, and M. I. Ahmad, "Fly ash porous material using geopolymerization process for high temperature exposure," *Int. J. Mol. Sci.*, vol. 13, no. 4, pp. 4388–4395, 2012.

[192] Ehsan Ul Haq, "Microwave synthesis of thermal insulating foams from coal derived bottom ash," no. February, 2015.

[193] C. Bai and P. Colombo, "Processing, properties and applications of highly porous geopolymers: A review," *Ceram. Int.*, vol. 44, no. 14, pp. 16103–16118, 2018.

[194] A. Hsu, R. H. Hurt, and E. M. Suuberg, "Adsorption of surfactants on unburned carbon in fly ash and development of a standardized foam index test," vol. 33, pp. 2091–2099, 2003.

[195] V. Vaou and D. Panias, "Thermal insulating foamy geopolymers from perlite," *Miner. Eng.*, vol. 23, no. 14, pp. 1146–1151, 2010.

[196] S. Delair *et al.*, "Durability of inorganic foam in solution : The role of alkali elements in the geopolymer network," vol. 59, pp. 213–221, 2012.

[197] H. Esmaily and H. Nuranian, "Non-autoclaved high strength cellular concrete from alkali activated slag," *Constr. Build. Mater.*, vol. 26, no. 1, pp. 200–206, 2012.

[198] K. Yang, C. Lo, and J. Huang, "Production and properties of foamed reservoir sludge inorganic polymers," *Cem. Concr. Compos.*, vol. 38, pp. 50–56, 2013.

[199] G. Masi, W. D. A. Rickard, L. Vickers, M. Chiara, and A. Van Riessen, "A comparison between different foaming methods for the synthesis of light weight geopolymers," *Ceram. Int.*, vol. 40, no. 9, pp. 13891–13902, 2014.

[200] Z. Abdollahnejad, F. Pacheco-Torgal, T. Félix, W. Tahri, and J. Barroso Aguiar, "Mix design, properties and cost analysis of fly ash-based geopolymer foam," *Constr. Build. Mater.*, vol. 80, no. May 2010, pp. 18–30, 2015.

[201] P. Hlaváček, V. Šmilauer, F. Škvára, L. Kopecký, and R. Šulc, "Inorganic foams made from alkali-activated fly ash: Mechanical, chemical and physical properties," *J. Eur. Ceram. Soc.*, vol. 35, no. 2, pp. 703–709, 2015.

[202] E. Kamseu *et al.*, "Cumulative pore volume, pore size distribution and phases percolation in porous inorganic polymer composites: Relation microstructure and effective thermal conductivity," *Energy Build.*, vol. 88, pp. 45–56, 2015.

[203] R. M. Novais, G. Ascensão, L. H. Buruberri, L. Senff, and J. A. Labrincha, "Influence of blowing agent on the fresh- and hardened-state properties of lightweight geopolymers," *Mater. Des.*, vol. 108, pp. 551–559, 2016.

[204] V. Ducman and L. Korat, "Characterization of geopolymer fl y-ash based foams obtained with the addition of Al powder or H 2 O 2 as foaming agents," *Mater. Charact.*, vol. 113, pp. 207–213, 2016.

[205] A. Hajimohammadi, T. Ngo, P. Mendis, and J. Sanjayan, "Regulating the chemical foaming reaction to control the porosity of geopolymer foams," *Mater. Des.*, vol. 120, pp. 255–265, 2017.

[206] A. Hajimohammadi, T. Ngo, and P. Mendis, "How does aluminium foaming agent impact the geopolymer formation mechanism?," *Cem. Concr. Compos.*, vol. 80, pp. 277–286, 2017.

[207] I. Beghoura, J. Castro-gomes, H. Ihsan, J. Pickstone, and N. Estrada, "Expansion volume of alkali activated foamed cork composites from tungsten mining mud waste with aluminium."

[208] G. Kastiukas, D. Ph, X. Zhou, D. Ph, K. T. Wan, and D. Ph, "Lightweight Alkali-Activated Material from Mining and Glass Waste by Chemical and Physical Foaming," vol. 31, no. 3, pp. 1–8, 2019.

[209] A. Hajimohammadi, T. Ngo, and P. Mendis, "Enhancing the strength of pre-made foams for foam concrete applications," *Cem. Concr. Compos.*, vol. 87, no. January 2018, pp. 164–171, 2018.

[210] J. He, Q. Gao, X. Song, X. Bu, and J. He, "Effect of foaming agent on physical and mechanical properties of alkali-activated slag foamed concrete," *Constr. Build. Mater.*, vol. 226, pp. 280–287, 2019.

[211] S. Soni, A. Jain, and H. Shrivastava, "Effect of Protein Based Foaming Agent on Geopolymer Foamed Concrete," vol. 7, no. 4, pp. 282–291, 2020.

[212] T. P. Huynh, V. H. Pham, N. D. Do, T. C. Nguyen, and N. T. Ho, "Performance evaluation of pre-foamed ultra-lightweight composites incorporating various proportions of slag," *Period. Polytech. Civ. Eng.*, vol. 65, no. 1, pp. 276–286, 2021.

[213] R. Krzywoń and S. Dawczyński, "Strength parameters of foamed geopolymer reinforced with gfrp mesh," *Materials (Basel).*, vol. 14, no. 3, pp. 1–19, 2021.

[214] I. Beghoura and J. Castro-Gomes, "Enhancing Density-Based Mining Waste Alkali-Activated Foamed Materials Incorporating Expanded Cork," *CivilEng*, vol. 2, no. 2, pp. 523–540, 2021.

[215] N. Ariffin *et al.*, "Effect of aluminium powder on kaolin-based geopolymer characteristic and removal of Cu2+," *Materials (Basel).*, vol. 14, no. 4, pp. 1–19, 2021.

[216] "(2021, November 01) Retrieved from https://patents.justia.com/patent/20140047999." .

[217] R. L. Heck, "A review of commercially used chemical foaming agents for thermoplastic foams," *J. Vinyl Addit. Technol.*, vol. 4, no. 2, pp. 113–116, 1998.

[218] C. Gmbh, "Chemical Foaming Agents," 1973.

[219] G. Masi, W. D. A. Rickard, L. Vickers, M. C. Bignozzi, and A. Van Riessen, "A comparison between different foaming methods for the synthesis of light weight geopolymers," *Ceram. Int.*, vol. 40, no. 9 PART A, pp. 13891–13902, 2014.

[220] V. Ducman and L. Korat, "Characterization of geopolymer fly-ash based foams obtained with the addition of Al powder or H2O2as foaming agents," *Mater. Charact.*, vol. 113, pp. 207–213, 2016.

[221] Joseph Davidovits, "Geopolymer chemestry & applications 3rd edition." 2011.

[222] J. Feng, R. Zhang, L. Gong, Y. Li, W. Cao, and X. Cheng, "Development of porous fly ash-based geopolymer with low thermal conductivity," vol. 65, pp. 529–533, 2015.

[223] D. D. Joseph, "Understanding foams & foaming," *J. Fluids Eng.*, p. To appear in the column entitled Significant Quest, 1997.

[224] M. Strozi Cilla, P. Colombo, and M. Raymundo Morelli, "Geopolymer foams by gelcasting," *Ceram. Int.*, vol. 40, no. 4, pp. 5723–5730, 2014.

[225] Z. Abdollahnejad, F. Pacheco-Torgal, T. Félix, W. Tahri, and J. Barroso Aguiar, "Mix design, properties and cost analysis of fly ash-based geopolymer foam," *Constr. Build. Mater.*, vol. 80, no. May 2010, pp. 18–30, 2015.

[226] Johan Alexanderson, "Relations between structure and mechanical properties of autoclaved aerated concrete. In: N. Narayanan and K. Ramamurthy, 'Structure and properties of aerated concrete: a review,' Cem. Concr. Compos., vol. 22, pp. 321–329, 2000.," *Cem. Concr. Res.*, vol. 9, no. 4, pp. 507–514, 1979.

[227] S. E. Petrov I, "Application of automatic image analysis for the investigation of autoclaved aerated concrete structure. In: N. Narayanan and K. Ramamurthy, 'Structure and properties of aerated concrete: a review,' Cem. Concr. Compos., vol. 22, pp. 321–329, 2000.," *Cem Concr Res*, vol. 24, no. 5, pp. 830–840.

[228] "Prim P, Witmann FH. Structure and water absorption of aerated concrete. In: Wittmann FH, editor. Proceedings Autoclaved Aerated Concrete, Moisture and Properties. Amsterdam: Elsevier; 1983. p. 43-53. In: N. Narayanan and K. Ramamurthy, "Structure and prop."

[229] S. Tada and S. Nakano, "Microstructural Approach To Properties of Moist Cellular Concrete.," *Dev. Civ. Eng.*, no. May, pp. 71–89, 1983.

[230] N. Narayanan and K. Ramamurthy, "Microstructural investigations on aerated concrete," *Cem. Concr. Res.*, vol. 30, pp. 457–464, 2000.

[231] K. Haněa, O. Koronthályová, and P. Matiašovský, "The carbonation of autoclaved aerated concrete," *Cem. Concr. Res.*, vol. 27, no. 4, pp. 589–599, 1997.

[232] V. RC, "Cellular concretes-composition and methods of preparation. In: N. Narayanan and K. Ramamurthy, 'Structure and properties of aerated concrete: a review,' Cem. Concr. Compos., vol. 22, pp. 321–329, 2000.," *J Am Concr Inst*, vol. 25, pp. 7737–795., 1954.

[233] C. Roulet, "Expansion of aerated concrete due to frost . Determination of critical," *Autoclaved*

aerated Concr. moisture Prop., no. January, 1983.

[234] C. G. J. P. Laurent, "Influence de la teneur en eau et de la temp6rature sur la conductivit6 thermique du b6ton cellulaire autoclav," *Mater. Struct.*, vol. 28, pp. 464–472, 1995.

[235] V. Vaou and D. Panias, "Thermal insulating foamy geopolymers from perlite," *Miner. Eng.*, vol. 23, no. 14, pp. 1146–1151, 2010.

[236] A. M. Papadopoulos, "State of the art in thermal insulation materials and aims for future developments," *Energy Build.*, vol. 37, no. 1, pp. 77–86, 2005.

[237] D. M. P. A. da Cunha, "Non - Structural Lightweight Concrete Produced with Volcanic Scoria from São Miguel Island," pp. 1–12, 2014.

[238] F. Puertas and A. Fern, "Mineralogical and microstructural characterisation of alkali-activated fly ash / slag pastes," vol. 25, pp. 287–292, 2003.

[239] A. Fernández-Jiménez and A. Palomo, "Composition and microstructure of alkali activated fly ash binder: Effect of the activator," *Cem. Concr. Res.*, vol. 35, no. 10, pp. 1984–1992, 2005.

[240] K. Srinivasan and A. Sivakumar, "Geopolymer Binders : A Need for Future Concrete Construction," vol. 2013, 2013.

[241] Helena Pereira, *Cork: Biology, Production and Uses. In: Carla Vilela et al. Novel sustainable composites prepared from cork residues and biopolymers. biomass and bioenergy, 55, (2013), 148-155.* 2007.

[242] S. P. Silva, M. A. Sabino, E. M. Fernandas, V. M. Correlo, L. F. Boesel, and R. L. Reis, "Cork: Properties, capabilities and applications," *Int. Mater. Rev.*, vol. 50, no. 6, pp. 345–365, 2005.

[243] "corklink (2016) available at: http://www.corklink.com/index.php/about-cork/(Accessed: 16 November 2016)." .

[244] L. Gil, "Cork powder waste; an overview," *Biomass ans Bioenergy*, vol. 13, no. C, pp. 59–61, 1997.

[245] H. Pereira, M. Emília Rosa, and M. A. Fortes, "The Cellular Structure of Cork from Quercus suber L," *IAWA J.*, vol. 8, no. 3, pp. 213–218, 1987.

[246] "Cork, How products are made, available at: http://www.madehow.com/Volume-5/Cork.html. (Accessed: 10 January 2021)." .

[247] Alessandro Gandini, "Polymers from Renewable Resources: A Challenge for the Future of Macromolecular Materials," *Macromolecules*, vol. 41, no. 24, 2008.

[248] M. Manso and J. P. Castro-Gomes, "Thermal analysis of a new modular system for green walls," *J. Build. Eng.*, vol. 7, pp. 53–62, 2016.

[249] T. M. Mata, A. Martins, J. C. G. Esteves, and S. T. Ana, "Carbon footprint of the insulation cork board," vol. 143, pp. 925–932, 2017.

[250] N. Pargana, M. Duarte, J. Dinis, and J. De Brito, "Comparative environmental life cycle assessment of thermal insulation materials of buildings," *Energy Build.*, vol. 82, pp. 466–481, 2014.

[251] J. D. Silvestre, N. Pargana, J. De Brito, M. D. Pinheiro, and V. Durão, "Insulation Cork Boards — Environmental Life Cycle Assessment of an Organic Construction Material," pp. 1–16, 2016.

[252] A. Cortês, J. Almeida, J. De Brito, and A. Tadeu, "Water retention and drainage capability of expanded cork agglomerate boards intended for application in green vertical systems," vol. 224, no. x, pp. 439–446, 2019.

[253] A. Brás, M. Leal, and P. Faria, "Cement-cork mortars for thermal bridges correction. Comparison with cement-EPS mortars performance," *Constr. Build. Mater.*, vol. 49, pp. 315–327, 2013.

[254] P. J. R. O. Nóvoa, M. C. S. Ribeiro, A. J. M. Ferreira, and A. T. Marques, "Mechanical characterization of lightweight polymer mortar modified with cork granulates," *Compos. Sci. Technol.*, vol. 64, no. 13–14, pp. 2197–2205, 2004.

[255] F. R. S. L. J. Gibson, K. E. Easterling, M. F. Ashby, "The structure and mechanics of cork," *J. Mater. Sci.*, vol. 377, pp. 99–117, 1981.

[256] M. E. Rosa and M. A. Fortes, "Rate effects on the compression and recovery of dimensions of cork," *J. Mater. Sci.*, vol. 23, no. 3, pp. 879–885, 1988.

[257] O. Anjos, H. Pereira, and M. E. Rosa, "Tensile properties of cork in the tangential direction: Variation with quality, porosity, density and radial position in the cork plank," *Mater. Des.*, vol. 31, no. 4, pp. 2085–2090, 2010.

[258] O. Anjos, H. Pereira, and M. E. Rosa, "Tensile properties of cork in axial stress and influence of porosity, density, quality and radial position in the plank," *Eur. J. Wood Wood Prod.*, vol. 69, no. 1, pp. 85–91, 2011.

[259] O. Anjos, C. Rodrigues, J. Morais, and H. Pereira, "Effect of density on the compression behaviour of cork," *Mater. Des.*, vol. 53, pp. 1089–1096, 2014.

[260] J. Davidovits, "Properties of Geopolymer Cements," *First Int. Conf. Alkaline Cem. Concr.*, pp.

131–149, 1994.

[261] A. Fernández-Jiménez and A. Palomo, "Characterisation of fly ashes. Potential reactivity as alkaline cements," *Fuel*, vol. 82, no. 18, pp. 2259–2265, 2003.

[262] P. Nath and P. K. Sarker, "Use of OPC to improve setting and early strength properties of low calcium fly ash geopolymer concrete cured at room temperature," *Cem. Concr. Compos.*, vol. 55, pp. 205–214, 2015.

[263] L. Dembovska, D. Bajare, V. Ducman, L. Korat, and G. Bumanis, "The use of different by-products in the production of lightweight alkali activated building materials," *Constr. Build. Mater.*, vol. 135, pp. 315–322, 2017.

[264] Siti Noorbaini Sarmin, "Characterization of Fly Ash / Metakaolin-based Geopolymer Lightweight Concrete Reinforced Wood Particles," in *International Conference on Sustainable Built Environment*, 2016, no. March.

[265] J. Feng, R. Zhang, L. Gong, Y. Li, W. Cao, and X. Cheng, "Development of porous fly ash-based geopolymer with low thermal conductivity," *Mater. Des.*, vol. 65, pp. 529–533, 2015.

[266] X. yan Zhou, F. Zheng, H. guan Li, and C. long Lu, "An environment-friendly thermal insulation material from cotton stalk fibers," *Energy Build.*, vol. 42, no. 7, pp. 1070–1074, 2010.